



*International*

**WOCE**

*Newsletter*



Number 20

September 1995

**IN THIS ISSUE**

**News from the IPO**

*We've Moved* W. John Gould 2

**Lagrangian Measurements**

*Global Drifter Program: Measurements of Velocity, SST and Atmospheric Pressure* Peter Niiler 3

*Lagrangian Measurements of the Mean Wind-Driven Currents in the Tropical Pacific* Elise Ralph and Peter Niiler 7

*Separation of the Kuroshio Water and its Penetration onto the Continental Shelf West of Kyushu* Heung-Jae Lie et al. 10

*Surface Currents in the Canary Basin from Drifter Observations* Jeffrey Paduan et al. 13

*The General Circulation of the Subtropical North Atlantic, near 700m Depth, Revealed by the TOPOGULF SOFAR Floats* Michel Ollitrault 15

*Trajectory Studies in a Model of the Indian Ocean Circulation* Meredith Haines et al. 19

*The Global Lagrangian Drifter Data Assembly Center at NOAA/AOML* Mark Bushnell 36

**Indian Ocean Cruises**

*WOCE Hydrographic Programme Stations in the Indian Ocean from December 1994 to July 1995* 22

*Repeat Hydrography Along WHP Lines I5W, I7N, and I1W* Amy Field et al. 23

*WHP Sections I8N/I5N in the Central Indian Ocean* Lynne Talley 25

*WHP Indian Ocean I9N* Arnold Gordon 26

**Other Science**

*On the Sensitivity of the Oceanic Meridional Heat Transport Implied by AGCMs to Simulated Cloud Radiative Effects* P.J. Gleckler and D.A. Randall 28

*WHP Repeated Hydrography Section PR14, Offshore Southern Chile* Ricardo Rojas et al. 31

*WOCE Sea Level Data – Plentiful and Available NOW!* Gary Mitchum and Bernard Kilonsky 33

*Exploring Oceanographic Data on the PC* Reiner Schlitzer 38

*WOCE Hydrographic Programme Underway Data Submission – An Update* Bertrand J. Thompson 40

**Miscellaneous**

*Joining WOCE on the World Wide Web (WWW)* 9

*Meetings Timetable 1995/96* 42

*WOCE IPO Move* 43

# We've Moved

*W. John Gould, Director*

## The move

The WOCE IPO is about to enter a new era. Since its establishment in 1984 the Office has been located in the Institute of Oceanographic Sciences in the countryside about 50 km southwest of London. In September, before you receive this Newsletter, we will be established in new offices in the Southampton Oceanography Centre. Our new location will be in the dock area of Southampton, the biggest commercial port in the UK and we will become part of one of the worlds' largest oceanographic laboratories.

Details of our new address, phone and fax numbers and e-mail addresses have been circulated by e-mail and are reproduced here on p. 43. As we used to say when television was in its infancy "Normal service will be resumed as soon as possible".

The process of moving from a building that IOS has occupied for over 40 years has resulted in large amounts of paper being consigned to the rubbish heap but the sifting process has turned up some interesting documents.

We were reminded that the first meeting of the WOCE Scientific Steering Group was held at Woods Hole in August 1983 and attended by steering group members Bretherton, Broecker, Crease, Kimura, Lefebvre, Wunsch and Woods (Hasselmann and Sarkisyan did not attend). These people were, I suppose, the founding fathers of WOCE and its good to see that some of them are still active in WOCE science.

WOCE has achieved a great deal since then and our ideas of how the project might be carried out have evolved, but the overall goals are still the same.

## Meetings

The Intergovernmental WOCE Panel (with 13 countries represented and 5 other representatives and observers) met in Paris in early June. It was followed by the IOC Assembly at which WOCE in the person of its co-chair Dr John Church made an impressive presentation on WOCE scientific results and on the challenges still facing WOCE. A resolution was passed by the IOC Assembly, the text of which has been passed to national WOCE Committee Chairmen for action. It called for actions on:-

- Resources for the analysis and synthesis of WOCE data,
- Access to territorial waters,
- Secondment of staff to WOCE DACs and SACs,
- Support for WOCE conferences and workshops,
- Continuing satellite missions.

Furthermore the letter requests that each nation sends a summary of its best WOCE results to the IPO so that a presentation pack of WOCE scientific highlights that is to be assembled after our office move can be as representative

and up-to-date as possible. Please make sure that your results and figures are made available to your national committee chairman or project co-ordinator.

At the IOC assembly the Canadian delegation agreed that Canada would host a major WOCE conference in Halifax, Nova Scotia in 1998. Initial planning is underway.

We are now entering the next cycle of WOCE meetings and there is a busy schedule up to the end of the year. The most important will be the first meeting of the WOCE Synthesis and Modelling WG under its co-Chairs Lynne Talley and Andrew Bennett. In the run-up, to the meeting there has been a lively discussion about what WOCE synthesis is. The discussion will be continued by the WG and its first report should make interesting reading and start to form a blueprint for the AIMS (Analysis, Interpretation, Modelling and Synthesis) phase of WOCE.

The WOCE Hydrographic Programme Planning Committee will be meeting in Hamburg in mid-October. Chuck Corry who worked in the WHPO in Woods Hole and was a point of contact with the WHPO for many WOCE scientists, left in early August. We wish him well in his new career but are faced with filling the hole that he has left. How this will be done will be a matter for discussion at the WHPPC and the US SSC meetings.

## Science

There were a number of WOCE-related sessions at the August IAPSO meeting in Honolulu. Although I wasn't there myself I hear that recent WOCE results made up an important element of the scientific presentations. This bodes well for the planned WOCE regional workshops.

The Indian Ocean campaign is past its half way point and is going extremely well. Problems with access to territorial waters have, in most cases been overcome, and a summary of recent cruises is included in this issue.

## This issue and next

This newsletter focuses on lagrangian measurements and, judging by the wide variety of articles and the presentations at IAPSO, this is a section of the WOCE science community that is working well together and producing new and exciting results. The transition from WOCE to CLIVAR is an important issue and the article by Allyn Clarke highlights some of the overlaps between the two programmes.

In our next newsletter we plan to have articles on modelling and data assimilation and WOCE synthesis and on oceanic and air-sea fluxes. So please let us know your latest results! The submission deadline is mid-November.

# Global Drifter Program: Measurements of Velocity, SST and Atmospheric Pressure

Peter Niiler, Scripps Institution of Oceanography, La Jolla, CA 92092-0230, USA

## Introduction

For the 1990s decade of climate research and monitoring, a more accurate and a more globally dense data set of the SST and surface circulation was needed than had been provided by Volunteer Observing Ships. ARGOS-tracked Lagrangian drifters were developed to acquire this data. Under the sponsorship of WCRP (WCRP-26), a Global Drifter Program (GDP) has been organized to deploy and interpret the data from drifters drogued in the mixed layer. In the past ten years, TOGA, WOCE, and several dozen other science programmes have contributed resources and data to this project. The future GCOS and CLIVAR programmes also include significant reliance on drifters for acquisition of the *in situ* ocean data (the Ocean Observing System Development Panel, 1995). Seven operational meteorological agencies now deploy drifters and use the data in real time for weather and climate prediction.

The Global Drifter Program objectives are to:

1. Provide global, operational data sets for SST and sea-level pressure that are used in real time for improving weather prediction and enhancing models of annual and interannual climate prediction.
2. Describe the mixed-layer velocity and its variability on a global basis resulting in new seasonal surface circulation charts of the oceans.
3. Assess the verity of global annual and interannual climate models of the oceans.
4. Enhance research data on upper ocean physical and biological processes.

GDP began in 1988 in the tropical Pacific, where since then 150 drifters have been in residence. In 1990, deployments were extended to the mid-latitude Pacific and in 1991, Atlantic deployments were started. The Indian Ocean and Southern Oceans were implemented in 1994/95. Fourteen countries have funded programmes to deploy drifters in support of GDP and several others aid in deployments. There is a continued need for ocean observations in support of annual and interannual climate analysis and prediction; therefore, observations of SST and surface current are an integral part of the required GCOS data set. To meet the sampling requirements, as set out in WOCE, four to six year-long time series from each basin were required on a 500 km x 500 km resolution. To meet the requirements of sampling annual and interannual climate anomalies, as in CLIVAR, a ten-year data set is needed.

The operations of GDP have been directed from two centres and the analysis and interpretation are distributed among the oceanographic community. The technology development is done at Scripps and ARGOS data is quality controlled and processed at the Data Assembly Center at AOML, Miami. Drifters are deployed from both VOS and

aircraft. The SST data (and sea-level pressure data) is reported in real time to GTS and, every six months, processed data tapes containing location and sensor data are sent to MEDS, Canada, which is the RNODC for the distribution of drifter data to scientists and other users.

## Technical achievements

### Global Lagrangian Drifter

A technical objective of GDP was to design and build a drifter which had a known water-following capability in different wind conditions at a specified depth and which would have a half life at sea in excess of one year. You will find a diagram as well as photos of the drifter on the World Wide Web (<http://larry.aoml.erl.gov:8000/www/drifter.html>). To determine how well a particular drifter follows water at the 15 m drogue level, two neutrally buoyant VMCMs were attached on top and bottom of the drogue in a variety of sea conditions and measured the slip of water past the drogue. The data showed that the most important parameter in controlling the water-following capability was the drag area ratio, R (the ratio of the product of the largest projected area of the drogue and its drag coefficient to the sum of the products of the largest projected areas of the tether and submerged surface floats and their drag coefficients). Eighty-four percent of the variability in 62 separate, 2-4 hour long measurements of slip velocity, U (cm/sec), of the drogue through the water was represented by a statistical model:

$$U = 3.5 (W/R) + 9.5 (DU/R), \quad (1)$$

where W (m/sec) is the wind at 10 m and DU (cm/sec) is the velocity difference across the drogue (Niiler et al., 1995). Therefore, to achieve water following capability of 1 cm/sec in 10 m/sec winds, a drifter has to be built with  $R > 35$ . The drag area ratio of Global Lagrangian Drifter is 40.

In 1988, deployment started of large numbers of drifters with large drag area ratio in the tropical Pacific in a pilot project, "The Pan Pacific Surface Current Study" (WCRP-26). In 1990, 12 drifters which had been at sea for 200 days were recovered from the eastern north Pacific. In 1993, 9 drifters were recovered after over 300 days. Inspection of these drifters led to a redesign of the tether attachments and a change of battery from lithium to alkaline. "The WOCE/TOGA Lagrangian Drifter Construction Manual" (Sybrandy and Niiler, 1991) describes the drifter manufacturing procedures, which are now used in ten countries. Since late 1990, the half-life has increased to 400 days. Projected costs in 1996 are about \$2600 per unit and in 1998, \$2200 per unit.

## Barometer Port Attachment

The Global Lagrangian Drifter is a platform from which sea-level pressure (and sea surface salinity) can be measured. This required the development of a barometer port for the surface float. Low cost barometers had already been tested for accuracy and long term stability for WOCE at WHOI (Payne *et al.*, 1990) so an AIR sensor was adopted for drifter applications. The drogues on GLDs are so large that the surface float often submerges. The shielded air intake was placed one radius distance above the float (Osmund and Painting, 1984). Because the port submerges, the barometers have overpressure signals. These submergence “spikes” are removed from a time series acquired once a second for 80 seconds by a de-spiking program installed into the data controller. A report entitled the “Global Lagrangian Barometer Drifter Construction Manual” (Sybrandy *et al.*, 1995) is available. Currently there are over 100 barometer drifters operational in the GDP.

## Sea Surface Salinity Attachment

SEACAT sensors have been used on moorings on the Pacific equator for many years and post-calibrations show that the six month stability of these sensors in the mixed layer was nominally 0.01 psu (McPhaden *et al.*, 1990). 72 unpumped SEACATs were attached to GLDs in the TOGA-COARE area, which acquired an average of 10, one-second samples every two hours and broadcast this average on 90 second intervals to ARGOS (Swenson *et al.*, 1992). In 1993, four SEACATs were recovered which had been

operational in the western Pacific in excess of 300 days. Post-calibrations show that these were offset by 0.020, 0.015, 0.005 and 0.035 psu. In 1995, 3 low cost salinity sensors made by Falmouth Scientific will be deployed in the North Atlantic.

## Drifter arrays

Fig. 1 shows global drifter tracks from January 1993 to March 1995. In the period July 1988–May 1995 the GDP deployed over 1600 drifters in the Pacific Ocean. The density of data return has not been spatially uniform, as drifters tend to spend about twice as much time in convergent regions, like the southern margin of the North Equatorial Countercurrent, than they do on the equator. Efforts are being made to correct this imbalance with the next 5 years of deployments. Fig. 2 is a map of the 15 m Pacific currents. This data is now mature for analysis. There are several lessons which have been learned from the first five years of WOCE drifter deployments:

- (i) The VOS network is an effective means to get drifters deployed. It takes several years to learn where drifters tend to congregate and where the deployment density should be increased. A rational plan for the seeding of drifters in the tropical and subtropical Pacific and North Atlantic Ocean, but this process has recently begun in the Indian and Southern Oceans.
- (ii) Even with tight specifications for manufacturing, there are differences in the survival rates of different lots of drifters. Continuous inspection of the manufacturing procedures and an open dialogue with the drifter manufacturers is needed.

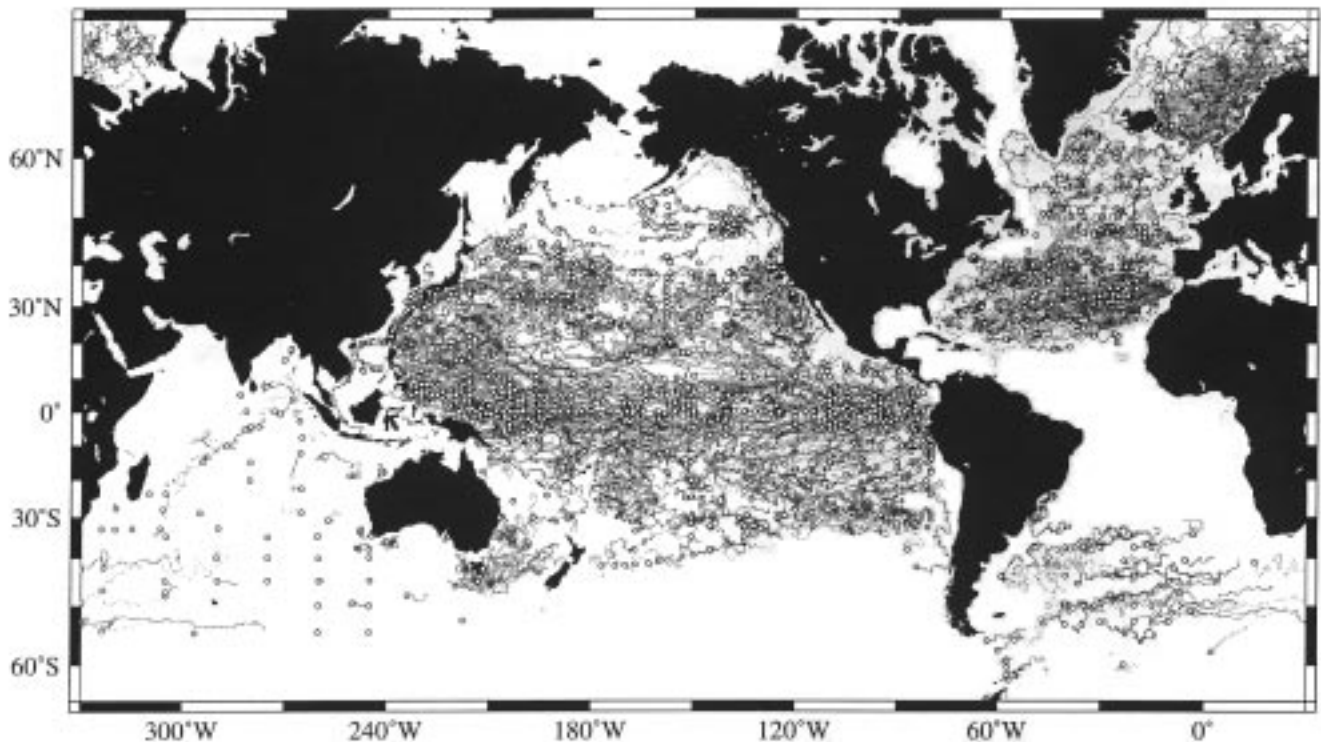


Figure 1. Tracks for all drifters transmitting from 1 January 1993 to 31 March 1995. The open circles mark the release location.

- (iii) Improvements in mechanical designs and information on the long-term stability of sensors are needed but this requires drifters to be recovered after being at sea for over one year, and hence dedicated ship time. Periodic recovery is a vital activity, considering the numbers of drifters which are proposed to be released in the GDP. The increase in data return from increasing the half-life by another 200 days (from the present 400 days) will more than compensate for the recovery expenses in the next year.

A number of research programmes and operational agencies require mixed layer drifters to be deployed in various parts of the global ocean. GDP has made its technical resources and deployment expertise available to these programmes, and has encouraged deployments of mixed layer drifters with drag area ratio greater than 40; thus, high quality GDP data has increased considerably. In several cases, GDC arranged for ARGOS tracking to continue when the original investigator was no longer interested in the data series. GDC has provided technical assistance to countries learning to build drifters, and to manufacturers who required aid in starting up the manufacturing process. Through this attention to the world requirements of drifter data and exchange of WCRP data with other programmes, the WOCE drifter data set has nearly doubled.

## Data and management

GDP data processing is done at the Drifter Assimilation Center at AOML/NOAA and data is stored at MEDS. A METADATA technical information sheet is also on file at

MEDS and documents the physical dimensions, manufacturer, drag area ratio, operation principles of sensors, etc. of every drifter released in the GDP.

Every year, a meeting of the global drifter community is held under WCRP auspices, the seventh of which, SVP-7, was held in La Jolla in November 1994. Convened by the WOCE/CLIVAR GDP Planning Committee, invitations are extended to national PIs, agency representatives, scientists with new analyses of drifter data, drifter manufacturers and others interested in the GDP. Reports of these meetings are published by the WOCE IPO.

## Scientific results/operational requirements

Scientific results from drifter data can be found in the CLIVAR/WOCE (formerly WOCE/TOGA) SVP Planning Committee meeting reports. The first comprehensive comparison between TOGA/NEG OGCMs and the Pacific GDP data set was done in November 1994 (WCRP, 1995). The Global Drifter Center at AOML maintains a bibliography accessible on INTERNET. Look for papers to appear in reviewed literature in the next year.

Drifters provide important operational SST and  $P_a$  data on a global basis. SST is used as a boundary condition for numerical weather prediction models and is a powerful analysis tool by itself for revealing the changing annual and interannual climate patterns over the global oceans. Sea level pressure ( $P_a$ ) is used in a variety of weather prediction schemes and as a powerful climate diagnostic tool. It is critical in producing dynamic sea level from satellite altimeter measurements and in ensuring that realistic fluxes of heat and momentum to the ocean are produced in

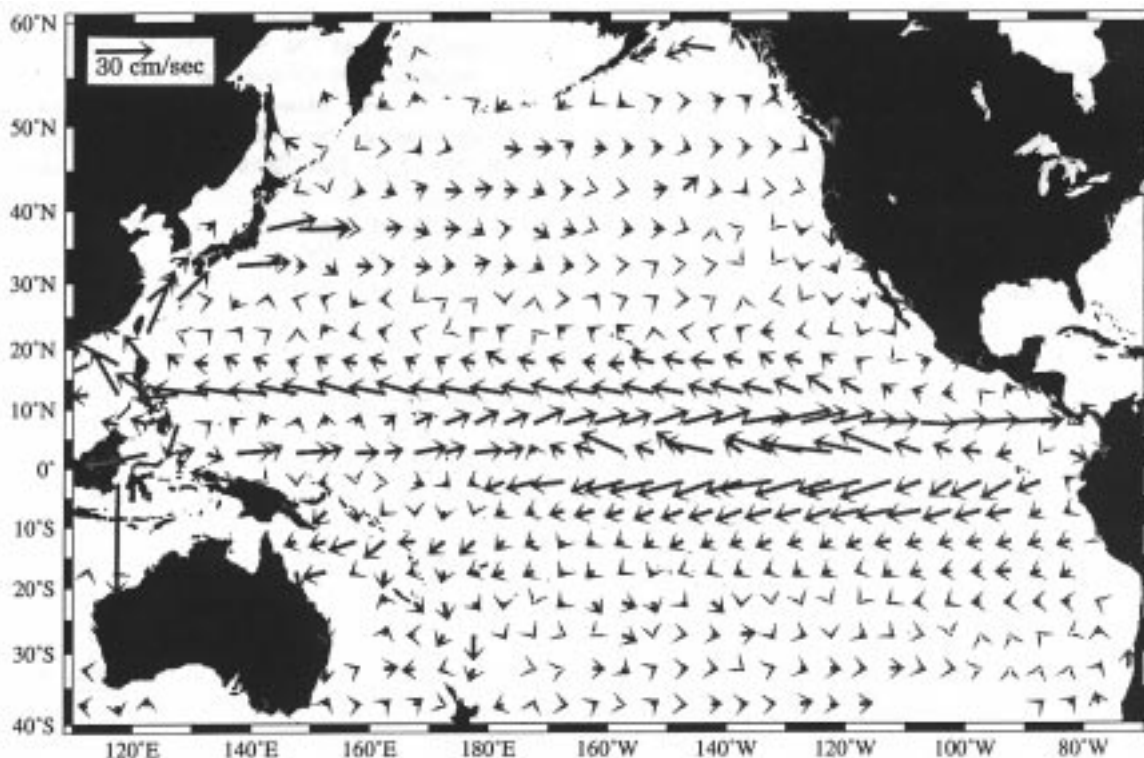


Figure 2. Map of currents at 15 m depth.

operational atmospheric models (Smith, 1991). NWS and other operational weather agencies directly use real time  $P_a$  for issuing marine weather nowcasts and forecasts. The scientific analyses of the global annual and interannual climate change over the oceans relies almost entirely on the fields of SST and  $P_a$  produced by the operational agencies. In these analyses, great attention is paid to the accuracy of the fields. WCRP put in place over the past ten years networks of *in situ* sensors for measuring SST to 10.1°C accuracy over entire ocean basins. Commencing in 1985, the construction of a global SST field was taken on by the Climate Analysis Center of NMC/NOAA. It is now produced on a one-degree grid using optimum interpolation (OI). The analysis uses SST observations from ships and buoys and multi-channel SST (MCSST) retrievals from satellites. Any large-scale biases in the MCSST are removed before the OI analysis is done. The correction of satellite biases requires the use of high quality *in situ* data, that now comes mostly from drifting and moored buoys. The highest priority for the SST analysis must be to continue to deploy drifters in southern middle latitudes, in all the oceans. Without these observations, the accuracy of the SST analysis will be degraded because bias correction of the satellite data would not be possible.

The  $P_a$  data is used by NWS and NMC and other operational numerical prediction centres as an integral part of the analysis forecast system (*i.e.*, GDAS). Sea level pressure data is an essential measurement used to anchor the remotely sensed temperature profiles from orbiting satellites that, when integrated vertically, provide the primary estimate of the extra-tropical Southern Hemisphere mass field. The forecast model dynamics provide the relationship of the mass and wind fields. Surface pressure observations from drifting buoys are required in the extra-tropical latitudes of the Southern Hemisphere, where there is limited land and VOS data (Seaman, 1994). The highest priority for  $P_a$  analyses must be to deploy drifters in the Southern Oceans and in mid-latitudes where real time  $P_a$  is needed for short term marine weather forecasts.

NMC estimates that one *in situ* device on the average in every 5 square is required to "tie down" the AVHRR and  $P_a$  retrievals on a global basis (Reynolds and Smith, 1994).

In summary, GDP is a mature, global ocean data acquisition project, which is organized to meet the needs of the scientific projects of WCRP and the operational agencies involved in predicting weather and climate. The next five years of activity has been proposed by a number of science and operational programmes to be a continuation of long

term climate observations of the oceans and providing a real-time operational marine data set. By the end of 5 years, GOOS/GCOS management will have a more direct participation in operating the drifter program. The transition of the deployments, data processing and program management to GOOS will be accomplished by designating the existing structure, that is already operational, as an official GOOS activity.

## References

- Comparison of TOGA Tropical Pacific Ocean model simulations with the WOCE/TOGA Surface Velocity Programme Drifter Data Set, 1995. WCRP Report No. 4/1995, 156pp.
- McPhaden, M.J., H.P. Freitag, and A.J. Shepherd, 1990: Moored salinity time series measurements at 0°, 140°W. *J. of Atmos. Ocean Tech.*, 7, 568–575.
- Niiler, P.P., A.L. Sybrandy, K. Bi, P-M Poulain, and D. Bitterman, 1995: Measurements of the water-following capability of holey sock and TRISTAR drifters. (Accepted by *Deep-Sea Res.*)
- The Observing System Development Panel, 1995: Scientific design for the common module of the Global Ocean Observing System and the Global Climate Observing System: An ocean observing system for climate. Department of Oceanography, Texas A&M University, College Station, Texas, 265pp.
- Osmund, A. and D.J. Painting, 1994: Static pressure heads for meteorological use. United Kingdom Meteorological Office, Tecemo/Reference III.15. WMO Technical Conference on Instruments and Cost Effective Meteorological Observations.
- Payne, R.E., G.H. Crescenti and R.A. Weller, 1993: Improved meteorological measurements from buoys and Ships (IMET): Preliminary report on barometric pressure sensors. WHOI Ref. No. 89-49.
- Reynolds, R.W., and T.M. Smith, 1994: Improved global sea surface temperature analyses. *J. Climate*, 7, 929–948.
- Seaman, R.S., 1994: Monitoring a data assimilation system for the impact of observations. *Aust. Met. Mag.*, 43, 41–48.
- Smith, N., 1991: The role of models in an ocean observing system. CCCO-JSC Ocean Observing System Development Panel, Texas A&M University, College Station, TX 77843-3146. OOSDP Background Report No. 1, 85pp.
- Swenson, M.S., P.P. Niiler, A.L. Sybrandy, and L. Sombardier, 1991: Feasibility of attaching Seacats to TOGA drifters. Scripps Institution of Oceanography Reference Series, 91-30, La Jolla, CA, 39pp.
- Sybrandy, A.L., and P.P. Niiler, 1991: The WOCE/TOGA SVP Lagrangian drifter construction manual. SIO Ref. 91/6, WOCE Report No. 63/91, 58pp.
- Sybrandy et al., 1995: Barometer Drifter Construction Manual.

### Subsurface Float and Ship Drift Data on CD-ROM

The WOCE Subsurface Float DAC in association with the US Naval Oceanographic Office and US-NODC have published two CD-ROMs containing historical subsurface float data and surface current (ship drift) data. All the data are in ASCII files, except the map of the grid system used for the ship drift data. Users will need to create their own routine from the format description, since no software is included on the disks. The CD-ROMs may be ordered as "Ocean Current Drifter Data on CD-ROM" at US\$110 per 2-disk set from US-NODC. By mail: National Oceanographic Data Center, User Services Branch, 1825 Connecticut Avenue, NW, Washington, D.C. 20235, USA; by phone: +1-202-606-4549; by Fax: +1-202-606-4586; or by World Wide Web: <http://www.nodc.noaa.gov>.

# Lagrangian Measurements of the Mean Wind-Driven Currents in the Tropical Pacific

Elise A. Ralph and Peter Niiler, Scripps Institution of Oceanography, University of California, San Diego, La Jolla, CA 92037-0230, USA

In response to the need of WOCE and TOGA for accurate surface current measurements, over 1500 WOCE/TOGA satellite-tracked drifters have been deployed in the tropical Pacific since 1988. These modern drifters have a drogue with a larger drag area than previous satellite-tracked drifters and follow the water to within 1 cm/sec in winds of 10 m/sec (Niiler *et al.*, 1995b). These drifters have recently been used to measure the tropical Pacific surface circulation (Niiler *et al.*, 1995a) and to monitor the oceanic response to westerly wind bursts (McPhaden *et al.*, 1992) and to an El Niño (Bi and Niiler, 1995).

The drogue of the drifters is centred at 15 m depth, which is generally within a layer which is influenced by wind (Davis *et al.*, 1981). The drifters are therefore influenced by surface geostrophic currents and ageostrophic Ekman currents. One goal of the WOCE/TOGA Surface Velocity Program is to infer wind driven currents by subtracting the geostrophic currents from the observed total currents. The residuals, or the Ekman currents, can be used to test models of vertical mixing due to wind stress and surface heat fluxes. This preliminary report contains what we have learned about the wind-driven currents deduced from the extensive data set of drifters in the tropical Pacific.

Five-day long segments of the drifter velocity measurements (with the down-wind slip removed (Niiler *et al.*, 1995b)) were binned into boxes of 1° latitude by 5° longitude and then averaged within each box. Any box that contained less than 25 independent (5 day) observations was discarded. Boxes within the equatorial region between -3°S – 3°N were also not used because the Ekman balance fails at such low latitudes (Bi, 1995). The average geostrophic velocity relative to 450 m calculated from Kessler's (1990) climatology of XBT data was subtracted from each box average to determine the average ageostrophic velocity within each box. The ECMWF-derived wind stress was interpolated along each drifter trajectory and then binned and averaged in the same fashion as the velocity measurements. The average mixed layer depth,  $H_m$ , was determined for each geographical box from the Levitus (1982) climatological data as the depth at which density varies from its surface value by more than 0.02 kg/m<sup>3</sup>.

The ageostrophic velocity typically lies to the right (left) of the wind stress in the Northern (Southern) hemisphere (Fig. 1). The angle with which the 15 metre currents veer from the wind is only weakly dependent on

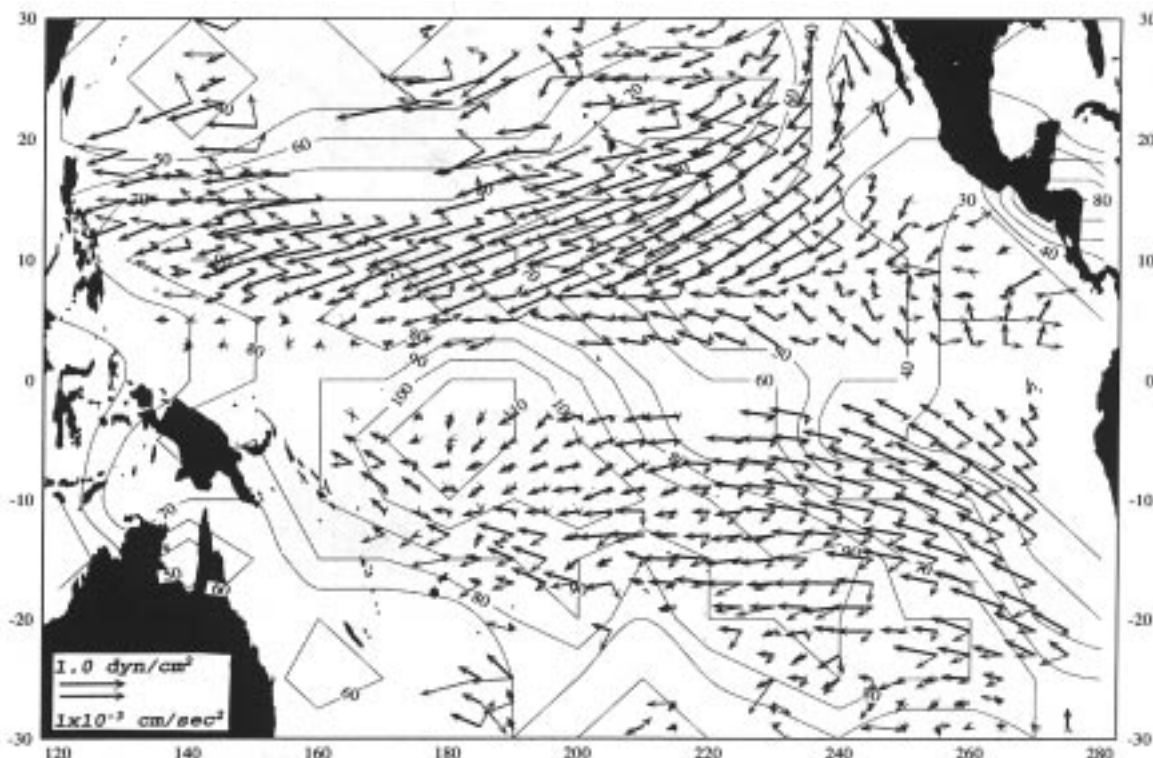


Figure 1. The mean wind stress and ageostrophic force measurements used in this study. Contours of  $H_m$ , the mean mixed layer depth were determined from the Levitus 1982 climatology.

latitude; the largest angles are in the eastern basin, where the 15 m drogue lies near the base of the mixed layer, which is on the order of 30 metres deep there. A best fit of the linear relationship:

$$(u + iv) = [e^{-i\theta} / H](\tau_o^x + i\tau_o^y) / \rho f \quad (1)$$

(which is implied by a bulk Ekman layer balance) is obtained using the basin-wide data set of drifters and wind stress and gives  $H = 23$  metres and  $\theta = 52^\circ$ . This calculation was also carried out for drifters with the Levitus geostrophic velocities relative to 3000 m removed. The mean rotation of the velocity and the coefficient  $H$  in (1) are independent of the climatology used. The relationship between the mean wind stress and the ageostrophic currents provides quite a remarkable demonstration of the earth's rotation.

This calculation suggests that, on average, the wind-driven stress only penetrates to a depth shallower than the average mixed layer depth of 56 m across the basin. However, there is a great deal of spatial variability about this mean. Can this variability be interpreted as being due to spatial variations in  $f$ ,  $\tau$  and the mixed layer depth,  $H_m$ ? Such an interpretation of the wind-driven circulation at 15 m relies on a model of the vertical distribution of stress between the surface (where it is equal to the wind stress) and the base of the mixed layer (where it is assumed to vanish). Since the 15 metre drifters sample different Coriolis parameters and different wind stresses as they move around the basin, they sample different levels of the vertical structure. The magnitude of the ageostrophic velocity at 15 metres was modelled as

$$|u_a| = Au_*^{1+a} f^b$$

where  $A$ ,  $a$  and  $b$  are determined by a least-squares fit. Using either the Levitus climatology or Kessler's climatology for the geostrophic velocity, we find that  $b \approx -0.5$ . This  $(1/\sqrt{f})$  scaling suggests two well-known models that may account for the variability we observe.

In Ekman's (1905) model, where the eddy viscosity  $K$  is assumed to be a constant, the ageostrophic velocity smoothly spirals with depth. Several studies (*i.e.* Price *et al.*, 1987 and Wijffels *et al.*, 1994) indicate that the observed spirals are "flatter" than Ekman's spiral, *i.e.* the amplitude decays more quickly than the angle rotates. This occurs in Ekman's solution where the stress vanishes at  $z = -H_m$ , a depth less than the Ekman depth. The solution for this system is (Gonella, 1971):

$$u(z) + iv(z) = \frac{u_*^2}{(fD_E)} \frac{(1+i)e^{2(1+i)H_m/D_E}}{(e^{2(1+i)H_m/D_E} - 1)} \left[ e^{(1+i)(z/D_E)} + e^{-(1+i)(z/D_E)} \right]$$

where  $D_E = \sqrt{2K/f}$  and  $u_*$  is the friction velocity.

Pollard *et al.*, 1973 (PRT hereafter), suggest that the depth of the mixed layer is determined as the depth at which the rate of production of turbulent mechanical energy by entrainment at the base of the mixed layer is balanced by the

production of turbulent mechanical energy by surface processes. This depth is  $H_p = u_* / \sqrt{fN}$ , where  $N$  is the buoyancy frequency,  $N^2 = g\Delta\rho / H_m\rho_0$  and  $H_m$  is determined from the Levitus data, as described above. Using this scaling of  $H_p$ , the magnitude of the ageostrophic velocity scales as

$$|u_a| = A(g\Delta\rho / \rho_0)u_* / \sqrt{f^4 H_m}$$

The constant  $A$  is the factor  $\sqrt{2^A/s}$ , where  $s$  is an empirical factor measuring the shear stability. Its value is typically 0.7 (Niiler and Kraus, 1977).

We can assess the validity of the two models by comparing the magnitude of the observed velocity to the magnitude of the predicted velocity as a function of  $u_*$ . The best fit to the Ekman model occurs for an eddy diffusivity of 30 cm<sup>2</sup>/sec, which leads to a mean Ekman depth of  $18 \pm 5$  metres. This value is much shallower than  $H_m$ , the depth at which the stress is assumed to vanish and the model is nearly identical to Ekman's solution; the model does not account for the observed rotation which is

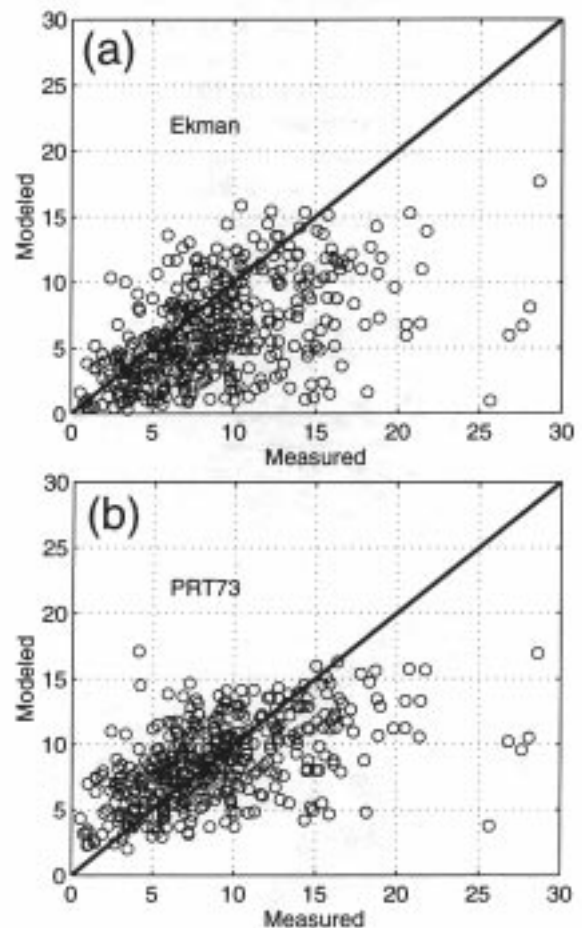


Figure 2. The modelled amplitude of the ageostrophic current vs. the measured amplitude for: (a) The Ekman model and (b) The Pollard, Rhines and Thompson (1973) model.

scattered around 50°. This model, which accounts for only 42% of the variance in the data, tends to under-predict the speed of the current when it is high (Fig. 2a). However, since wind-driven velocities as large as 25 or 30 cm/sec are rare in the ocean, it is possible that these ageostrophic velocities, as described here with non-synoptic data, are incorrect. The PRT model has less scatter (Fig. 2b) than the Ekman model, and accounts for 70% of the variance in the data. The mean scale depth for this model is also shallow, at  $16 \pm 5$  metres. An unbiased linear regression analysis between the PRT model and the observed magnitudes, assuming homogeneous errors in  $H$  (10 metres),  $u_*$  (0.1 cm/sec), and  $|u_a|$  (2.5 cm/sec), indicates that the PRT model is acceptable at the 97.5% confidence level. A similar analysis for the Ekman model does not support that scaling.

The mean amplitude of the ageostrophic current can be predicted to within 5 cm/sec using either the turbulent Ekman model or the PRT model. However, the Ekman model underpredicts the observed currents, and so is less robust than the PRT model. These results must of course be viewed with caution; the variability in the ageostrophic velocity can be attributed to uncertainties associated with measuring the drifter velocities and geostrophic velocities during different climatologies. A weighted regression analysis, with the estimate of errors made for each measurement, must be performed, and is being done. Also, neither model is able to predict the observed rotation of the current from the wind. Nevertheless, the results are encouraging, since 15 m measurements made from a wide variety of locations, during a wide range of times, and under variable wind stress, support the idea that there is a "universal" model to account for the turbulent mixing of momentum. This analysis continues with using TOPEX/POSEIDON sea level data which is contemporaneous with drifter velocities.

## References

- Bi, K., and P.P. Niiler, 1995: The equatorial Pacific response to the 1991-92 ENSO as observed with Lagrangian mixed layer drifting buoys. *J. Geophys. Res.*, submitted.
- Bi, K., 1995: Variability of the surface layer circulation in the western equatorial Pacific. PhD thesis, University of California, San Diego.
- Davis, R.E., R. deSzoeko, and P.P. Niiler, 1981: Variability in the upper ocean during MILE. Part II: Modeling the mixed layer response. *Deep-Sea Res.*, 28A, 1453-1475.
- Ekman, V.W., 1905: On the influence of the earth's rotation on ocean-currents. *Ark. Mat. Ast. Fys.*, 2, 1-52.
- Gonella, J., 1971: The drift current from observations made on the Bouee Laboratoire. *Cah. Oceanogr.*, 23, 19-33.
- Kessler, W., 1990: Observations of long Rossby waves in the northern tropical Pacific. *J. Geophys. Res.*, 95, 5183-5217.
- Levitus, S., 1982: Climatological Atlas of the World Ocean. NOAA Professional Paper 13, U.S. Dept. of Commerce, NOAA.
- McPhaden, M.J., F. Bahr, Y. du Penhoat, E. Firing, S.P. Hayes, P.P. Niiler, P.L. Richardson, J.M. and Toole, 1992: The response of the western equatorial Pacific Ocean to westerly wind bursts during November 1989 to January 1990. *J. Geophys. Res.*, 97, 14289-14303.
- Niiler, P., and E.B. Kraus, 1977: One-dimensional models of the upper ocean, in *Modelling and Prediction of the upper layers of the ocean*, edited by Kraus, E. pp. 143-172, Pergamon Press, Oxford.
- Niiler, P., D. Hansen, D. Olson, P. Richardson, G. Reverdin, and G. Cresswell, 1995a: The Pan Pacific Current Study Lagrangian drifter measurements: 19G. 88-1994. *J. Geophys. Res.*, submitted.
- Niiler, P.P., A.S. Sybrandy, K. Bi, P.M. Poulain, and D. Bitterman, 1995b: Measurements of the water-following characteristics of Tristar and holey-sock drifters. *Deep-Sea Res.*, accepted.
- Pollard, R., P. Rhines, and R. Thompson, 1973: The deepening of the wind-mixed layer. *Geophys. Fluid Dyn.*, 3, 381-404.
- Price, J.F., R.A. Weller, and R.R. Schudlich, 1987: Wind-driven ocean currents and Ekman transport. *Science*, 238, 1534-1538.
- Wijffels, S., E. Firing, and H. Bryden, 1994: Direct observations of the Ekman balance at 10°N in the Pacific. *J. Phys. Oceanogr.*, 24, 1666-1679.

## Joining WOCE on the World Wide Web (WWW)

An excellent way of keeping up to date on WOCE information and data availability is to make use of the WWW. If you have not already installed the software, *Mosaic* can be freely obtained over the internet from ftp.ncsa.uiuc.edu - logon as ftp, give your ID, and change directory to Mosaic. Use 'ls' to list the contents and pick the appropriate directory - Mac, Windows, Unix. Again use 'ls', select the files you like the look of, and the commands 'binary' and 'get (filename)' should download the software.

*Netscape* software (an alternative preferred by many) can be obtained from ftp.netscape.com, by following a similar procedure to that described above.

To get on the WOCE network open the URL with

<http://diu.cms.udel.edu/woce/oceanic.html>

and explore the wealth of options. I am confident you will be amazed.

# Separation of the Kuroshio Water and its Penetration onto the Continental Shelf West of Kyushu

Heung-Jae Lie, Chel-Ho Cho, Jae-Hak Lee, Korea Ocean Research and Development Institute, Ansan P.O. Box 29, Seoul 425-600, Korea; Peter Niiler, Scripps Institution of Oceanography, UCSD, La Jolla, CA 92093-0230, USA; and Jian-Hwa Hu, National Taiwan Ocean University, 20224 Keelung, Republic of China

The Kuroshio has long been known to have a branch current west of Kyushu, the Tsushima Warm Current (TWC). TWC transports heat and salt not only for the northern East China Sea (ECS), but also for the East Sea through a deep trough west of Kyushu (Nitani, 1972). The separation and penetration of TWC are of great importance for exchange processes between shelf and Kuroshio waters, and in the circulation of ECS, Yellow Sea, and East Sea. Recently, Lie and Cho (1994) observed a persistent northward flow along the western shelf edge of the deep north-south trough west of Kyushu and suggested that part of the weak inshore fringe of the Kuroshio, separated from the Kuroshio near the continental slope at the entrance to the trough. Hsueh et al. (1995) applied a theoretical model of the bifurcation of a baroclinic current incident upon step rise in topography to the turning and branching of the Kuroshio west of Kyushu. However, the separation and penetration are not evident in CTD casts and direct current measurements. The Korea Ocean Research and Development Institute (KORDI) has deployed satellite-tracked surface drifters since 1991 as a Korean contribution to the WOCE Surface Velocity Programme (WOCE-SVP),

supplemented by CTD surveys in December 1993 and April–May 1995. Other drifter data collected by KORDI and WOCE-SVP were also used.

A map of drifter trajectories was constructed from the combined data set of 170 drifters, in the ECS between 1988 and 1995 (Fig. 1). It shows dense trajectories off the east coast of Taiwan, along the ECS continental slope, and the Okinawa Trough. These are in good agreement with the topographically controlled path of the Kuroshio, from hydrographic and GEK data. A small number of trajectories meander northeast of Taiwan and at the mouth of the deep trough west of Kyushu. Southwest of Kyushu, the Kuroshio main stream is observed to turn its direction to the east around 29°N 127°30'E, and to cross the trough toward the Tokara Strait, located south of Kyushu. Near the turning point of the Kuroshio, some drifters crossed the continental slope, and others released near the western shelf edge of the trough moved northward along the 100–400 m isobaths. Thus, the trajectories clearly demonstrate more clearly than before (*e.g.*, Nitani, 1972), the eastward turning of the Kuroshio main stream toward the Tokara Strait, and provide for the first time direct evidence for the separation of the

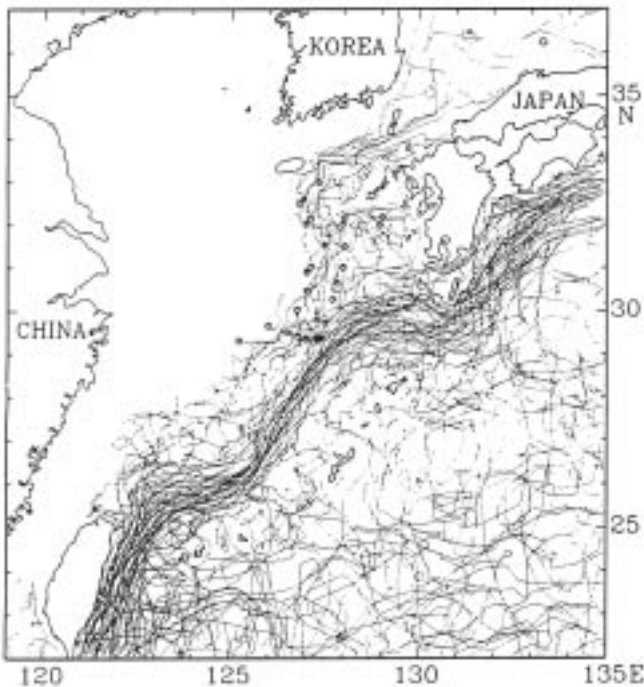


Figure 1. A composite map of trajectories of satellite-tracked surface drifters conducted by the WOCE-SVP until September 1994 and by the KORDI until June 1995. Release points of KORDI drifters are marked by circles.

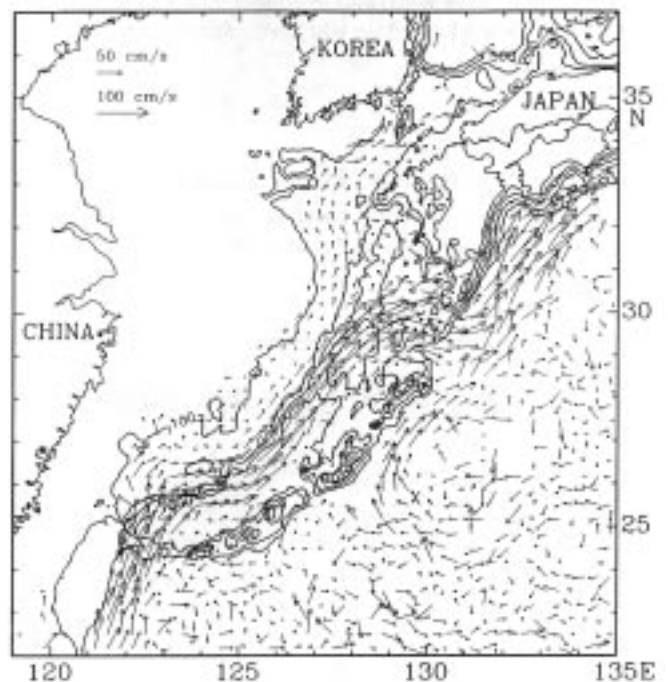


Figure 2. Surface current vectors derived from trajectories in Fig. 1 by 20' x 20' box averaging. Vectors were computed using  $\geq 3$  drifters passing through corresponding boxes. For vector scale see upper left panel.

Kuroshio around the turning point. An average surface current pattern of the eastern ECS computed by 20' x 20' box-averaging is shown in Fig. 2. Arrow vectors are the means obtained from three or more drifters in each box. The main Kuroshio high speed axis in Fig. 2 coincides with the dense trajectories on the continental slope in Fig. 1. A northward current prevails on the 100–200 m deep shelf west of the trough, but in the area south of 29°N, the shelf current is not unidirectional even though the Kuroshio touches the shelf edge. The northward shelf current separates from the Kuroshio main stream near the continental slope at the western entrance of the trough. After separation, it continues northward nearly along the western shelf edge of the trough between 29.5° and 33.5°N. Figs. 1 and 2 reveal that the branch current corresponds to the inshore part of the Kuroshio, immediately before the separation. The anticyclonic eddy discussed by Lie and Cho, 1994 is observed in the northern trough.

The Kuroshio water is characterized by high temperature and salinity, while shelf water of the ECS is colder and fresher. T and S of both waters have a great seasonality, due to seasonal heating and heavy summer precipitation and flooding. T and S can be used to trace the northward penetration of the Kuroshio water onto the continental shelf of the ECS. Horizontal maps of T, S, and  $\sigma_t$  at 50 m for the winter (December 1993 Fig. 3) and spring surveys (April–May 1995 Fig. 4) show hydrographic structures that are relatively simple compared with those in summer. Daily mean velocity vectors were estimated from drifter trajectories during the two surveys and are marked as arrows. Horizontal distributions at 15 m, the drifter dogue depth, are very similar to those at 50 m. The velocity vectors are plotted for the first 10 days after release since the Kuroshio fluctuates with predominant periods, especially in spring, of 14–20 days, (e.g., Qiu et al., 1990).

During the winter survey, isotherms and isopycnals diverged toward the north, and Kuroshio water of  $T > 22.5^\circ\text{C}$ ,  $S > 34.7$ , and of  $\sigma_t < 24.0$  occupied the southeastern quadrant of the survey area. The radial pattern of isolines of high T and S implies the eastward turning of the Kuroshio main stream. Surface currents measured by a ship-borne ADCP (not shown) indicate the Kuroshio main stream located approximately in the Kuroshio core water of  $T > 22.5^\circ\text{C}$  and  $S > 34.8$ . On the other hand, water of  $21.5\text{--}22.0^\circ\text{C}$  and  $34.5\text{--}34.8$  intruded into the shelf across the continental slope. Three drifters, deployed in the usual separation area, moved northward almost along isolines. The northward movement of drifters suggests a northward penetration of the saline Kuroshio water onto the shelf after crossing the slope. The northward movement of drifters suggests a northward penetration of the saline Kuroshio water onto the shelf after crossing the slope. Three drifters almost followed the 34.3–34.75 isohalines. In particular, a drifter, released at the shelf edge, crossed the continental slope in a northwestward direction parallel to isohalines in the neighbourhood of the releasing point. The similarity of the northwest trajectory and the isohaline is direct proof of the penetration of saline Kuroshio water onto the shelf.

During the spring survey, the eastward turning of the Kuroshio at the mouth of the trough was clearly detected by

the ADCP. The Kuroshio core water with maximum T ( $> 23^\circ\text{C}$ ) and S ( $> 34.70$ ) at 50 m depth was consistent with the main axis of the Kuroshio. Inshore Kuroshio water was characterized by high S of 34.6–34.7 and T of  $18\text{--}23^\circ\text{C}$ , slightly lower than the maximum values of the Kuroshio

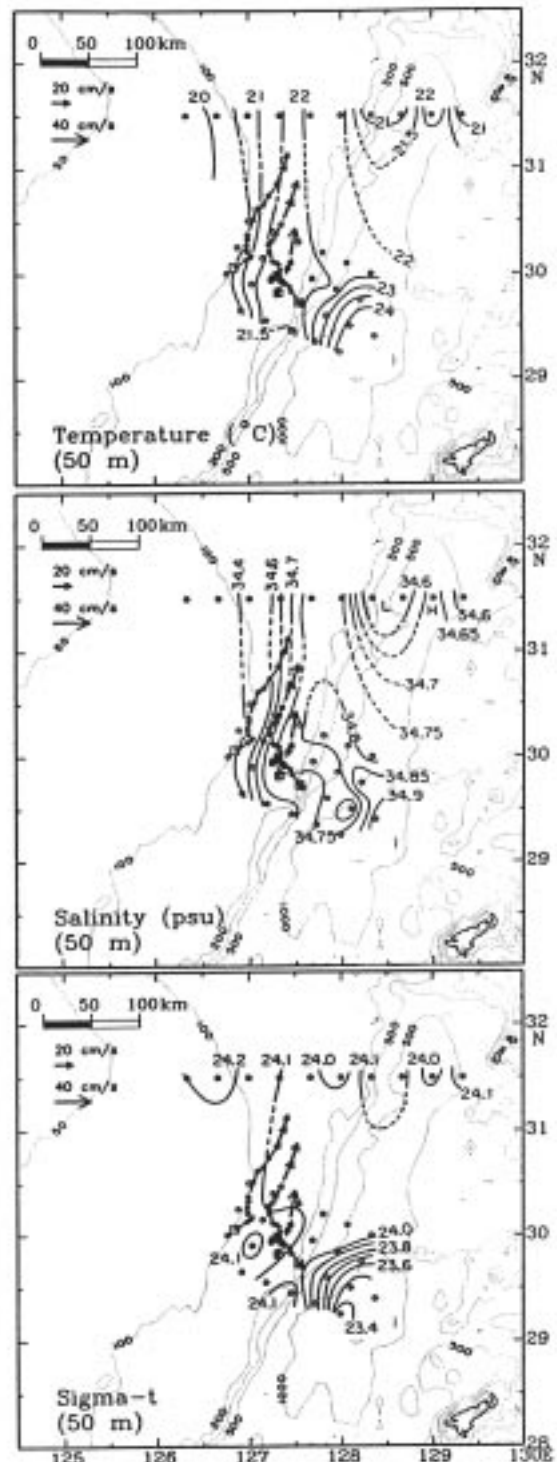


Figure 3. Temperature, salinity, and  $\sigma_t$  at 50 m depth in December 1993, with daily mean current vectors derived from drifter trajectories during the first 15 days after release. The scale of arrow vectors is shown on the upper left corner.

core water, which lay on the continental slope. The inshore Kuroshio water intruded northward in a tongue shape along the western shelf break of the trough and then penetrated onto the continental shelf, mainly between lines I and B. Mixed water with  $S$  of 34.3–34.5 occupied a narrow band

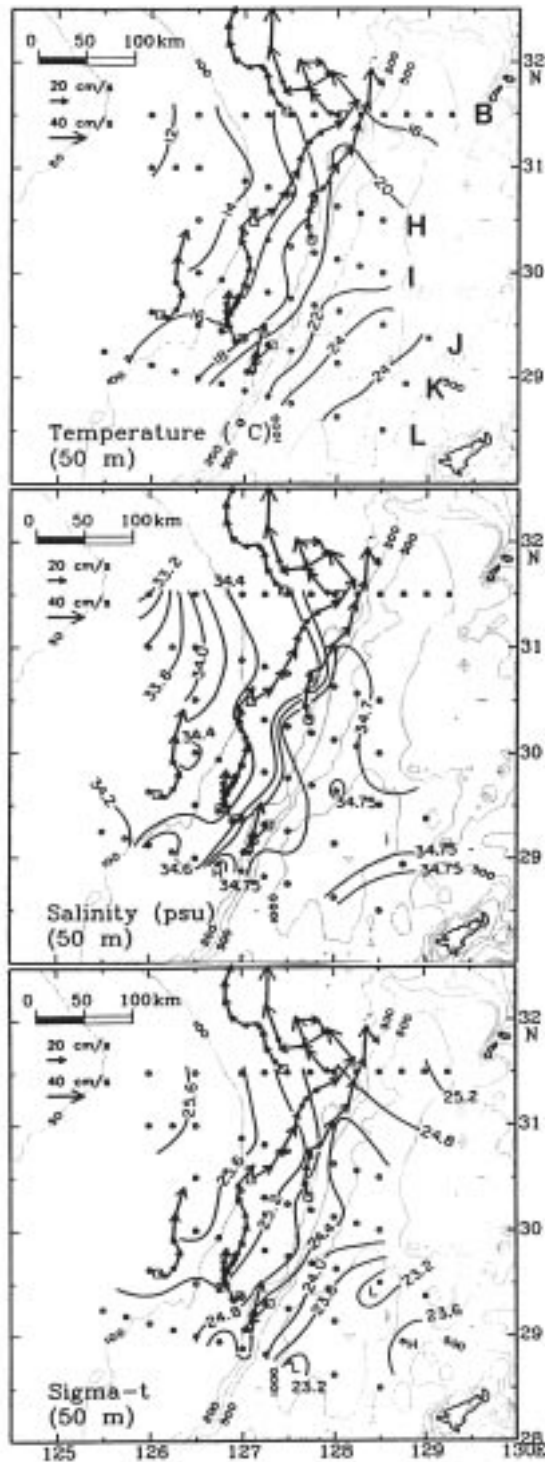


Figure 4. Temperature, salinity, and  $\sigma_t$  at 50 m in late April-early May 1995, with daily mean current vectors derived from drifter trajectories during the first 10 days after release. The scale of arrow vectors is shown on the upper left corner.

on the shelf, located between the 100 m isobath and the inshore Kuroshio water. The band widened from line K to line B, due to mixing between fresher shelf water and the inshore Kuroshio water from the south. The inshore water separated from the Kuroshio core water almost in the same area as for the winter survey. However, a small portion of inshore Kuroshio water intruded into the shelf in the neighbourhood of the separation area. Two drifters deployed on line K on the shelf moved northward almost along isolines with different speeds, but two near the shelf edge moved southwestward for a few days after release and then moved north in a small eddy-like trajectory. This suggests large current variability at the southern three lines which might be related to a frontal meander or eddy during the survey as is frequently observed in spring. Two drifters, released at line I, converged towards the northeast along the isoline for the first several days between lines I and H, and continued in the same direction crossing isolines between line B and H. The crossing could be due to a frontal meander. Two drifters, released at the northernmost line B, were displaced northwest to shallower depths, approximately normal to the 200–500 m isobaths. The inshore Kuroshio water near the shelf edge was warmer and slightly saltier than in the central trough, with isolines crossing the shelf edge. The northwest movement and the distribution of isolines across the continental slope north of line H shows that the inshore Kuroshio water penetrated mainly onto the shelf across the northwestern trough. Vertical sections of  $S$  also reveal that the penetration took place mainly on the northwestern flank of the trough and partly in the neighbourhood of its separation.

### Summary

The separation of the Kuroshio water and its penetration onto the continental shelf west of Kyushu were evidenced for the first time from drifters and CTD data. The separation took place near the continental slope at the western entrance of the deep trough west of Kyushu, where the northeast Kuroshio main stream turns east. The northward branch transported inshore Kuroshio water. The separated water penetrated onto the shelf, mainly in the neighbourhood of the separation area during the winter survey and on the northwestern flank of the trough during the spring survey. The drifter trajectories were nearer parallel to isohalines than to isotherms and isopycnals. Application of an inverse method to the CTD data also supports the separation and penetration of the Kuroshio, and a resemblance of stream lines to isohalines. The volume transport of the branch current is about  $4.0 \times 10^6 \text{ m}^3/\text{s}$  and  $4.5 \times 10^6 \text{ m}^3/\text{s}$  for the winter and spring surveys, respectively, which is approximately twice that of the transport through the Korea Strait.

### Acknowledgement

We appreciate staffs of KORDI and crew of RV Onnuri for the surveys in the East China Sea. The study was

supported by Korea Ministry of Science and Technology, National Science Foundation and NOAA in USA, and National Science Council of ROC.

## References

Hsueh, Y., H.-J. Lie, and H. Ichikawa, 1995: On the branching of the Kuroshio west of Kyushu. Submitted to *J. Geophys. Res.*

Lie, H.-J. and C.-H. Cho, 1994: On the origin of the Tsushima Warm Current. *J. Geophys. Res.*, 99, 25081–25091.

Nitani, H., 1972: Beginning of the Kuroshio, in *Kuroshio*, edited by H. Stommel and K. Yoshida, University of Tokyo Press, Tokyo, pp. 353–369.

Qiu, B., T. Toda, and N. Imasato, 1990: On Kuroshio front fluctuations in the East China Sea using satellite and *in situ* observational data. *J. Geophys. Res.*, 95, 18191–18204.

# Surface Currents in the Canary Basin from Drifter Observations

Jeffrey D. Paduan, Department of Oceanography, Naval Postgraduate School, Monterey, CA 93943, USA; Meng Zhou and Pearn P. Niiler, Scripps Institution of Oceanography, University of California, San Diego, La Jolla, CA 92093-0230, USA

## Introduction

The region of the northeast Atlantic Ocean in the vicinity of the Canary Basin has been intensely sampled using WOCE-quality surface drifters; the sampling began in July 1991. The study region is important because of the ventilation of mid-depth waters that is thought to occur there. If the complex interaction between surface layer processes and thermocline water masses can be understood in this region, it will be possible to predict the circulation of much of the potential vorticity-conserving deep ocean (Luyten *et al.*, 1983). Focus on drifter deployments was placed on this area, first, by the ONR-sponsored SUBDUCTION Experiment. The drifter deployments were conducted within the context of the larger-scale WOCE Surface Velocity Programme (SVP) and intensive deployments culminated with the activities of the French SEMAPHORE Experiment in fall 1993.

## Data

The composite of all surface current trajectories in the northeast Atlantic based on WOCE quality drifters is shown in Fig. 1. The deployment locations are denoted by solid symbols and the trajectories derive from data through March 1995. The data used in this study derive from WOCE-TOGA Lagrangian drifters drogued at 15 m (Sybrandy and Niiler, 1991; Niiler *et al.*, 1987) and compiled by the SVP Data Assembly Center at NOAA/AOML in Miami. Positions and temperatures were uniformly interpolated to 6-hourly time series for each drifter according to

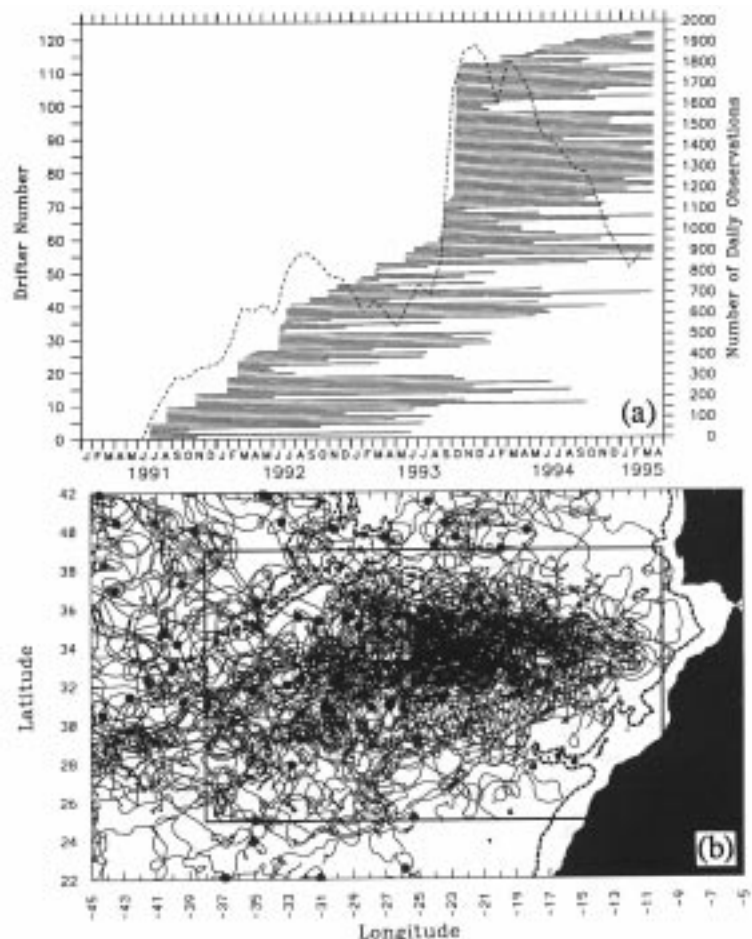


Figure 1. Composite trajectories from WOCE/TOGA Lagrangian drifters drogued at 15 m in the northeast Atlantic Ocean (a) and the time history of drifter observations in the boxed region between 25°N, 38°W and 39°N, 10°W (b) for individual (solid) and combined (dashed) drifters. Solid symbols denote deployment locations and heavy dashed contours show the 2000 m isobath.

the method of Poulain and Hansen (1995) and an additional low-pass filter subsampled daily was applied for this study.

The temporal distribution of drifter sampling in the SUBDUCTION region (Fig. 1) derives from a total of 122 drifters within the region between 25°N, 38°W and 39°N, 10°W (boxed area in Fig. 1). The monthly average number of daily drifter observations in the region illustrates how the observations peaked during the time period October 1993 through October 1994. This is because of the large number drifter deployments made during the field phase of the French SEMAPHORE Experiment in fall 1993.

For this study, drifter observations were analyzed within 1° latitude by 2° longitude subregions. The spatial distribution of data in those sub-regions ranges up to 900 drifter days in the area around 35°N, 23°W with typical values between 300 and 600 drifter days. Statistical properties of drifter observations, such as mean currents, can be biased by uneven data distribution. In this study, we correct for these biases where possible and to exclude geographic regions with low numbers of observations.

## Results

The mean surface currents in the SUBDUCTION region of the Canary Basin are shown in Fig. 2 based on long-term averages in 1° x 2° sub-regions. Mean current vectors from areas with less than 100 drifter days of observations are not shown. In addition, any areas with less than seven different months represented in the average are also eliminated. The current vectors shown in the figure

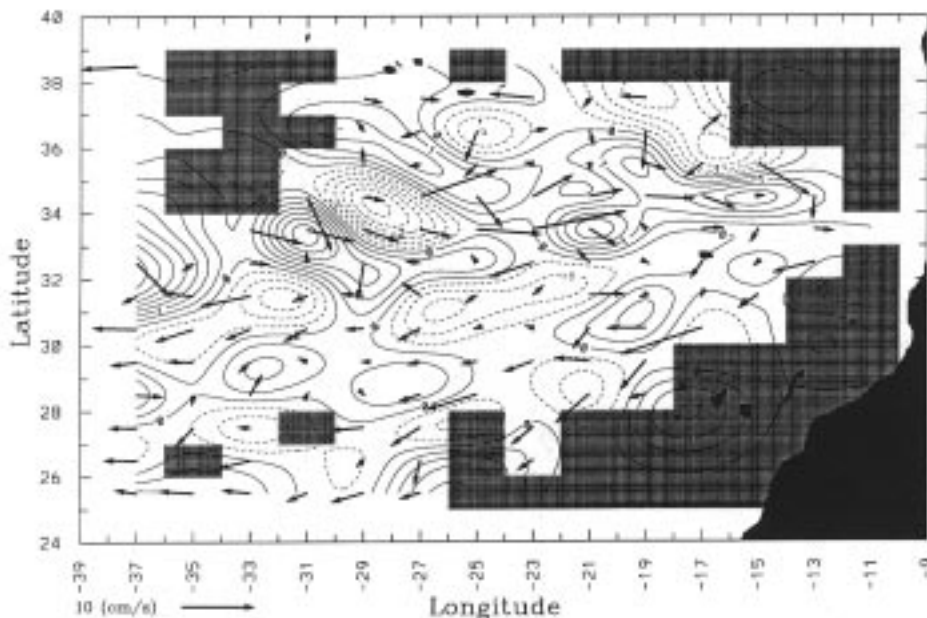


Figure 2. Mean surface currents from drifter observations (vectors) and the associated eddy kinetic energy levels (dashed contours). Mean values are not shown where the total number of daily observations is less than 100, or where the number months represented in the average is less than 7.

have been corrected for array bias due to variations in data concentration in the presence of diffusion as suggested by Davis (1991). The corrected mean velocities are given by

$$\langle \vec{u} \rangle = \frac{\int [\vec{u}(\vec{x})C(\vec{x}) - \vec{K}^\infty(\vec{x}) \cdot \nabla C(\vec{x})] d\vec{x}}{\int C(\vec{x}) d\vec{x}} \quad [1]$$

where  $\vec{K}^\infty(\vec{x})$  is the horizontal drifting particle diffusivity vector whose components were estimated from ensembles of drifter segments passing through each sub-region (Poulain and Niiler, 1989) and the integrals in [1] are computed as summations over each sub-region. The numerical values of the diffusivity components,  $K_{xx}$  and  $K_{yy}$  range between 3000 m<sup>2</sup> s<sup>-1</sup> and 9000 m<sup>2</sup> s<sup>-1</sup>, which is similar to ranges reported previously for the northeast Atlantic (Krauss and Böning, 1987) and slightly larger than values reported for the northeast Pacific (Poulain and Niiler, 1989; Paduan and Niiler, 1993). The largest diffusivities are associated with the strongest flows in the Azores Current. Despite the factor of two change in data concentration over much of the SUBDUCTION area, the maximum correction applied to the mean currents has a magnitude of 6 cm s<sup>-1</sup>, and most of the array biases are less than 2 cm s<sup>-1</sup>.

The current system associated with the subtropical convergence zone in this area (the Azores Current) is clearly visible in the mean currents around 34°N. Mean speeds within the Azores Current system are typically 10–15 cm s<sup>-1</sup>. The Azores Current is observed to bifurcate around 22°W with a major branch of the current continuing eastward and circling the Madeira Plateau (~32.5°N, 17°W). This Azores Current Extension is oriented along the continental slope and flows between the Madeira Plateau and the Canary Islands toward the southwest with speeds similar to those observed in the current at 34°N. The minor branch of the Azores current moves southward near 22°W and joins the extension current near 30°N, 20°W, northwest of the Canary Islands. The current barrier formed by the Madeira Plateau is a robust result of these observations. Large numbers of drifters pass around the area during the nearly four year period of these observations. (The “hole” left by this bifurcation

process is clearly seen in the composite trajectories in Fig. 1). Historical observations of the large scale dynamic height field in the area show the general anticyclonic sweep of the surface currents in the vicinity of the Madeira Plateau (e.g. Käse *et al.*, 1986; Stramma, 1984) but the details visible in these drifter observations have not previously been available.

Eddy kinetic energy levels are shown as contours on the mean current field of Fig. 2. The maximum values of  $\sim 200 \text{ cm}^2 \text{ s}^{-1}$  (rms speeds  $\sim 15 \text{ cm s}^{-1}$ ) are centred along the negative vorticity (southern) side of the Azores Current. These eddy speeds are similar to the mean current speeds, which is unusual for open ocean surface currents. This suggests that eddy activity in the SUBDUCTION region is dominated by features generated locally by undulations and pinching of the current similar to Gulf Stream rings.

Further dynamical insights will be gained by investigating the heat, momentum, and energy balances in the SUBDUCTION region from these long-term drifter observations combined with surface temperature and wind data. Preliminary computations of the mean surface divergence field show convergence (downwelling) north of the Azores Current and divergence (upwelling) to the south. This is consistent with the vertical circulation in one of the hypothesized mechanisms for subduction in which persistent frontal dynamics dominate the areawide ventilation of thermocline waters (Niiler and Reynolds, 1984).

## References

- Käse, R.H., J.F. Price, P.L. Richardson, and W. Zenk, 1986: A quasi-synoptic survey of the thermocline circulation and water mass distribution within the Canary Basin. *J. Geophys. Res.*, 91, 9739–9748.
- Luyten, J.R., J. Pedlosky, and H. Stommel, 1983: The ventilated thermocline. *J. Phys. Oceanogr.*, 13, 292–309.
- Niiler, P.P., R.E. Davis, and H.J. White, 1987: Water-following characteristics of a mixed layer drifter. *Deep-Sea Res.*, 34, 1867–1882.
- Niiler, P.P., and R.W. Reynolds, 1984: The three-dimensional circulation near the eastern north Pacific subtropical front. *J. Phys. Oceanogr.*, 14, 217–230.
- Paduan, J.D., and P.P. Niiler, 1993: Structure of velocity and temperature in the northeast Pacific as measured with Lagrangian drifters in fall 1987. *J. Phys. Oceanogr.*, 23, 585–600.
- Poulain, P.-M., and Hansen, 1995: Quality control and interpolations of WOCE/TOGA drifter data. *J. Atmos. Ocean. Tech.* (submitted).
- Poulain, P.-M., and P.P. Niiler, 1989: Statistical analysis of the surface circulation in the California Current using satellite-tracked drifters. *J. Phys. Oceanogr.*, 19, 1588–1603.
- Stramma, L., 1984: Geostrophic transport in the warm water sphere of the eastern subtropical North Atlantic. *J. Marine Res.*, 42, 537–558.
- Sybrandy, A.L., and P.P. Niiler, 1991: WOCE/TOGA Lagrangian drifter construction manual, SIO Ref. 91/6, WOCE Report 63/91, 58pp.

## The General Circulation of the Subtropical North Atlantic, Near 700 m Depth, Revealed by the TOPOGULF SOFAR Floats

*Michel Ollitrault, Laboratoire de Physique des Océans, IFREMER, 29280 Plouzané, France*

### Summary

Twenty-six subsurface floats drifting at  $700 \pm 100$  dbar, acoustically tracked between July 1983 and June 1989, reveal a very turbulent circulation of the North Atlantic Ocean between  $30^\circ\text{N}$  and  $45^\circ\text{N}$ . The eulerian mean circulation, however, shows continuity between the Gulf Stream and the North Atlantic current, intense recirculations south of the Gulf Stream and the Azores current to the east of the Mid-Atlantic ridge. The ridge axis separates higher eddy kinetic energy values of the western basin from the smaller ones of the eastern basin. Communication over the ridge is rare, but does exist.

### Introduction

The general circulation of intermediate waters in the North Atlantic (near the base of the main thermocline) is

not well known (Schmitz and McCartney, 1993) with information coming mainly from hydrography (Reid, 1994). Near 700 dbar however, 82.7 float-years of data collected with 81 subsurface floats, between September 1976 and March 1989, have provided a statistical description of water mass motions within the Gulf Stream and its recirculations (Owens, 1991). To complement this data base and to study large-scale communications over the Mid-Atlantic Ridge (MAR), 26 floats were launched between July 1983 and September 1985 around 700 dbar on both sides of the MAR axis. These SOFAR floats are part of the TOPOGULF experiment (the TOPOGULF Group, 1986, 1987) and were tracked acoustically by an array of 20 listening stations until June 1989 (Ollitrault, 1994). Statistical results of these 26 floats are presented briefly in this paper (a more detailed version in French may be found

in Ollitrault, 1995).

## Float data

53.0 float-years of data have been collected in the depth range 600 to 800 dbar. Raw positions estimated every 12 h were filtered to suppress periods of less than 3 days, and velocities were obtained through cubic spline fit. All the trajectories are given in Fig. 1. Absolute error on position is 5 km, but is only a few hundred metres on the displacement between 2 positions a few days apart, implying an error smaller than 1 cm s<sup>-1</sup> on “instantaneous” velocities.

The western floats (14 launched in July 1983, within a 75 km diameter circle near 36°N, 40°W) have dispersed all over the western basin, between 30°N and 45°N (except for one that crossed the MAR eastward), while the eastern floats (9 launched in October 1984 and 3 launched in September 1985, within a 50 km diameter circle near 33°N, 33°W) remained in the region between 30°N and the continental slope to the south of the Azores, and between 20°W and the MAR axis (except for one that crossed the MAR westward).

## Turbulent diffusion

To obtain a rough global estimate of turbulent diffusivities and lagrangian time scales, within western and eastern basins, trajectories have been partitioned between those found to the west (33.2 float-years) and those found to the east (19.3 float-years).

Sample probability distribution of instantaneous velocities is quasi-gaussian and quasi-isotropic.

$$\langle u_i'^2 \rangle \approx \langle u_j'^2 \rangle \approx 115 \pm 10(2\sigma) \text{cm}^2 \text{s}^{-2}$$

and

$$\langle u_i' u_j' \rangle \approx 6 \pm 6(2\sigma) \text{cm}^2 \text{s}^{-2}$$

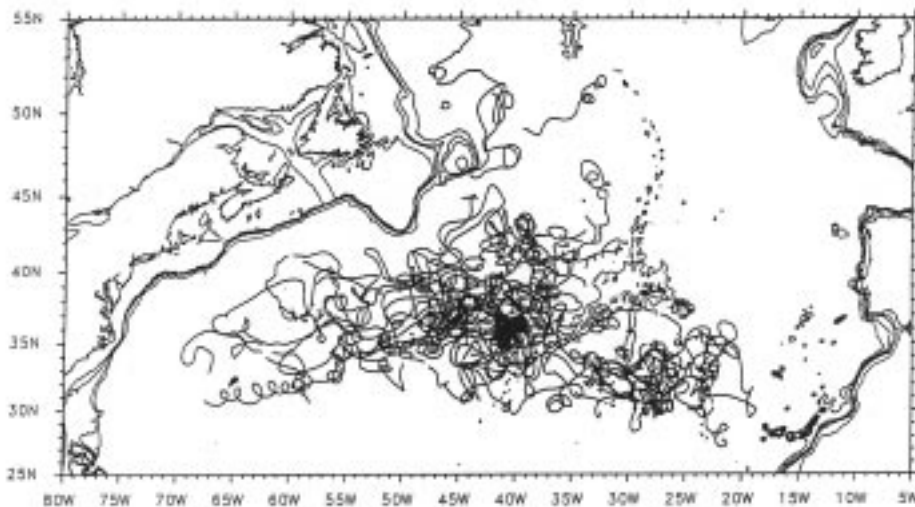


Figure 1. Trajectories of the 26 SOFAR floats from the TOPOGULF experiment (float depths are between 600 and 800 dbar).

for the western basin, while

$$\langle u_1'^2 \rangle \approx \langle u_2'^2 \rangle \approx 28 \pm 4(2\sigma) \text{cm}^2 \text{s}^{-2}$$

and

$$\langle u_1' u_2' \rangle \approx -2 \pm 2.5(2\sigma) \text{cm}^2 \text{s}^{-2}$$

for the eastern basin. Brackets denote stochastic means;

$$u_i = \langle u \rangle + u_i', i = 1, 2$$

are the velocity components.

Covariance functions

$$\langle u_1' u_1'(\tau) \rangle, \langle u_2' u_2'(\tau) \rangle \text{ and } \langle u_1' u_2'(\tau) \rangle,$$

estimated for  $0 \leq \tau \leq 240$  days, with a rms error of a few  $\text{cm}^2 \text{s}^{-2}$ , are not significantly different from 0 for  $\tau > 30$  days. However, meridional functions seem to show a negative lobe near 50–60 days.

Integrating covariance functions, one obtains integral time scales  $T_{ij}$  and one-particle diffusivity  $K_{ij}$ . Under spatial homogeneity and temporal stationarity hypothesis (Taylor, 1921; Batchelor, 1949)  $T_{ij}(t)$  and  $K_{ij}(t)$  should tend to  $T_{ij}^\infty$  and  $K_{ij}^\infty$  for  $t \gg T_{ij}^\infty$ . One observes (Fig. 2) a quasi-isotropic diffusion up to 30 days and a “plateau” between 20 and 30 days ( $K_{11} \approx K_{22} \approx 5 \cdot 10^7 \text{cm}^2 \text{s}^{-1}$  to the west and  $2.2 \cdot 10^7 \text{cm}^2 \text{s}^{-1}$  to the east, for  $20 \leq t \leq 30$  days). Between 60 and 210 days, in the eastern basin, zonal and meridional diffusivities are rather constant near  $2.5 \cdot 10^7 \text{cm}^2 \text{s}^{-1}$  and  $1.5 \cdot 10^7 \text{cm}^2 \text{s}^{-1}$  respectively. Corresponding time scales are of the order of 10 days (zonal) and 6 days (meridional). In Fig. 2, dots give the diffusivities

estimated from  $\frac{1}{2} \frac{d}{dt} \langle X_i'^2 \rangle$ , where  $X_i', i=1,2$  are the particle excursions (eastward and northward) relative to the ensemble mean displacement. The almost coincidence of covariance-based and dispersion-based diffusivities is a confirmation that Taylor hypothesis applies for the eastern basin.

Beyond 30 days, in the western basin, diffusivities exhibit large fluctuations indicating that they are not well determined. The homogeneity assumption is not verified over such a large area as the western basin. However, as in the east, a markedly smaller meridional diffusivity, may reflect the observation that floats disperse rather zonally on the large scale (Fig. 1). Western time scales are probably smaller and diffusivities greater than eastern ones by a factor of two.

## Mean circulation

The eulerian mean circulation (Fig. 3) and Eddy Kinetic Energy (EKE) (Fig. 4) have been obtained for

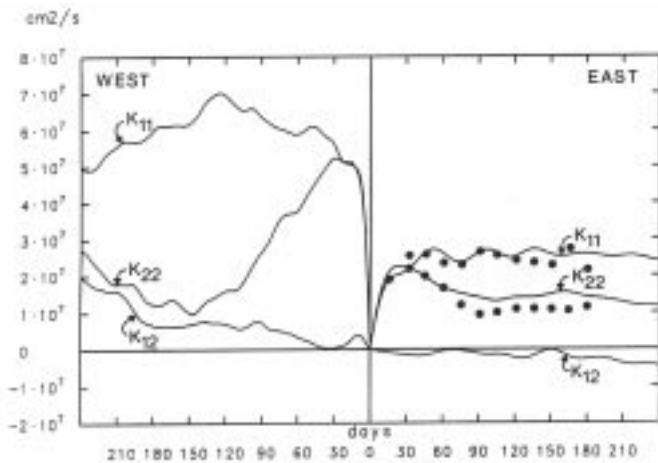


Figure 2. Diffusivity coefficients for the western and eastern basins of the North Atlantic (30°N – 45°N).

2° latitude by 5° longitude bins, by using floats as roving current meters. Size of bins was dictated so that there are enough float-days per bin. Since bins are centred every degree in latitude and longitude, this amounts to a spatial filtering which reveals the large scale features. Only 20 boxes, mainly in the eastern part, contain enough data to estimate mean velocities with a  $\pm 1 \text{ cm s}^{-1}$  95% confidence interval. However, in Fig. 3, mean velocities are given whenever the mean speed is greater than its rms error, which allows a wider coverage.

The continuity between the Gulf Stream and the beginning of the North Atlantic Current (NAC) is indicated by the mean “eulerian” circulation at 700 dbar round the south-east Newfoundland Rise. One float (the trajectory near 50°N, 35°W on Fig. 1) shows a possible path from there to the MAR over a 2.5 year period. In fact, south-east of the Grand Banks, where the Gulf Stream bifurcates between the NAC and a southern branch, float trajectories show a very confused circulation. Near 40° – 42°N and between 35°W and 40°W, 3 floats reveal an eastward current towards the ridge (but two floats also show westward motions there), then a tendency (for one float) to flow northward along the ridge between 42°N and 47°N. Near 42°N, 43°W there is something that resembles the Northern gyre of Mann (1967) and Clarke *et al.* (1980).

The Gulf Stream itself is revealed between 58°W and 50°W but only by the high values of EKE which mark its way (Fig. 4). The synoptic circulation given by floats is

wiped out by the eulerian means (Hogg, 1992). West of 50°W and south of the Stream the Worthington (1976) recirculation appears, which is fed in part by a strong westward current near 37°N, between 38°W and 50°W. The southern branch of the Gulf Stream, associated with a tongue of  $\text{EKE} > 100 \text{ cm}^2 \text{ s}^{-2}$  near 39°N, 35°W divides to the north and south because of the ridge. Floats show a southward flow down to 36°N, along the ridge, then a westward flow. Some crossings of the ridge occur episodically near 35°N, 35°W (there is no mean current on Fig. 3 because of opposite crossings) and more frequently near 33°N, 40°W (there is an eastward mean current). Except for a tongue of  $\text{EKE} > 50 \text{ cm}^2 \text{ s}^{-2}$  penetrating eastward around 34°N, 33°W, and showing the temporal and spatial variability of the Azores current, systematically revealed by floats launched in the eastern basin, the axis of the ridge separates western EKE values higher than  $50 \text{ cm}^2 \text{ s}^{-2}$  from smaller eastern ones. An examination of individual float trajectories indicates a strong influence of the seamounts (along 29°W) on the floats advected by the Azores jet. Another feature of mean eulerian circulation is the southward flow between these seamounts and the Canary Islands.

### Future work

The TOPOGULF lagrangian data will be combined with historical lagrangian data, which will amount to 135.7 float-years, over the 13-year period from late 1976 to mid 1989. It is hoped that this data base will make it possible to resolve the mean eulerian circulation over smaller size bins (*e.g.* of 1° latitude by 2° longitude) and map the spatial variation of horizontal (one-particle) diffusivities. It will also be used as a reference level via an inversion of hydrographic data, to obtain a diagnostic 3D mean circulation over the North Atlantic.

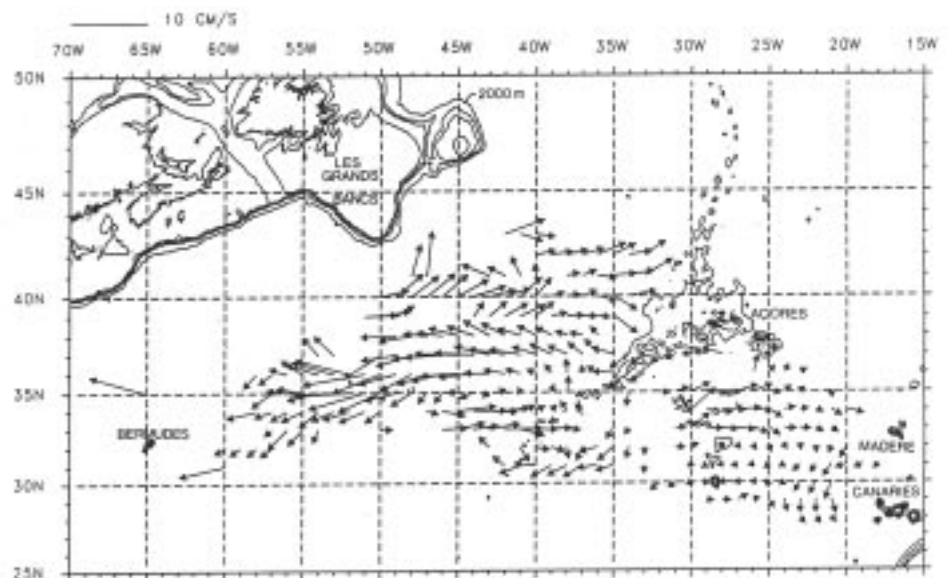


Figure 3. Mean velocity vectors at  $700 \pm 100 \text{ dbar}$  within  $2^\circ \times 5^\circ$  bins, obtained with at least 150 days of data. Excluded are estimates for which the mean speed is smaller than the root mean square standard velocity error.

The TOPOGULF data will be delivered to WOCE float DAC, under the responsibility of Phil Richardson for general use, beginning in 1997. However, the data can be made available for those who would like to collaborate in combining them with other data or models.

## Epilogue

Fig. 5 which gives global displacements over 15 days, shows that most of the general circulation features would have been preserved, had we used WOCE-type floats rising periodically to the surface to be positioned by system ARGOS, like the ALACE (Davis *et al.*, 1992) or MARVOR (Ollitrault *et al.*, 1994), although the latter can also be positioned acoustically at depth.

## References

Batchelor, G.K., 1949: Diffusion in a field of homogeneous turbulence. *Austral. J. Sci. Res.*, A2, 4, pp. 437-450.

Clarke, R.A., H.W. Hill, R.F. Reiniger and B.A. Warren, 1980: Current system south and east of the Grand Banks of Newfoundland. *J. Phys. Oceanogr.*, 10, pp. 25-65.

Davis, R.E., D.C. Webb, L.A. Regier and J. Dufour, 1992: The autonomous lagrangian circulation explorer (ALACE). *J. Atmos. Ocean. Techn.*, 9, pp. 264-285.

Hogg, N., 1992: On the transport of the Gulf Stream between Cape Hatteras and the Grand Banks. *Deep-Sea Res.*, 39, 7/8, pp. 1231-1246.

Mann, C.R., 1967: The termination of the Gulf Stream and the beginning of the North Atlantic current. *Deep Sea Res.*, 14, pp. 337-359.

Ollitrault, M., 1994: The TOPOGULF experiment lagrangian data. *Repères Océan*, 7, IFREMER, 622pp.

Ollitrault, M., 1995: La circulation générale de l'Atlantique Nord subtropical vers 700 m de profondeur révélée par des flotteurs dérivants de subsurface. *C.R. Acad. Sci. Paris*, t. 320, Série IIa.

Ollitrault, M., G. Loaec and C. Dumortier, 1994: MARVOR: a multicycle RAFOS float. *Sea Techn.*, 35, pp. 39-44.

Owens, W.B., 1991: A statistical description of the mean circulation and eddy variability in the northwestern Atlantic

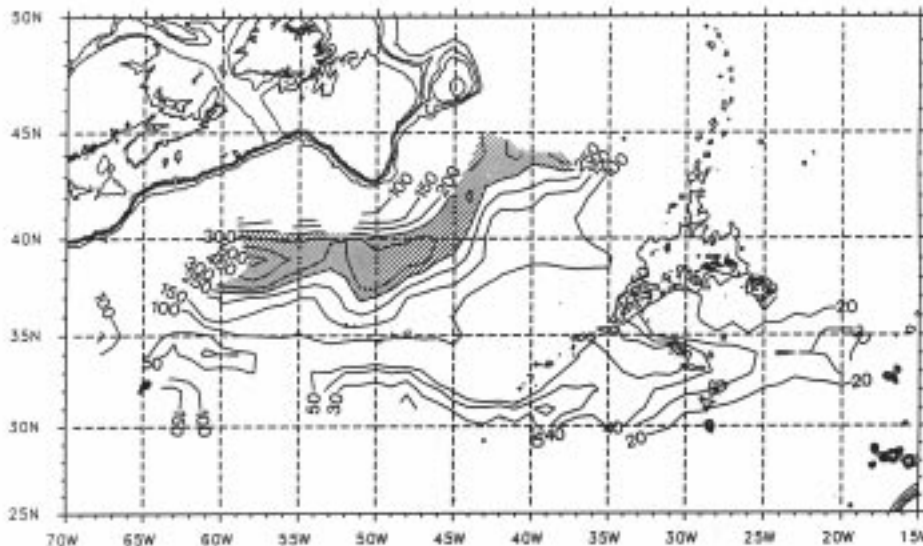


Figure 4. Distribution of eddy kinetic energy ( $\text{cm}^2 \text{s}^{-2}$ ) at  $700 \pm 100$  dbar depth (obtained with  $2^\circ$  lat. by  $5^\circ$  long. bins and at least 50 days of data per bin).

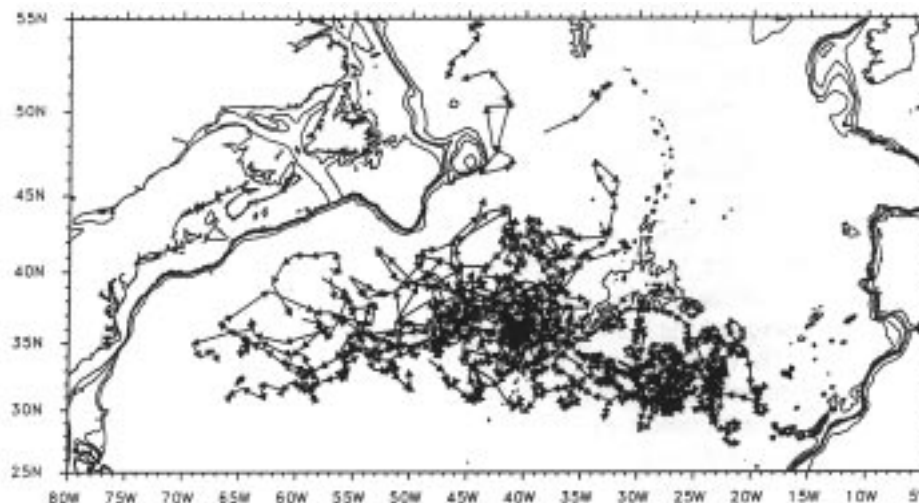


Figure 5. 15-day global displacements for the 26 SOFAR floats from the TOPOGULF experiment, whose depths are between 600 and 800 dbar.

using SOFAR floats. *Prog. Oceanogr.*, 28, pp. 257-303.

Reid, J.L., 1994: On the total geostrophic circulation of the North Atlantic Ocean: Flow patterns, tracers and transports. *Prog. Oceanogr.*, 33, pp. 1-92.

Schmitz, W.J. and M.S. McCartney, 1993: On the North Atlantic circulation. *Reviews of Geophysics*, 31, 1, pp. 29-49.

Taylor, G.I., 1921: Diffusion by continuous movements. *Proc. London Math. Soc.*, 20, pp. 196-212.

The TOPOGULF Group, 1986: TOPOGULF data report. Vol. 1 : CTD,  $\text{O}_2$  and nutrients. *Berichte auf dem IFM Kiel*, 154, 183pp.

The TOPOGULF Group, 1987: Long term current measurements along  $48^\circ\text{N}$  in the central North Atlantic. TOPOGULF data report. Vol. 2 : *Camp. Oceanogr. Franc.*, 5, IFREMER, 198pp.

Worthington, L.V., 1976: On the North Atlantic circulation. *The Johns Hopkins Oceanographic Studies*, 6, 110pp.

# Trajectory Studies in a Model of the Indian Ocean Circulation

Meredith A. Haines, Mark E. Luther, Department of Marine Science, University of South Florida, St. Petersburg, FL 33701-5016, USA; and Rana A. Fine, Rosenstiel School of Marine and Atmospheric Science, University of Miami, Miami, FL 33149-1098, USA

A numerical model of the Indian Ocean circulation is employed to investigate the pathways and timescales of horizontal spreading of water masses. A primary goal of the research is to combine the numerical model with chlorofluorocarbon (CFC) observations to give some insight on the interpretation of distributions of CFCs as they will be measured during the WOCE one-time survey in the Indian Ocean.

CFCs are passive tracers which provide ventilation information on the decadal timescale. In the model, CFCs penetrate the interior Indian Ocean from their source in the atmosphere and also by horizontal advection of ventilated waters. The eddy transport of heat and of chemical tracers by the chaotic eddy field and by the seasonally reversing boundary currents is likely to dominate the mean transport of water mass properties. In this study Lagrangian trajectories of tags introduced at the Indonesian Throughflow (IT) are presented as they are calculated using the archived

velocities of a high horizontal resolution circulation model that is driven by a climatology of observed atmospheric fields.

## Circulation Model and Experiments

The ocean circulation model of Luther and O'Brien (1985) as modified by Jensen (1991) is extended by Ji and Luther to include thermodynamic forcing and active mixed layer physics. The model domain covers the Indian Ocean basin to 30°S (as illustrated in Fig. 1) at a resolution of 1/12 degree in latitude and longitude. There are open boundaries in the south, corresponding to the middle of the South Indian subtropical gyre, and in the east at the IT. The purely dynamical version of the circulation model is currently run in near real-time with observed monthly averaged winds. Resultant GIF images are available on the World Wide Web (URL <http://kelvin.marine.usf.edu>) or

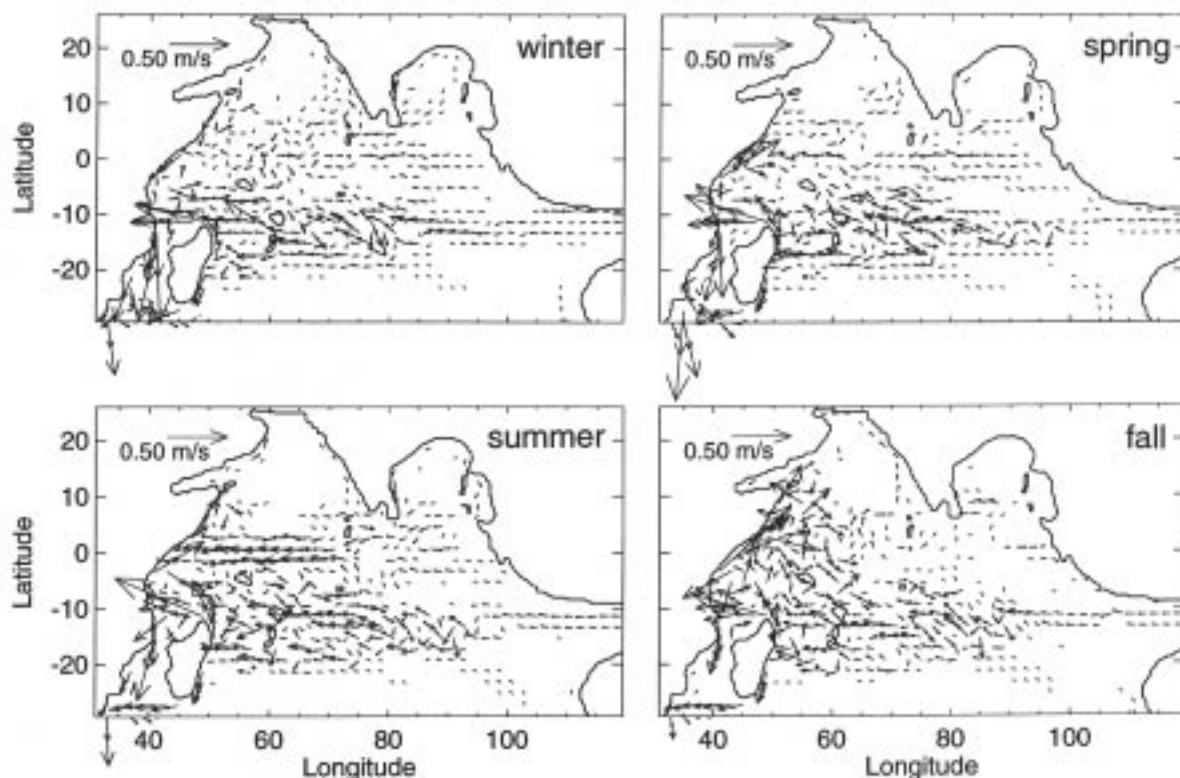


Figure 1. The Indian Ocean model domain spans the region illustrated at a resolution of 1/12 degree. The 200 metre isobath is used as the solid wall boundary between ocean and land or islands. Illustrated are snapshots of velocities in the thermocline layer at the mid-point of each season. For clarity vectors are shown every 2°, those over 1.0 m/s are truncated and those less than 0.03 m/s are suppressed. Near-real time model products are available as GIF images from our WWW site (see text).

by anonymous ftp (kelvin.marine.usf.edu: ~ftp/pub/ndnocr).

The model has 4 layers with a surface mixed-layer embedded in the first layer and the lowest layer at rest (the reduced gravity approximation). The second layer spans the mid-thermocline and the third layer corresponds to the lower thermocline. Initial conditions are chosen according to observations (Wyrki, 1971) with a first layer thickness of 80 m, second layer thickness of 250 m, and a third layer thickness of 500 m. A zero-gradient condition for scalar variables is applied at the open boundaries and a radiation condition is specified for the velocities. Entrainment (and detrainment) occurs between the shallow layers, but there is no exchange of water between the second and third layers. The model settles into a steady annual cycle after about 10 years of spin-up using monthly mean climatological atmospheric fields of Rao *et al.* (1989) as forcing.

Features of the circulation are illustrated in Fig. 1. The South Indian subtropical gyre is bisected by the southern open boundary and has the westward flowing South Equatorial Current (SEC) as its northern limit at 10–15°S. The northern limit of the open boundary in the east is also

at 10°S, where the IT is into the basin at all times, peaking in the summer and winter. The SEC divides into two branches at the coast of Madagascar, a southward and a northward branch. The northward branch flows around the tip of Madagascar and along the African Coast, meeting the seasonally reversing Somali current. During the northeast (northern hemisphere winter) monsoon, these waters flow eastwards along 3°S in the South Equatorial Counter Current (SECC). The eddy activity is highest in the west, particularly during the southwest (summer) monsoon.

The horizontal penetration of water masses is modeled by tagging water parcels at their entry points along the open model boundary in the east and tracking their Lagrangian trajectories as they are advected by archived model velocities in the mid-thermocline (layer 2). The velocities are those generated in the model by monthly mean climatological forcing (in wind stress, solar radiation, air temperature, and specific humidity) and archived as 6-day averages at 1/3 degree resolution. Mixing between the 1st and 2nd layer is necessarily ignored at present as the patterns of horizontal mixing in each layer must first be determined. Later iterations will incorporate vertical mixing. The IT in the model

is 12 Sv and is forced by dynamics internal to the Indian Ocean only, with no contribution from the Pacific. The volume transport is in the mid-range of observations (*e.g.* Gordon, 1986; Toole and Warren, 1993; Feix *et al.*, 1994).

Lagrangian trajectories are calculated using a 4th-order Runge-Kutta scheme with adaptive step-size control. At each time step the linearly interpolated archived velocities are integrated to give the distance each tagged water mass moves with an accuracy requirement set at 5 ppm. The average timestep taken is 30 minutes and the same annual climatological cycle of model velocities was applied repeatedly for 50 years, corresponding to the timescale over which CFCs have been present in the ocean in measureable amounts. Tags are introduced at 1/12 degree separation, and their position recorded every 30 days as they are advected according to this scheme.

## Trajectories and Timescales

Fig. 2 shows the progression of the tags in five year intervals. The first tags cross the basin within 5 years, and the majority do so within 10 years, following fairly direct paths. It is only when tags reach a solid boundary, Madagascar or Africa, that there is significant and rapid north and south scattering of the tags by the fast boundary currents. Tags escape out the southwest corner of the model domain, from where they are not permitted to return. After 10 years less than 50% of the tags remain in the basin and after 20 years, order 20% remain. About 10% of the original tags remain after 50 years of integration.

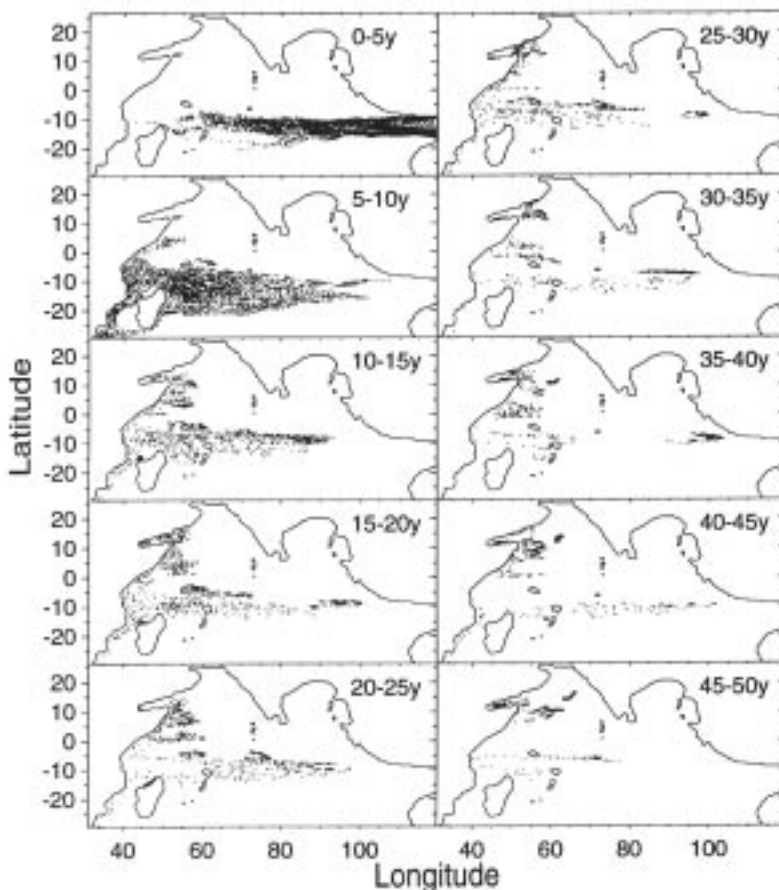


Figure 2. Illustrated is the progression of 93 tags from their entry points along the eastern boundary (initially at 1/12 degree separation) in the thermocline layer of the model. The location of each tag is plotted every 30 days in 5 year intervals; the result of repeatedly applying an annual cycle of velocities beginning in mid-winter. Tags escape the model domain in the southwest corner and are not permitted re-entry.

Sample trajectories are illustrated in Fig. 3 for tags introduced at mid-winter in the annual cycle. Experiments were also run with tags introduced at the mid-point of the other seasons, with the same variety of results. The main route of escape (63%) is southwards in the African Coastal Current, while 18% travel down the east coast of Madagascar and around its southern tip. About 30% of the tags penetrate farther north than 10°S. From there, 10% reach the Arabian Sea after 10–15 years, by way of the Somali Current, and the remainder are swept back eastwards into the interior of the basin by the SECC.

### CFC Application

F-11 measurements collected in mid 1989 in the IT region were kindly supplied to us by C. Andrié (Fieux *et al.*, 1994). The saturations measured at depths corresponding to the second model layer are used as a boundary condition to superimpose CFC concentrations on our model trajectories. It is assumed that tag positions at given times correspond directly to the relative age of water masses at those positions. Also, a constant percent saturation is assumed with an atmosphere whose known F-11 content has been varying nearly exponentially since the late 1930's. The resultant picture (Fig. 4) is of the CFC content in the Indian Ocean from waters of IT source.

### Conclusions

The timescale for IT thermocline waters to traverse the Indian Ocean from east to west has been estimated here to be in the range 5-10 years. About 10% of the tags released in the IT thermocline reach and remain in the Northern Arabian Sea after 10-15 years, while the majority exit the basin in the southwest corner of the domain within 20 years.

The same treatment has been applied to trajectories originating on the southern open boundary, for which F-11 measurements are also available (Fine, 1993), and from both open boundaries in the deep thermocline model layer 3. Tags in the mid-thermocline layer progress generally northwestwards from the southern boundary. The first tags reach the Arabian Sea, via the western boundary currents, after 5 to 10 years. The modeled layer 2 F-11 concentrations compare well at 90 degrees East with a north-south transect of F-11 observations (SAGA II data supplied by R. Gammon). Trajectories of tags released from the marginal seas are also being studied.

In future work vertical mixing will be incorporated, including the direct atmospheric source of CFCs to the surface ocean. We also intend to assess the role of eddy transport by generating trajectories using model velocities produced by both higher and lower time resolution forcing than the current monthly mean climatological forcing. We intend to sample the model results in the same locations as the WHP will sample the real ocean for CFCs, and to provide some context for the level of variability to be expected in these observations.

### References

Fieux, M., C. Andrié, P. Delecluse, A.G. Ilahude, A. Kartavtseff, F. Mantisi, R. Molcard, and J.C. Swallow, 1994: Measurements within the Pacific-Indian Oceans throughflow region. *Deep-Sea Res.*, 41, 1091–1130.

Fine, R.A., 1993: Circulation of Antarctic Intermediate water in the South Indian Ocean. *Deep-Sea Res.*, 40, 2021–2042.

Gordon, A.L., 1986: Inter-ocean exchange of thermocline water. *J. Geophys. Res.*, 91, 5037–5046.

Jensen, T., 1991: Modelling the seasonal undercurrents in the Somali Current system. *J. Geophys. Res.*, 96, 22,151–22,168.

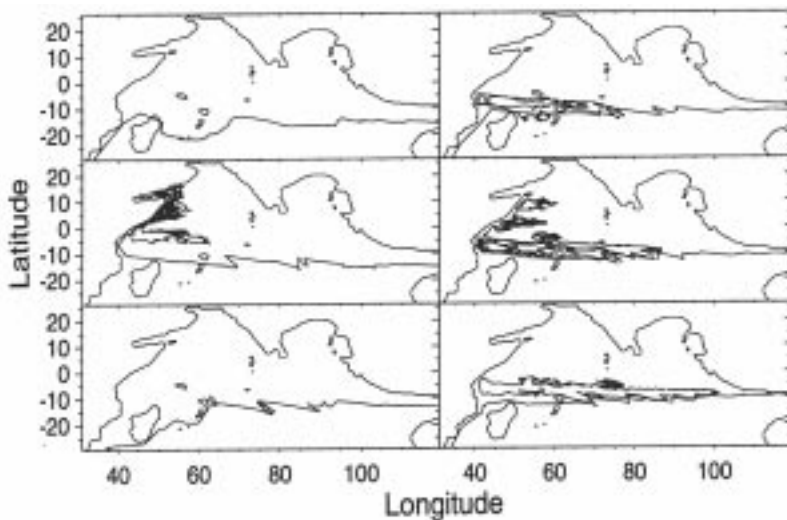


Figure 3. Sample individual trajectories of tags introduced at the Indonesian Throughflow model boundary. The resolution of the trajectories is 30 days.

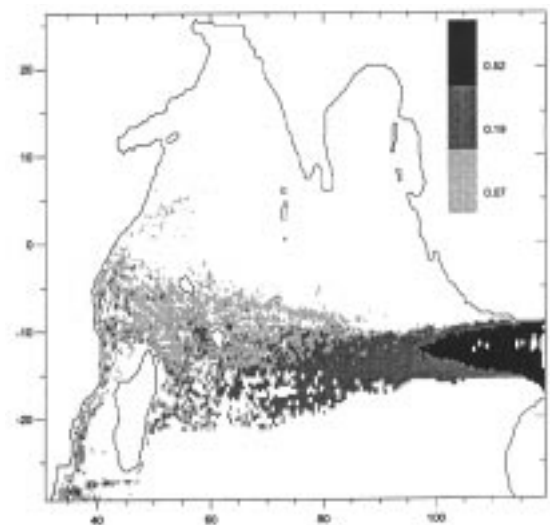


Figure 4. Modelled F-11 concentrations (simulating late 1980's conditions) in the second (mid-thermocline) model layer in waters originating from the IT.

Luther, M.E. and J.J. O'Brien, 1985: A model of the seasonal circulation in the Arabian Sea forced by observed winds. *Prog. Oceanogr.*, 14, 353–385.

Murray, S.P., and D. Arief, 1988: Throughflow into the Indian Ocean through Lombok Strait, January 1985–January 1986. *Nature*, 333, 444–447.

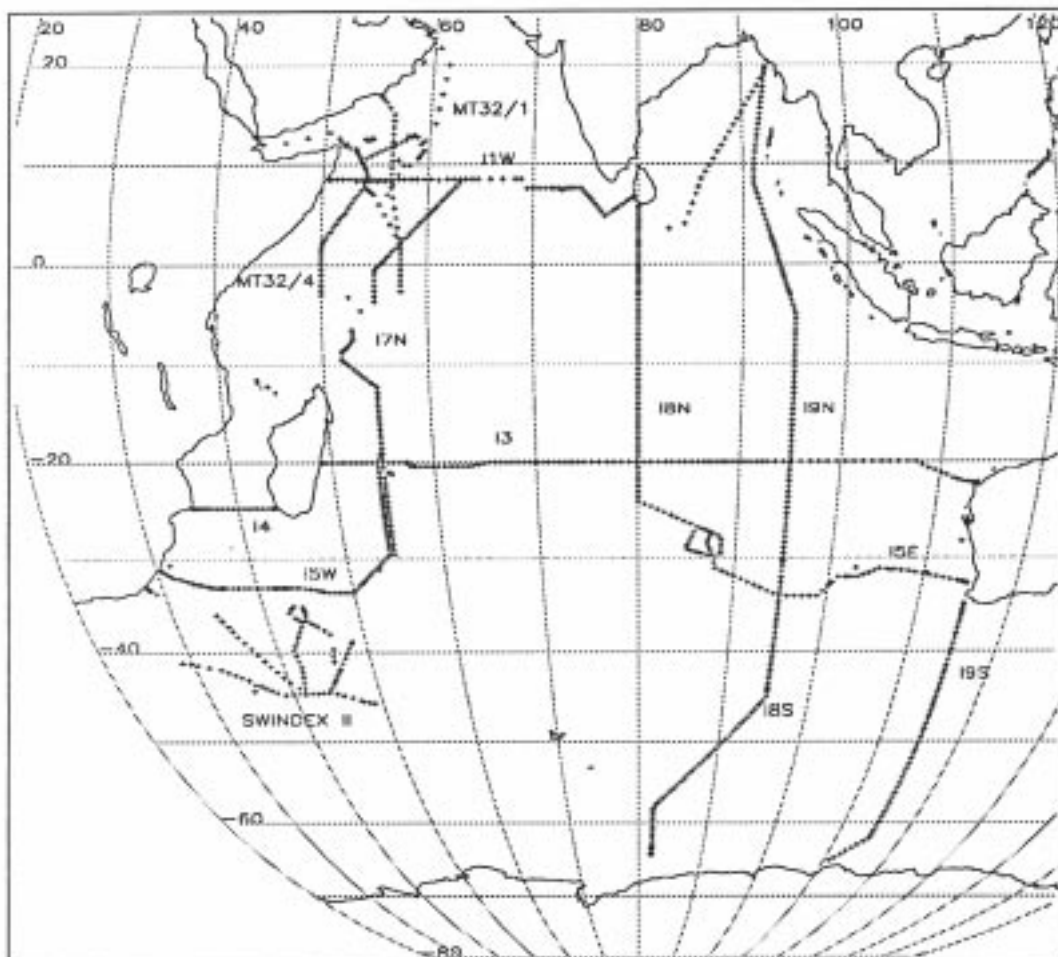
Rao, R.R., R.L. Molinari, and J.F. Festa, 1989: Evolution of the climatological near-surface thermal structure of the tropical Indian Ocean. 1. Description of monthly mean mixed layer

depth, and sea surface temperature, surface current, and surface meteorological fields. *J. Geophys. Res.*, 94, 10801–10815.

Toole, J.M., and B.A. Warren, 1993: A hydrographic section across the subtropical South Indian Ocean. *Deep-Sea Res.*, 40, 1973–2019.

Wyrtki, K., 1971: *Oceanographic Atlas of the International Indian Ocean Expedition*. National Science Foundation, Washington, DC, 531pp.

## WOCE Hydrographic Programme Stations in the Indian Ocean from December 1994 to July 1995



Chief Scientists for the one-time survey stations were McCartney (I8S/I9S), Gordon (I9N), Talley (I8N/I5E), Nowlin (I3), Toole (I4/I5W/I7N). Chief Scientists for the repeat sections and special study areas were Ffield (I5W/I7N), Molinari (I1W), Pollard (ISS1-SWINDEX II), Quadfasel (ISS2-MT32/1,4).

A regularly updated version of this map is available from the WWW using, e.g. NETSCAPE or MOSAIC. The address is: <ftp://nemo.ucsd.edu/woce/plots/> then click on: [woceind\\_label.gif](#).

# Repeat Hydrography Along WHP Lines I5W, I7N, and I1W

Amy Ffield, Bob Molinari, Doug Wilson, and Rik Wanninkhof, NOAA/AOML, 4301 Rickenbacker Causeway, Miami, FL 33149, USA.

During the Indian Ocean intensive 1995 field period, the NOAA ship Malcolm Baldrige is occupying portions of the same WHP lines as the RV Knorr one-time cruises. The Baldrige cruises occur during opposing monsoon seasons in recognition of the large seasonal variability related to the reversing monsoon winds. Baldrige measurements include temperature, salinity, oxygen, velocity, and a suite of chemistry and atmospheric variables. We have surveyed ISS1 (I5W), IR03 (I7N), and IR01 (I1W) at this time, and IR04 (I8N) is scheduled to begin in September (for location see page 22). Fig. 1 illustrates the relative timing between the repeat and one-time surveys; the cruise tracks are illustrated previously in this newsletter. In part, the goals of our cruises are to determine the representativeness of the one-time WHP survey results, assess the large seasonal variability in the basin, and to determine the role of the ocean circulation in redistributing the radiatively important gases. Using preliminary data, a few of the observed features are noted below.

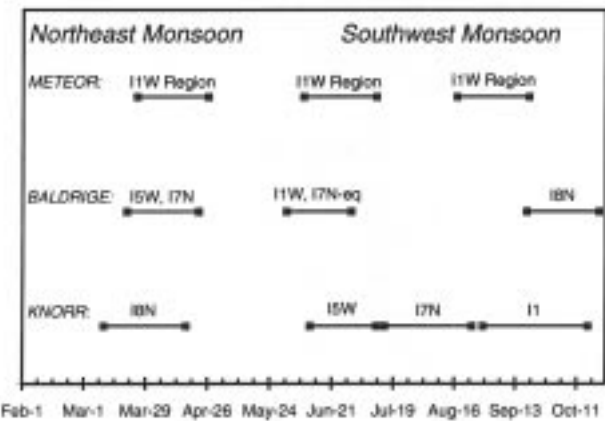


Figure 1. The relative timing between the repeat NOAA ship Malcolm Baldrige and RV Meteor cruises and the one-time RV Knorr cruises.

The Agulhas western boundary current balances the slower northward interior flow of the Indian Ocean and input by the Indonesian throughflow. Using geostrophy, we calculate a  $51 \times 10^6 \text{ m}^3/\text{s}$  (Sv) southward transport in the upper 2000 m between the African coast and west of the Mozambique Ridge (Fig. 2). With direct current measurements from the lowered acoustic doppler profiler (LADCP) we obtain a 62 Sv southward flow in the upper 2000 m. (Several eddies are evident in the Baldrige data.) In comparison, Toole and Warren (1993) measure a 80 Sv southward geostrophic transport along the same transect in December 1987. Two of the Baldrige stations reveal

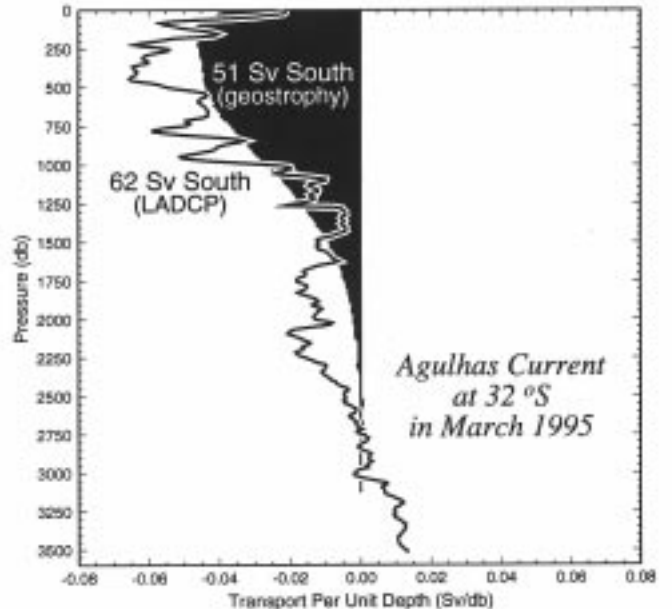


Figure 2. The transport per unit depth of the Agulhas Current between 31.0°S, 30.4°E and 33.0°S, 35.3°E. (Preliminary data)

Tropical Surface Water, Tropical Thermocline Water, and relatively pure Red Sea Water (Fig. 3). These water masses may have flowed south through the Mozambique Channel to become the inner edge of the Agulhas Current; a

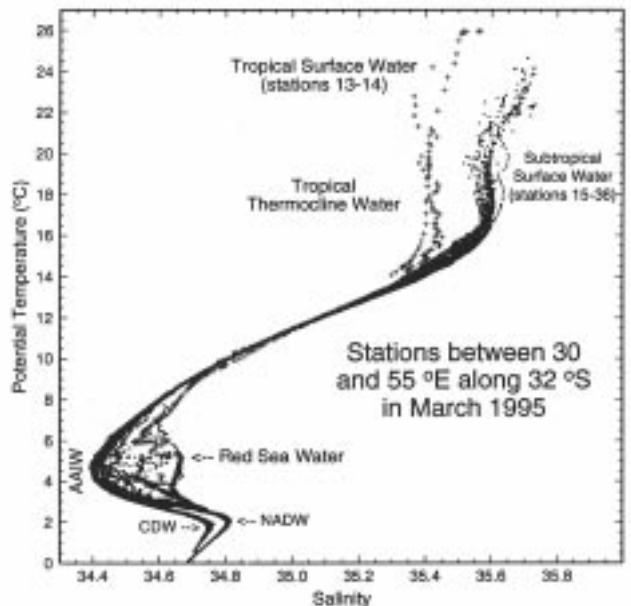


Figure 3. Potential temperature vs salinity curve of the I5W stations. (Preliminary data)

transport on order of 4 Sv is estimated for these stations.

The strong monsoonal forcing in the Indian Ocean produces a rapidly varying circulation in the equatorial and northern regions. Consequently, frequent sampling is necessary to resolve the basic circulation features. The equatorial portion of 17°N along 55°E was surveyed twice by the *Baldrige*, in April and in June. The transition between the monsoon currents is clearly evident in the LADCP direct current measurements (Fig. 4). In April there is the 75 cm/s eastward flowing equatorial undercurrent centred at 80 m, typical of the transition between the monsoons. By June the equatorial undercurrent has disappeared. During both April and June, a moderately strong westward flow is found between 100 and 500 m. This deeper flow intensifies to 54 cm/s westward in June, and the current core rises to 115 m. Leetmaa and Stommel (1980) also observed this westward flow along 55°E, but with only 20 cm/s in June 1975 and 40 cm/s in June 1976.

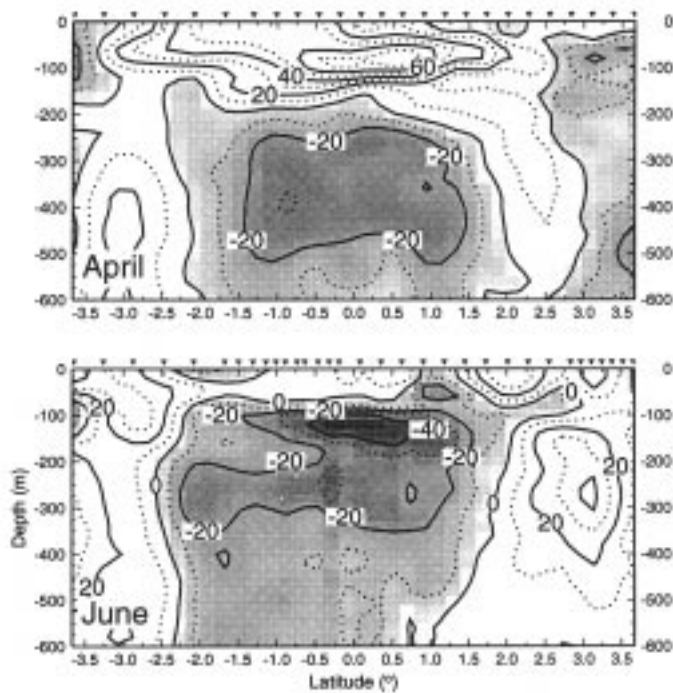


Figure 4. Direct velocity measurements of the equatorial currents along 55°E in April (upper panel) and in June 1995 (lower panel). (Preliminary data)

The Indian Ocean represents a major unknown in closing the global meridional overturning circulation. Time-varying features such as the Great Whirl can complicate resolving this circulation, and the associated fluxes of carbon and nutrients out of the Arabian Sea. During I1W, the early stages of the Whirl are apparent near the coast of Somalia, where winds gusted to over 30 knots after 8 June. Using direct current measurements, the upper 250 m meridional transport within the onshore branch of the Whirl is 9 Sv to the north, and 8 Sv to the south in the offshore branch. While the net transport may be of order

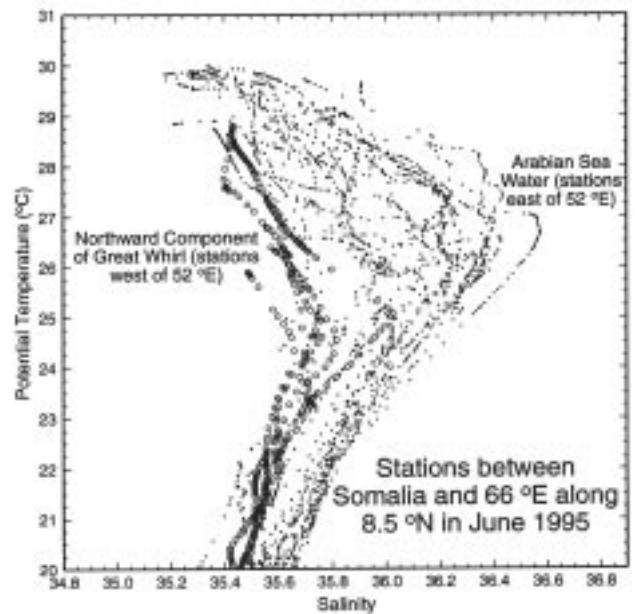


Figure 5. Upper water column potential temperature – salinity curve of the western portion of I1W. (Preliminary data)

0 Sv in the upper 250 m, the onshore branch of the Whirl carries low salinity water northward, and the offshore branch carries high salinity water southward (Fig. 5).

During all the *Baldrige* cruises, surface water carbon and associated parameters are measured quasi-continuously from an intake at the bow. Hourly underway nitrate, PAR, chlorophyll, pH, and pCO<sub>2</sub> measurements, along with 6-hour samples of total dissolved inorganic carbon (DIC) offer the opportunity to determine air-water pCO<sub>2</sub> disequilibria, and factors controlling the source and sink strength of pCO<sub>2</sub> in the Indian ocean. The ocean was a weak sink of about 10 μatm between 30 and 23°S along 17°N during March–April. From this point northward surface water pCO<sub>2</sub> levels gradually increased to supersaturated values of 50 to 60 μatm just south of the equator.

## References

- Leetmaa, A., and H. Stommel, 1980: Equatorial current observations in the western Indian Ocean in 1975 and 1976. *J. Phys. Oceanogr.*, 10, 258–269.
- Toole, J.M., and B.A. Warren, 1993: A hydrographic section across the subtropical South Indian Ocean. *Deep-Sea Res.*, 40, 1973–2019.

You will find more cruise reports from previous WHP cruises as well as cruise plans on the WWW. If you have for example NETSCAPE open: '<http://www.cms.udel.edu>', which brings you to the WOCE Data Information Unit (DIU). Then choose 'Indian Ocean' from the 'WOCE Field Programme Information' menu and click on 'Cruise plans/reports'.

## WHP Sections I8N/I5E in the Central Indian Ocean

Lynne D. Talley, Scripps Institution of Oceanography 0230, La Jolla, CA 92093-0230 USA

One of the central purposes of the WHP Indian Ocean expedition is to determine the fate of the deep water which enters from the south. Toole and Warren (1993) and Fu (1986) both suggest that there is anomalously large upwelling in the Indian Ocean compared with the Pacific and Atlantic; Warren (1995) has hypothesized the net heat gain in the tropics to account for it. The apparent anomaly may well reflect the lack of a sizeable northern source of intermediate or deep water, leaving the Indian Ocean far more asymmetric than the other two, and thus not masking the actual amount of upwelling of southern-source deep water by production of another northern deep water on top of it. It is not known whether monsoonal forcing in the Indian Ocean also plays a role in the deep upwelling.

To study the distribution and circulation of deep waters in the Central Indian Basin, and other items of interest (see the cruise plan for I8N) RV Knorr departed Colombo, Sri Lanka on 10 March 1995, and arrived in Fremantle, Australia on 15 April 1995 to carry out its third WOCE hydrographic leg in the Indian Ocean. Eighteen principal investigators were involved. Basic technical support was provided by Scripps Institution of Oceanography's Oceanographic Data Facility. ADCP

operations were carried out by U. Hawaii (Firing). Water samples were collected for analyses of salt, oxygen and nutrients on all stations and of CFC-11, CFC-12, carbon tetrachloride, helium-3, helium-4, tritium, AMS C14, pCO<sub>2</sub>, total dissolved inorganic carbon, alkalinity, and barium on selected stations. The basic sampling program was accomplished very smoothly. The full cruise report listing all parameters sampled can be obtained from the author. A longer report of the physical oceanography results might be published in a later edition of the WOCE Newsletter.

The cruise track for these sections is shown in the overview figure for this newsletter (page 22). The goals of the sampling were to obtain a section through the centre of the Central Indian Basin to observe the distribution and possible sources of bottom water in the basin, and to repeat the crossing of the northward flow of deep water just to the west of Australia. The northern end of the section lay close to a current meter array set out by Schott *et al.*, (1994). Particular attention was paid to a potential source of deep water for the Central Indian Basin, through a sill in the Ninety-East Ridge, located at about 28°S. The section along 33°S was a nominal repeat of the 1987 section (Toole and Warren, 1993). There was time to deviate from the

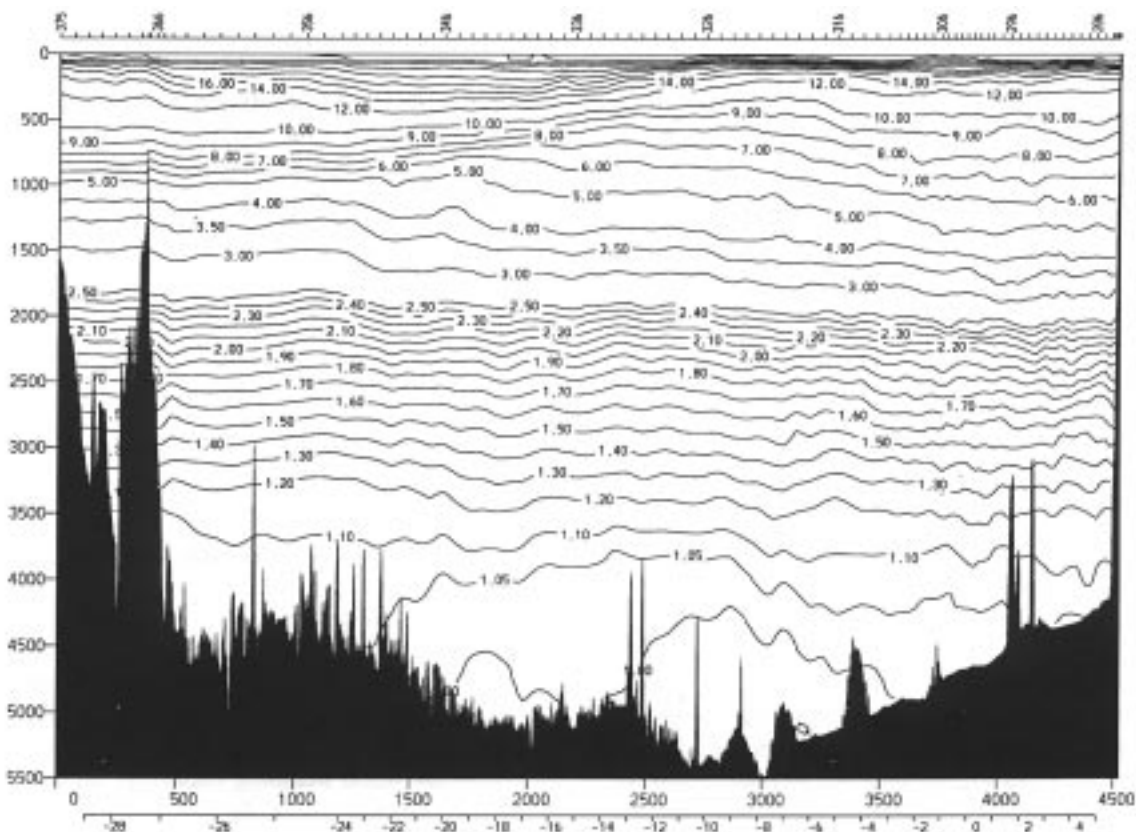


Figure 1. Potential temperature along I8N at 80°E, illustrating the deep cold water in the Central Indian Basin.

32°S section, and sample in the deep water south of Broken Ridge instead of along the top of the ridge. Between Broken Ridge and Australia we chose to move the section slightly north of the original position of I5E in order to resolve whether the deep flow splits around Dirck Hartog Ridge.

Preliminary observations indicate that the 11°S sill in the Ninety-East Ridge is indeed the principal source of bottom water. A preliminary estimate of flow through the 28°S sill indicates that about 2 Sv enter there, and turn southward. Northward flow into the Perth Basin, based on water properties, is almost all between the Broken and Dirck Hartog Ridges. There are differences in properties throughout the water column between the 1987 and 1995 sections between Broken Ridge and Australia; some of the differences are not attributable to the slight difference in location of the sections.

Shallower features of note on I8N south of the equator were the westward flow of water between 10°S and 14°S originating partially in the Indonesian throughflow (surface flow >70 cm/sec based on ADCP and geostrophic transport relative to the bottom of 21 Sv), and a swift equatorial countercurrent south of the equator (surface flow >70 cm/sec based on ADCP and eastward geostrophic transport of approximately 55 Sv). At the equator appeared a well-defined equatorial undercurrent centred at about 80 metres carrying saline Arabian Sea water eastward beneath the westward flow of fresher Bay of Bengal water. The halocline separating them was particularly intense off the equator, especially in the Sri Lankan coastal jet, which carried about 6 Sv of fresh surface water westward and 30 Sv of more saline water eastward beneath. Brunt-Vaisala frequency shows short vertical scales to the ocean bottom within 3 degrees of the equator like in the Pacific and Atlantic Oceans, indicating the presence of the stacked equatorial jets.

The surface layer north of 10°S was very warm (29°C) and essentially well mixed down to the strong halocline (except for a very shallow diurnal thermocline), suggesting that there is a continual forcing. Because the

winds were light during the cruise and because the climatological winds for this period are light, and because the surface layer was very warm and fresh, we hypothesize that evaporation might be an important component in the mixing.

South of 14°S lies the oxygen-rich subtropical gyre with very saline surface or subsurface water (subtropical underwater). An oxygen maximum is apparent along the whole of the I8N and I5E section centred at about  $26.8\sigma_\theta$ ; this is the northward extension of the Subantarctic Mode Water (SAMW) which is ventilated in the southeastern Indian Ocean and enters the subtropical circulation there. All along the I5E section the SAMW is apparent as a potential vorticity minimum, reflecting its origin as a deep convective layer north of the Subantarctic Front. In contrast, the Antarctic Intermediate Water along these sections has no signature in potential vorticity or oxygen, and it does not extend north of the subtropical gyre as a salinity minimum; while AAIW represents the densest thermocline ventilation in the South Pacific and South Atlantic, the SAMW originating in the southeast Indian Ocean dominates ventilation in the Indian Ocean's lower thermocline.

In summary, the cruise went very smoothly and we observed a number of interesting features which will form the basis of further work with this and the other Indian Ocean data sets.

## References

- Fu., L.-L., 1986: Mass, heat and freshwater fluxes in the South Indian Ocean. *J. Phys. Oceanogr.*, 16, 1683–1693.
- Schott, F., J. Reppin, J. Fischer, and D. Quadfasel, 1994: Currents and transports of the monsoon current south of Sri Lanka. *J. Geophys. Res.*, 99, 25127–25141.
- Toole, J.M., and B.A. Warren, 1993: A hydrographic section across the subtropical South Indian Ocean. *Deep-Sea Res.*, 40, 1973–2019.
- Warren, B.A., 1995: Driving the meridional overturning in the Indian Ocean. *Deep-Sea Res.*, 41, 1349–1360.

## WHP Indian Ocean I9N

*Arnold L. Gordon, Lamont-Doherty Earth Observatory of Columbia University, Palisades, NY 10964-8000, USA*

The RV Knorr commenced cruise 145-6, WOCE WHP Indian Ocean section I9N (for location see page 22) on 24 January 1995 from Fremantle, Australia, terminating in Colombo, Sri Lanka on 5 March 1995. Arnold L. Gordon was Chief Scientist; Don Olson was co-Chief Scientist. The average station spacing along this section is 30 nm, with a minimum spacing of 20 nm from 3°S to 3°N and with

a maximum spacing of 36 nm. There was ample time to obtain an additional section along the central axis of the Bay of Bengal at a station spacing of 46 nm. This section allows for some mapping capability within this poorly sampled embayment of the Indian Ocean. Stations 148, 149, 150, 152 repeated stations of the previous Knorr cruise, I8S and I9S. The last station is 277 at 80°E in the

same position as a planned station on the Lynne Talley I8N cruise. A total of 130 stations were obtained on I9N.

The I9N suite of measurements included: CTD with 36 bottle rosette (SIO/ODF), with water samples analyzed for salinity and oxygen for calibration of the CTD sensors; nutrients; CFC (RSMAS); tritium/helium (RSMAS); carbon dioxide parameters (Princeton); C-14; and hull mounted and lowered Acoustic Doppler Current Profiler (University of Hawaii); underway meteorological and sea surface temperature and salinity were logged. ALACE floats and WOCE drifters were deployed along the route.

Fig. 1 shows full depth, computer contoured temperature and salinity along 95°E (nominal), the primary

I9N section, from 31°S to the head of the Bay of Bengal. The meridional WOCE lines pass through many different climate zones (and the Indian Ocean has a lot of 'zones' to offer). As soon as one gets some understanding of the water mass composition within any one regime, the ship passes into the next. I9N transversed four distinct regimes within the thermocline layer, beginning with the subtropical gyre of the southern Indian Ocean, crossing the trans-Indian Indonesian throughflow plume near 11°S; the equatorial regime; and finally the Bay of Bengal. In most cases the intermediate and deep water displayed 'changes in phase' with the upper layer regimes. There is the interplay of the sharply contrasting Antarctic Intermediate Water with Red

Sea outflow, and the build up of silicate in the deep water emanating from the sediment cone of the Bay of Bengal.

The subtropical gyre of the southern Indian Ocean is similar to the other southern hemisphere systems, except for a strong presence of a mid-thermocline 'stad-like' water mass near 10°C (McCartney's subantarctic mode water). Traces of this water can be found north of the Equator. Separating the subtropical thermocline from the equatorial regime is a band of water near 11°S derived from the Indonesian Seas throughflow, the Timor Sea water extends to a depth of 360 m. This band stretches across the Indian Ocean neatly dividing the surface waters of the subtropics from the equatorial zones. Presumably only in the western Indian Ocean is there significant meridional flow. The Bay of Bengal is highly stratified, estuary-like regime, established by massive river outflow from Asia. Some very sharp benthic gradients in oxygen and silicate reveal significant interaction with the sediments.

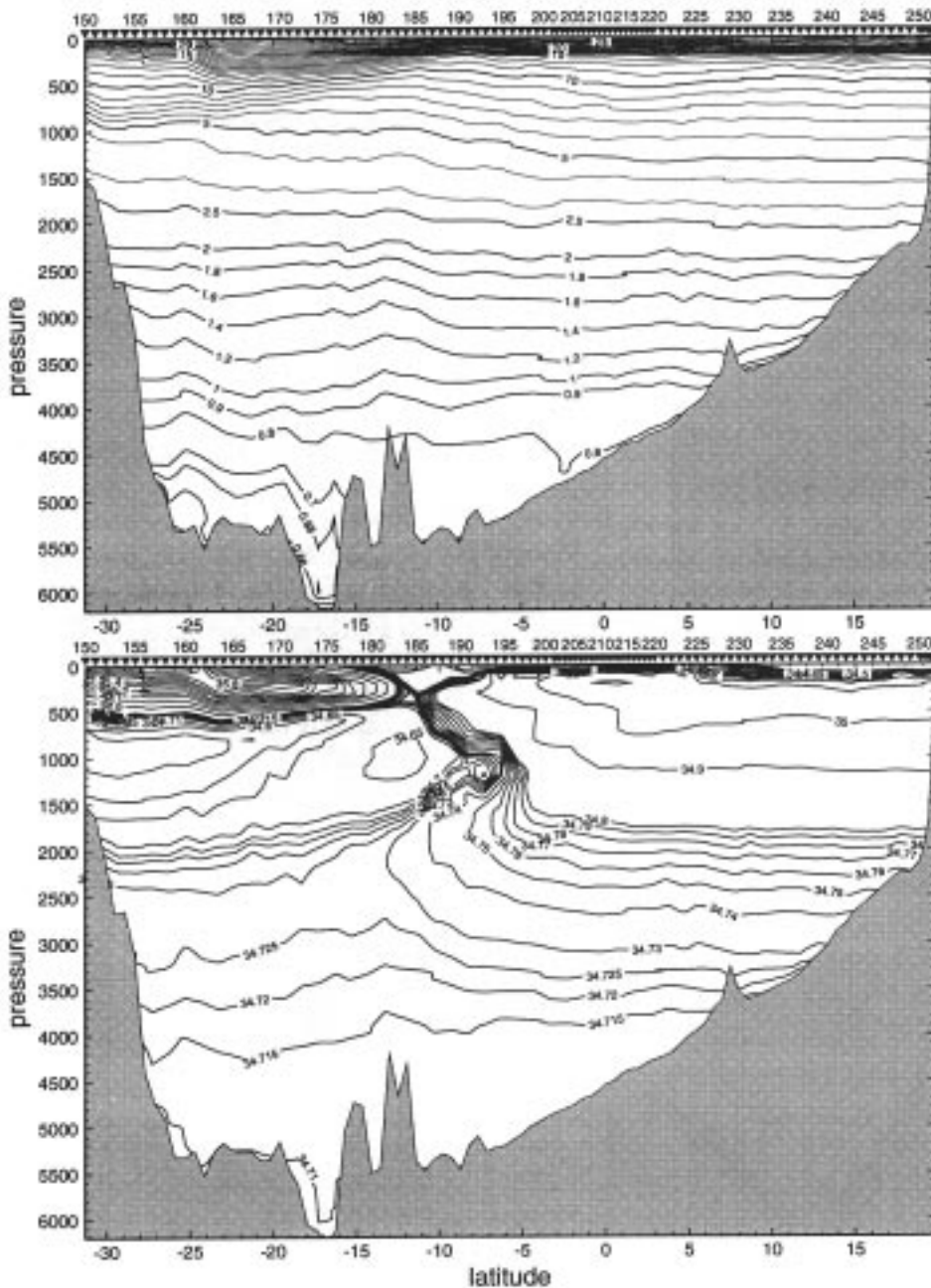


Figure 1. Vertical distribution of potential temperature (upper panel) and salinity (lower panel) along 95°E (nominal) from 31°S to 20°N.

# On the Sensitivity of the Oceanic Meridional Heat Transport Implied by AGCMs to Simulated Cloud Radiative Effects

P. J. Gleckler, Program for Climate Model Diagnosis and Intercomparison, Lawrence Livermore National Laboratory, P.O. Box 808, L-264, Livermore, CA 94551; and D. A. Randall, Department of Atmospheric Science, Colorado State University, Fort Collins, CO 80523, USA

The Atmospheric Model Intercomparison Project (AMIP, Gates 1992) provides a unique opportunity to evaluate atmospheric general circulation model (AGCM) simulations made with realistic boundary forcing. Here we report on findings from AMIP Subproject No. 5, the focus of which is on the simulated surface energy fluxes and the implied partitioning of meridional energy transport between the atmosphere and the ocean. The implied oceanic meridional energy transport varies dramatically from model to model, and we show that these differences are largely due to cloud-radiative effects. This result has important implications for coupled atmosphere-ocean general circulation models.

Uncoupled AGCM simulations are performed by prescribing sea-surface temperatures (SSTs) and sea ice distributions. In a similar way, uncoupled ocean general circulation models (OGCMs) are integrated with prescribed surface wind stresses and relaxation of surface temperatures and salinity toward prescribed climatological values. Simulations produced by these models are quite realistic, but they are strongly constrained by the prescribed boundary conditions. Climate change studies must account for interactions between the ocean and the atmosphere, and so efforts are underway to couple AGCMs and OGCMs. When the boundary constraints are removed, as in the coupled models, the simulated climate typically “drifts” towards an unrealistic state. To prevent this, most coupled models use “flux corrections,” including *ad hoc* adjustments to the surface energy flux distribution (e.g. Manabe and Stouffer, 1993). It is important to understand why such corrections are needed, so that ultimately they may be

minimized or altogether eliminated. The results of this study shed light on this issue.

We must emphasize that when AGCMs are run with specified SSTs and sea ice, as in the AMIP runs, the surface radiation fluxes over the oceans are largely immaterial to the simulated atmospheric circulation. The simulated atmospheric circulation can be very realistic even if the surface radiation fluxes are not realistic. It is only when the AGCM is used as the atmospheric component of a coupled atmosphere-ocean model that the surface radiation fluxes become critical for the simulated climate.

Annual-mean meridional energy transports can be inferred for the atmosphere,  $T_A$ , the ocean,  $T_O$ , and the combined ocean-atmosphere system,  $T_{A+O}$  by:

$$\begin{aligned} & (T_{A+O}, T_A, T_O)(\phi) \\ &= 2\pi a^2 \int_{-\pi/2}^{\phi} (R_{top}, R_{top} - N_{ocn}, N_{ocn}) \cos \phi' d\phi' \end{aligned} \quad (1)$$

where  $\phi$  is the latitude,  $a$  the radius of the earth, and  $R_{top}$  and  $N_{ocn}$  represent the zonal mean top-of-the-atmosphere net radiative flux and ocean surface net energy flux respectively. In Eq. 1 northward transports and downward vertical fluxes are defined as positive.

In our calculations of the implied heat transports, any non-zero annual mean of the globally averaged boundary fluxes (the right hand side of Eq. 1) is removed uniformly over the globe. Tests have demonstrated that the assumed

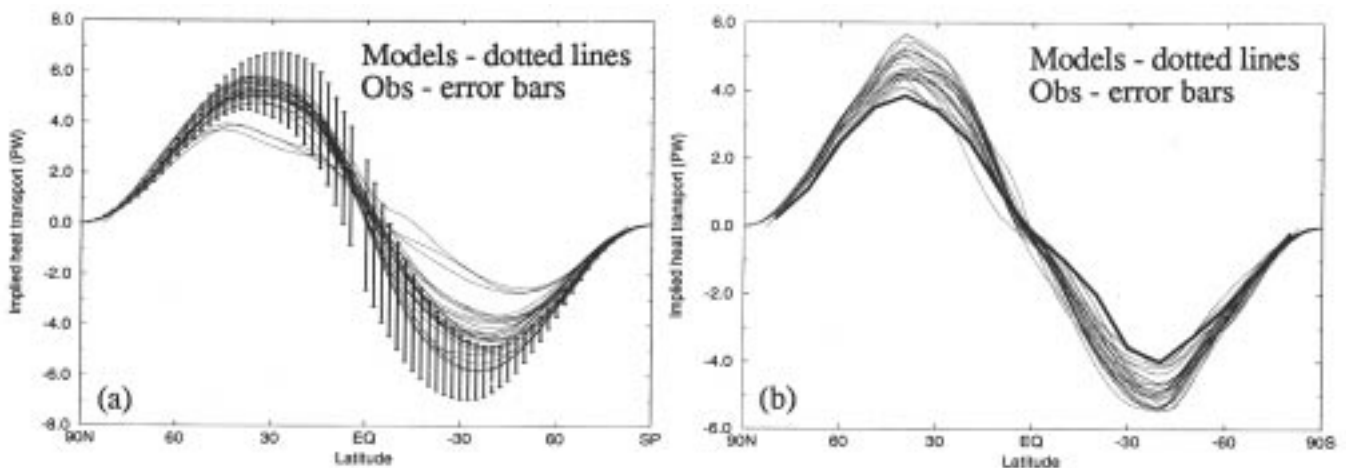


Figure 1. Observed and modeled annual mean heat transport for (a) atmosphere+ocean and (b) atmosphere.

geographical distribution of the globally averaged energy imbalance does not alter the conclusions presented here.

Fig. 1a shows  $T_{A+O}$  as inferred from Eq. 1. The uncertainties (Gleckler, 1993) associated with integrating net top-of-the-atmosphere radiation as observed from ERBE (Barkstrom *et al.*, 1990) are shown as vertical bars, and the models are shown as dotted lines. Note the broad range of simulated transports in the Southern Hemisphere, which are generally much less than observed. Fig. 1b shows observationally derived (Trenberth, 1994) annual mean estimates of  $T_A$  (solid line), and the  $T_A$  implied by the models (dotted lines). In the mid latitudes, the models all yield a greater  $T_A$  than that of the observations even though Trenberth's estimate is larger than previous observationally based estimates (c.f., Carisimo *et al.*, 1983).

Fig. 2 shows the implied  $T_O$  obtained from  $N_{ocn}$  fluxes of the AMIP simulations. For the Northern Hemisphere the AGCMs are in general qualitative agreement with the observations (not shown), although there is a large spread of results among the models. For the Southern Hemisphere the range in the models' implied  $T_O$  is much larger; the implied  $T_O$  is northward (equatorward) in many cases, and southward (poleward) in only a few. There is a strong downward  $N_{ocn}$  at 50°S in many of the models which acts to force northward ocean transport between 50°S and the Equator.

It is important to identify the causes of these large discrepancies between the observed and simulated surface fluxes and implied ocean transports in the Southern Hemisphere. AGCMs are known to disagree considerably in their simulations of the effects of clouds on the Earth's radiation budget (Cess *et al.*, 1990), and hence the effects of simulated cloud-radiation interactions on the implied meridional energy transports are immediately suspect. Unfortunately, we do not have global data on the effects on clouds on the surface energy budget, either as simulated by the models or from observations. We do, however, have observations of the effects of clouds on  $R_{top}$  and thus  $T_{A+O}$ .

The cloud radiative forcing (CRF) is defined (Ramanathan *et al.*, 1990) as the difference between the net radiation at the top of the atmosphere with the given distribution of cloudiness, and  $R_{clr}$ , which we define to be the net radiation at the top of the atmosphere which would have been observed if no clouds were present but all else (e.g. temperature and water vapour) remained the same. Thus  $CRF \equiv R_{top} - R_{clr}$ . Clouds influence atmospheric heating primarily by trapping longwave energy within and beneath the cloud layer, and by reflecting sunlight back to space. There are large differences among the CRF simulated by the various models, and for the most part also between the observed and simulated cloud radiative forcing. In comparison with the ERBE data, many of the models underestimate the magnitude of the CRF at mid-latitudes but overestimate it in the tropics. The underestimate of the CRF in the Southern Hemisphere mid-latitudes is especially

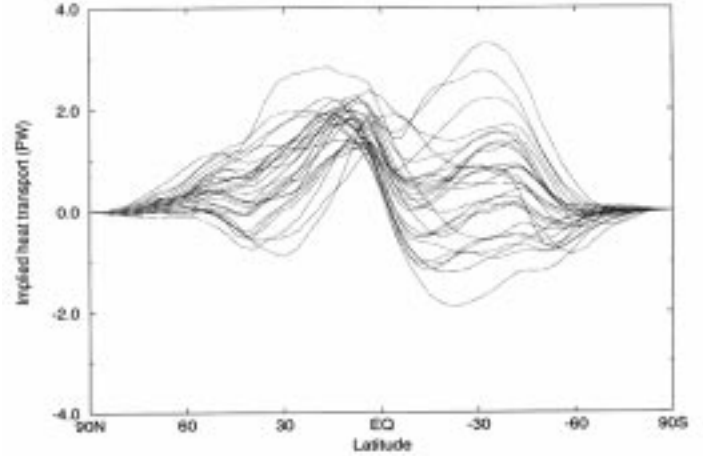


Figure 2. Annual mean global ocean heat transport by AMIP model.

important for the implied  $T_O$  because the Southern Hemisphere oceans are much more extensive than those of Northern Hemisphere. A comparison of the CRF and  $N_{ocn}$  simulated in AMIP suggests that there is a strong correlation between the magnitudes of the CRF and  $N_{ocn}$ , and that differences in  $T_{A+O}$  and  $T_O$  are linked and largely due to cloud effects in the models. The discrepancies between the simulated and observed CRFs suggest that the simulated implied northward  $T_O$ , in the Southern Hemisphere is erroneous and is due to inadequate simulations of the CRF.

We may connect the implied oceanic transport to the cloud radiative forcing using Eq. 1:

$$T_{A+O} = 2\pi a^2 \int_{-\pi/2}^{\phi} \{R_{clr} + (R_{top} - R_{clr})\} \cos \phi d\phi \quad (2)$$

$$= 2\pi a^2 \int_{-\pi/2}^{\phi} \{R_{clr} + CRF\} \cos \phi d\phi \quad (3)$$

$$= T_{clr} + T_{CRF}, \quad (4)$$

where  $T_{clr}$  represents the  $T_{A+O}$  inferred from a “clear-sky” atmosphere, and  $T_{CRF}$  is that due to the radiative effects of clouds. We have computed a “hybrid”  $T_O$  defined by:

$$\tilde{T}_O \equiv T_{A+O}^{ERBE} - T_A \quad (5)$$

$$= (T_{A+O} - T_A) + (T_{A+O}^{ERBE} - T_{A+O}) \quad (6)$$

$$= T_O + \delta T_{clr} + \delta T_{CRF}. \quad (7)$$

Here  $T_{A+O}^{ERBE}$  is the  $T_{A+O}$  inferred from the ERBE data. The  $\delta T_{clr}$  and  $\delta T_{CRF}$  represent the difference between the observed and simulated  $T_{A+O}$  resulting from the effects of clouds and a clear-sky atmosphere respectively. Comparison of the simulated cloudy and clear-sky fluxes has

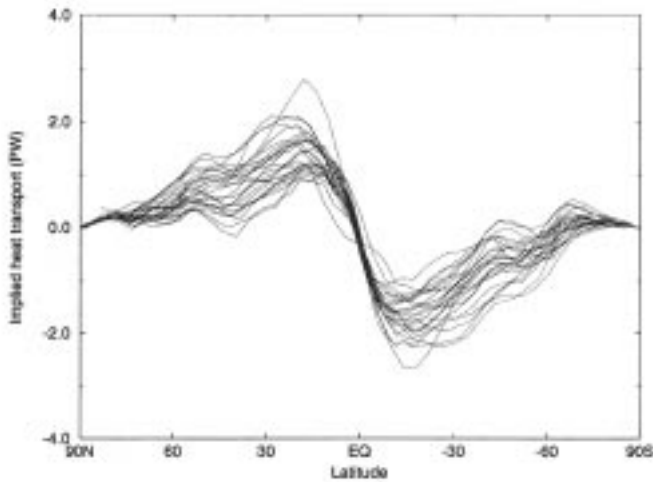


Figure 3. Hybrid ocean heat transport  
 $T_{A+O}(ERBE) - T_A(\text{models})$

demonstrated that we can neglect the clear-sky effects on the implied  $T_O$  and thus:

$$\tilde{T}_O \cong T_O + \delta T_{CRF} \quad (8)$$

The resulting hybrid  $T_O$ , which is based partly on observations and partly on simulations, is shown in Fig. 3. The contrast with Fig. 2 is remarkable; in Fig. 3, all of the hybrid results show poleward  $T_O$ , in both hemispheres as a consequence of the cloud forcing “corrections.” This calculation yields a result which is physically more plausible and the models are now also in much better agreement with one another.

The AGCMs shown here were run with fixed SSTs. The ocean energy transports inferred from these runs are not necessarily the same as the ocean energy transports that would be produced in coupled ocean-atmosphere simulations with the same AGCMs.

Nevertheless, our results show that prescribed realistic SST distributions lead current AGCMs to produce surface energy budgets (Figs. 1-3) that imply ocean energy transports that vary widely from model to model, especially in the Southern Hemisphere. These implied ocean energy transports cannot all be right, although they can all be wrong. Observations of the surface energy budget and/or the ocean circulation are not adequate to say which of the AGCM-implied ocean energy transports, if any, is correct. It is difficult to believe however, that the ocean energy transports could be equatorward at all latitudes in the Southern Hemisphere.

This summary presents quantitative evidence that the model-to-model variations in the implied ocean energy transports are largely due to model-to-model differences in the simulated cloud radiative forcing, which is a comparatively well observed quantity except at high latitudes. Our results thus indicate that as future AGCMs

produce more realistic cloud radiative forcing, the simulated surface energy budget should improve as should coupled model simulations without flux corrections.

The results presented here are an update to Gleckler *et al.* (1995a). Further works resulting from AMIP Diagnostic Subproject No. 5 are in progress, including a more comprehensive analysis and discussion of the implied heat transports (Randall *et al.*, 1995) and an evaluation of the seasonal cycle of the simulated surface heat fluxes (Gleckler *et al.*, 1995b).

## Acknowledgement

This work was performed under the auspices of the Department of Energy Environmental Sciences Division at the Lawrence Livermore National Laboratory under contract W-7405-ENG-48.

## References

- Barkstrom, B., H. Harrison, and R. Lee, 1990: The earth radiation budget experiment, EOS, 71, No. 9, 297.
- Carissimo, B.C., A.H. Oort, T.H. Vonder Haar, 1985: Estimating the meridional energy transports in the atmosphere and ocean. J. Phys. Oceanogr., 16, 82 (1985).
- Cess, R.D. et al., 1990: Intercomparison and interpretation of climate feedback processes in 19 atmospheric general circulation models. J. Geophys. Res., 95, 16,601.
- Gates, W.L., 1992: The Atmospheric Model Intercomparison Project. Bull. Amer. Met. Soc. 73, 1962–1972.
- Gleckler, P.J., 1993: The partitioning of meridional energy transport between the atmosphere and the ocean, Ph.D. dissertation, University of California at Davis, 183pp.
- Gleckler, P.J., D.A. Randall, G. Boer, R. Colman, M. Dix, V. Galin, M. Helfand, J. Kiehl, A. Kitoh, W. Lau, X.-Z. Liang, V. Lykossov, B. McAvaney, K. Miyakoda, S. Planton, 1995a: Cloud-radiative effects on implied oceanic energy transports as simulated by atmospheric general circulation models. Geophys. Res. Lett., 22, 791–794.
- Gleckler, P.J., D.A. Randall, *et al.*, 1995b: On the evaluation of the seasonal cycle of ocean surface heat fluxes simulated by AGCMs. In preparation.
- Manabe, S., and R.J. Stouffer, 1993: Century-scale effects of increased atmospheric CO<sub>2</sub> on the ocean atmosphere system. Nature, 364, 216.
- Phillips, T.J., 1994: A summary documentation of the AMIP models. PCMDI Report No. 18, Lawrence Livermore National Laboratory, P.O. Box 808, L-264, CA 94551.
- Ramanathan, V., *et al.*, 1989: Cloud-radiative forcing and climate: results from the Earth radiation budget experiment. Science, 243, 57.
- Randall, D.A., P.J. Gleckler, *et al.*, 1996: The implied partitioning of meridional heat transport between the atmosphere and ocean as simulated by AGCMs. In preparation.
- Trenberth, K., and A. Solomon, 1994: The global heat balance: heat transports in the atmosphere and ocean. Clim. Dyn., 10, 107–134.

# WHP Repeated Hydrography Section PR14, Offshore Southern Chile

Ricardo Rojas, Nelson Silva, Wanda Garcia and Yenny Guerrero, Servicio Hidrográfico y Oceanográfico de la Armada (SHOA), Casilla 324, Valparaiso, Chile

Between latitudes 35° – 48°S in the southeast Pacific, the Antarctic Circumpolar Current (ACC), impinges the South American continent. In this area the ACC splits in two major branches, one flows northward as the Humboldt

(or Peru) Current (HC) and the other flows southward closer to the Chilean coast as the Cape Horn Current (CHC). The CHC carries a mixture of subantarctic water with surface waters from the adjacent coastal zone.

The ACC bifurcation off the Chilean coast is a poorly studied feature on a synoptic sampling scheme. It can be seen in global historical data analysis of temperature and dynamic topography surfaces (Sverdrup *et al.*, 1942; Wyrki, 1975; Reid, 1961). Silva and Neshyba (1977), made a more focused study of the ACC bifurcation, also based on historical data. They proposed that this split takes place around 43° – 44°S. Neshyba and Fonseca (1980), performed a XBT section across the ACC at about 92°W, and proposed a counterflow to explain the ubiquitous tongue of low salinity surface water extending westward off southern Chile.

The synoptic study of the dynamics and variability of the ACC bifurcation is a major goal to be carried out during the WOCE programme.

Five cruises have been performed in the area. The first two aboard AGS *Yelcho* (October 14–November 07 1991, and August 17–22 1992). The last three cruises aboard AGOR 60, *Vidal Gormaz* (October 07–16 1993, October 04–25 1994 and May 16–June 23 1995). These vessels belong to the Chilean Navy and during each cruise, scientific and technical personnel from the Department of Oceanography of SHOA operated the instruments. In all the cruises, a SeaBird CTD, model Seacat SBE19 has been used. The accuracy of the instrument is 0.01°C and 0.001 for conductivity. The instrument has been recently (April 1995) calibrated at the SeaBird Laboratory in Bellevue, WA, USA.

The track for PR14 is composed of two east-west oriented sections (at 38°S and 48°S), and one north-south

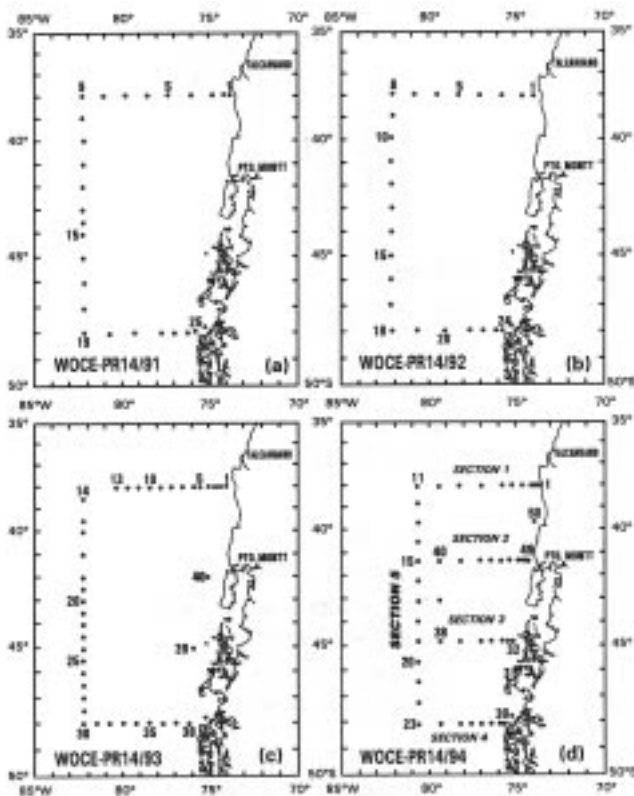


Figure 1. Positions of the CTD stations performed aboard AGS *Yelcho* during (a) 1991 and (b) 1992 and aboard AGOR 60 *Vidal Gormaz* during (c) 1993 and (d) 1994. Cruise WHP repeated section PR14.

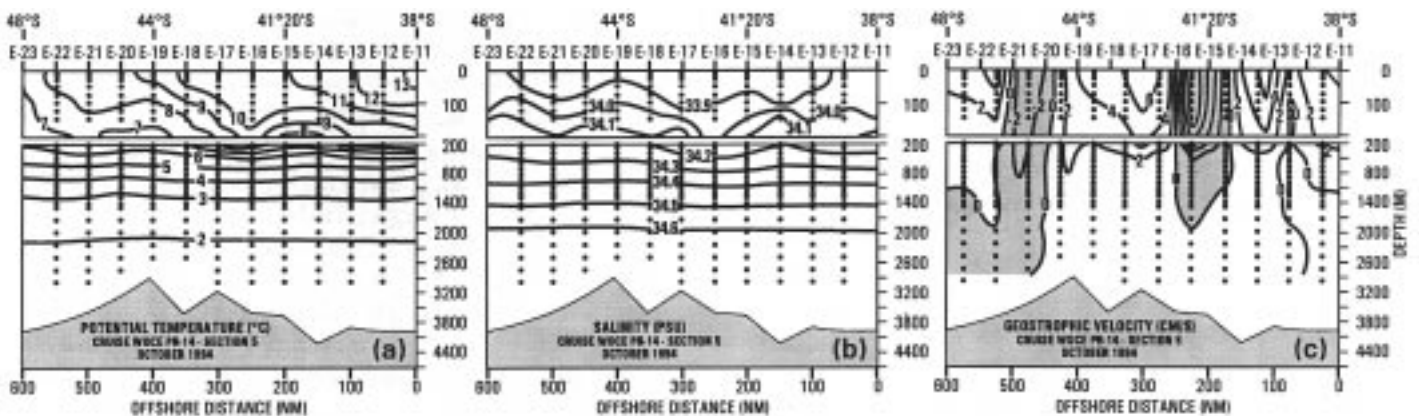


Figure 2. Sections of (a) potential temperature, (b) salinity and (c) geostrophic velocity relative to 3000 dbar level of stations pairs on section 5 cruise WHP repeated section PR14 (October 1994). Shaded zones in Fig. 2(c) mean east-west flow.

section on 82°W. Fig. 1 (a,b,c) shows the tracks occupied by the first three cruises (1991 to 1993). During 1991–1992 the cruises had about the same number of stations and sampling depth (1000 m). In 1993 the sample density increased (40 stations to 1500 m).

In 1994 additional tracks were added to the basic C-shape (Fig. 1d) and also the sampling reached close to 3000 m. This was to help with the plotting horizontal sections, overcome the huge distance between the northernmost (section 1) and the southernmost section (section 4). With this new sampling strategy, the main goals for these cruises, *i.e.* monitor the thermohaline structure and study the dynamics and variability of the ACC bifurcation, are more easily accomplished. The same track was used again during 1995.

While a more comprehensive paper is being prepared, we will show now some descriptive results obtained during the PR14-1994 cruise. Fig. 2 (a), (b) shows the distribution of temperature and salinity for section 5 (meridional oceanic section). Meridionally the horizontal temperature gradient is about 0.5°C/100 km while in the upper 100 m the water column is relatively well mixed. The salinity shows almost no meridional horizontal gradient. However it does show homogeneous conditions in the upper 100 m as in temperature. Below 200 m both temperature and salinity show a vertical stratification and homogeneous conditions on the horizontal.

Fig. 3 shows the T-S curves along section 5. At least

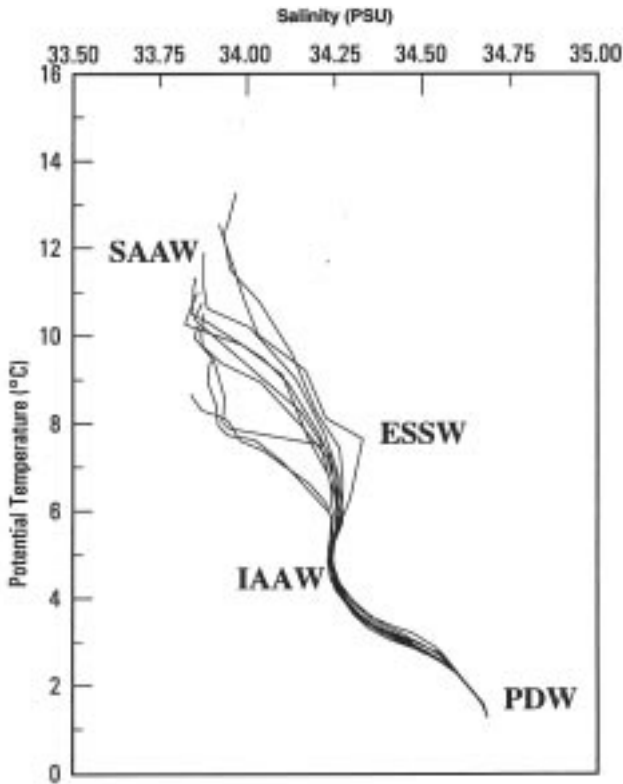


Figure 3. T-S diagram for all CTD casts in section 5. Cruise WHP repeated section PR14 (October 1994).

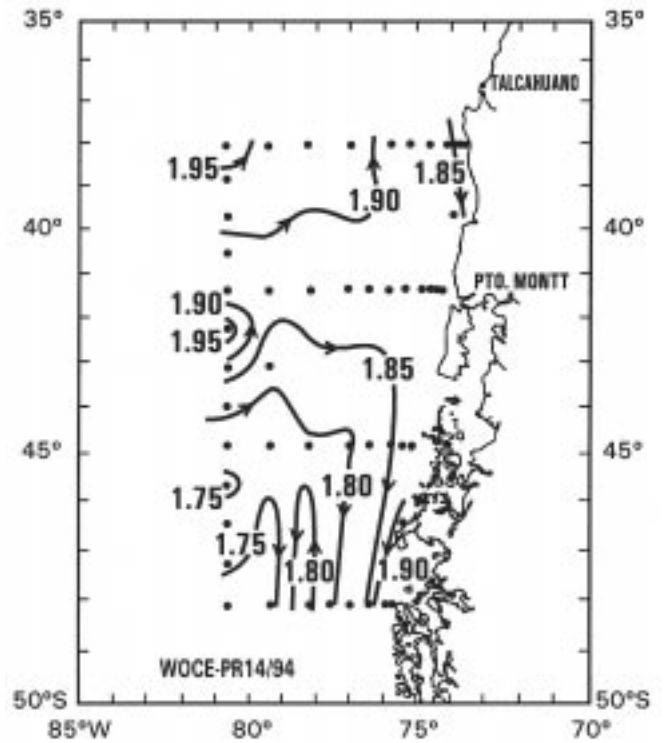


Figure 4. 0/2000 dbar dynamic topography of the area where the ACC impinges the southern part of Chile. Cruise WHP repeated section PR14 (October 1994).

four water masses can be identified: the Subantarctic Water (SAAW), Equatorial Subsurface Water (ESSW), Antarctic Intermediate Water (AAIW) and Pacific Deep Water (PDW). The ESSW is a remnant in the zone from the subsurface equatorial water transported southward by the Peru–Chile Undercurrent (Silva and Konow, 1975; Silva and Neshyba, 1979).

The hydrographic data were used to calculate the geostrophic velocity relative to 3000 dbar. The general flow is eastward with maximum speeds of 6 cm/s transporting about 17 Sverdrups. Two westward flows are evident within the general eastward flow of the ACC transporting about 9 Sverdrups. As mentioned in a previous paragraph, one tends to relate the northernmost flow to the counterflow proposed previously by Neshyba and Fonseca (1980). This can be inferred from the magnitudes of the velocities as well as the location of this flow (see Fig. 2, Neshyba and Fonseca, 1980).

Nevertheless, if the surface dynamic topography chart, relative to 2000 db, is taken into account (Fig. 4) one can find out that this flow appears to be more related to an eddy-like structure than a counterflow. In this figure the bifurcation of the ACC is located around 41° – 42°S, that is, further north than previously reported by Silva and Neshyba (1977). The difference may be the result that the Silva and Neshyba estimated the dynamic topography relative to 500 dbar using composite historical oceanographic data, while in PR14 cruise the data is quasisyntopic and relative to 2000 dbar.

## Acknowledgements

We would like to thank all the participants involved in the PR14 cruises, both officers and crew from AGS Yelcho and AGOR Vidal Gormaz and the scientific and technical personnel of the Department of Oceanography of SHOA.

## References

- Neshyba, S., and T. Fonseca, 1980: Evidence for counterflow to the West Wind Drift Off South America. *J. Geophys. Res.*, Vol. 85 C9, 4888–4892
- Silva, N., and D. Konow, 1975: Contribucion al conocimiento de las masas de agua en el Pacifico Sudoriental. Expedicion KRILL. Crucero 3-4. Julio-Agosto 1974. *Revista Comision Permanente Pacifico Sur*, 3:63–75.
- Silva, N., and S. Neshyba, 1977: Corrientes superficiales a lo largo de la costa austral de Chile, *Cienc. Tec. Mar*, 3.
- Silva, N., and S. Neshyba, 1979: On the southernmost extension of the Peru–Chile Undercurrent. *Deep-Sea Res.*, 26A: 1387–1393.
- Sverdrup, H., M. Johnson and R. Flemming, 1942: *The Oceans, their physics, chemistry and general biology*. Prentice Hall, New York, 1087 pp.
- Reid, J., 1961: On the geostrophic flow at the surface of the Pacific Ocean with respect to the 1000 decibar surface. *Tellus*, 13 (4), pp 489–502.
- Wyrtki, K., 1975: Fluctuations of the dynamics topography in the Pacific Ocean. *J. Phys. Oceanogr.*, 5, 450–459.

## WOCE Sea Level Data – Plentiful and Available NOW!

Gary Mitchum and Bernard J. Kilonsky, *Department of Oceanography and JIMAR, 1000 Pope Road, MSB 307, University of Hawaii at Manoa, Honolulu, HI 96822, USA*

### Historical perspective

*In situ* sea level measurements are capable of providing time series at fixed locations over periods of many decades. These observations are used for the analysis and interpretation of the ocean's dynamics, for monitoring the relative variations of land and sea, tectonic changes, the adjustment of water and ice volumes, and short-term climatic variations, and are proving very useful as ground truth for satellite altimetry heights. Under the direction of Klaus Wyrtki, the University of Hawaii Sea Level Center (UHSLC) began installing tide gauges in the tropical Pacific Ocean in the early 1970s. The maturation of this activity in the intervening years resulted in the Indo-Pacific Sea level network (IPSLN), which is presently the largest open ocean sea level network in the world that is operated by a single group. In 1985 the data collection activity represented by the IPSLN was complemented with the establishment at the UHSLC of the Tropical Ocean-Global Atmosphere (TOGA) Sea Level Center (TSLC). The TSLC does not operate any tide gauges, but collects hourly sea level data from many data originators, of which the IPSLN is a primary one. The TSLC data set is distributed directly from the UHSLC and is also provided to the World Data Center system and the U.S. National Oceanographic Data Center (NODC) for additional distribution. The UHSLC also operates a Specialized Oceanographic Center (SOC) for the Integrated Global Ocean Services System (IGOSS). The IGOS Sea Level Project in the Pacific (ISLP-Pac) is an early, and very successful, example of operational oceanography. Since June 1984 monthly maps of the Pacific sea level topography have been produced without fail. The ISLP-Pac analysis

includes monthly mean sea level data from 93 participating stations in 33 countries throughout the Pacific basin. When WOCE recognized the need for sea level data, the WOCE “Fast Delivery” Sea Level Center (WSLC) was established at the UHSLC in order to take advantage of the experience with sea level data that already existed there.

In the WOCE Implementation Plan, *in situ* sea level data were identified as being useful for two major purposes: (1) to compare the observations made during the WOCE period to longer time series in order to evaluate the representativeness of the WOCE time frame, and (2) for joint use with satellite altimeters, such as TOPEX/POSEIDON, which are expected to greatly increase our understanding of the circulation of the world's oceans. The WOCE plan called for a heavy reliance on sea surface height measurements derived from satellite-borne altimeters, but it is important to remember that this technology is still evolving. The altimeter data need to be carefully checked against the *in situ* data, and results obtained with the altimetry data should be checked where possible against the more traditional, and well-understood, sea level data from tide gauges. It was recognized, however, that this second requirement meant that sea level data would have to be collected, processed, and made available to scientists much more quickly than has been done in the past. The altimetry data are available within a month or so of collection; if the sea level data are to be of maximum utility, then they should be available on a comparable time scale. Again, the experience at the UHSLC with operational delivery of sea level data made it a logical place to establish such an effort.

## Data collection, processing, and distribution

The creation of the WSLC was a major new initiative for the UHSLC. Before the establishment of the WSLC, sea level data were collected, processed, and distributed to users within one to two years after the calendar year in which the data were acquired. The WSLC, on the other hand, needs to process data from a globally-distributed set of stations and make it available to users within one to three months of data collection. The turnaround time for this data set is much faster than the standard set for the TOGA data set, and the geographical extent of the data set exceeds that of the TOGA and ISLP-Pac data set. Fortunately, the IPSLN had upgraded over 40 of its stations to upload data via the NOAA's Geostationary Operational Environmental Satellite Data Collection System (DCS), Japan's Geostationary Meteorological Satellite DCS, and the European Organization for the Exploitation of Meteorological Satellites and Meteorological Satellite DCS (Kilonsky, 1984). These upgraded sites provide the nucleus of the WSLC data set. The WSLC has also expanded upon the contacts made by the UHSLC with other national agencies contributing sea level data to the TOGA and IGOSS projects. Through these activities, we have significantly expanded our collection of near-real time sea level data. Currently, ORSTOM and Service ARGOS contribute data from two stations, the Flinders University in Australia provides data from 7 stations, the U.S. National Ocean Service provides 31 additional stations, and, building upon their contribution to the ISLP-Pac, the Japanese Meteorological Agency supplies 7 stations along the coast of Japan. There are now 94 stations contributing in near-real time to the WOCE "fast delivery" sea level data set (see

Fig. 1).

All of the activities of the WSLC have been organized to take maximum advantage of the work already being done by the UHSLC. The software used by the WSLC is taken from collocated projects and is maintained by the UHSLC data manager. The satellite-transmitted data comes at no cost over channels established by the UHSLC, and computing resources are shared. Thus, the processing of sea level information for the WSLC closely parallels the procedures described elsewhere (Mitchum et al., 1994; Kilonsky and Caldwell, 1991; Wyrki *et al.*, 1988), and only a brief description will be presented here.

As it arrives at the UHSLC, the sea level data are logged onto a network of microcomputers. A daily review of the data is conducted, and instrument problems are identified and queries are made to the data originators when appropriate. The initial quality control procedures include inspecting the data for consistency with past data from that station, setting reference levels, and removing any obviously inaccurate data. Emphasis is on verifying the timing of the samples and the linking of the data to a stable reference level. More specifically, differences of consecutive values are calculated and compared to threshold values. Time series plots of the original sea level data and the residuals between different channels and the predicted tides for a station are analyzed for possible problems. Detectable errors include random erroneous signals, reference level shifts, timing errors, and data gaps. All of these errors are generally evident in the residual plots, and usually can be resolved to produce a quality data set. IPSLN stations also include a tide staff and an automated reference level switch, which are linked by surveying with local bench marks. Measurements from these devices are used to align the gauge measurements with a common stable zero reference



Figure 1. Stations contributing to the WOCE "Fast Delivery" Sea Level Center. Stations available as of June 1995.

level.

Once the initial quality control checks are done, the data are processed to obtain the hourly, daily, and monthly time series that comprise the products of the WSLC. Sea level data are typically taken at a sampling rate ranging from several samples per second to several samples per hour. These high frequency samples are filtered to obtain hourly data, which is the first “standard” sampling interval. The hourly data are used to compute daily sea level values that preserve sea level variability at time scales longer than about 2.5 days. The daily values are computed by subtracting estimates of the major diurnal and semidiurnal tides and then applying a convolution-type numerical filter. Note that the long period tides are not removed from the daily values. Finally, the daily values are averaged to obtain traditional monthly means. At all stages of the processing, various quality control procedures are applied to the data. Among other things, every time series is checked visually by the data manager and by the WSLC director before being approved for inclusion in the WSLC data set. Our experience tells us that one of the best possible quality control checks is simply having a scientist familiar with the data set look at it.

Turning now to data distribution, we note that several years before the establishment of the WSLC, the UHSLC instituted an “anonymous ftp” system on the Internet computer network that allowed users to log into one of our computers and obtain copies of files containing the most up to date versions of all of our IGOSS products and the latest version of the TOGA *in situ* sea level data set. Although such ftp sites are now common, it should be noted that the UHSLC version was one of the earliest implementations. As the goal of the WSLC is the rapid distribution of *in situ* sea level data, it was natural to expand our Internet facility to include the near-real time WOCE data. By the time the funding for the WSLC arrived in fall 1993, a new ftp section had been added that contained data for over 50 stations, and in the first month of operation the WSLC handled 51 requests for 1179 sea level station files. Since that time, there have been 469 data requests, and 11,340 data files have been distributed to users. Also, a 1994 e-mail survey, which was certainly less than comprehensive, identified over 80 scientific users with 14 papers published in scientific journals.

### An application of the WSLC data set

It was pointed out earlier that the need for the sea level data included verification of the altimeter heights against a well-understood data set. Mitchum (1994) has done such an evaluation of the TOPEX altimetric heights using the data from the WSLC. It was found that for time scales longer than 10 days, the TOPEX sea surface heights agreed with the WSLC sea levels to 4 cm rms. It was also found that attempting once per revolution orbit error corrections actually degraded the quality of the intercomparison, which testifies to the excellence of the TOPEX orbit calculations. Examples were found where propagating Rossby waves

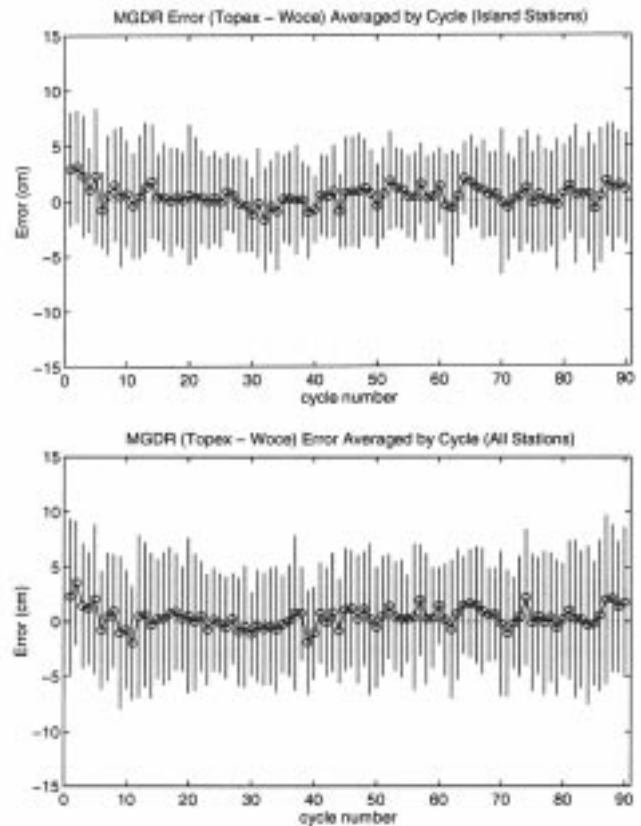


Figure 2. T/P differences from the WSLC sea levels (open circles) averaged over all tide gauge stations. In principle, if the two data sets are the same except for noise, and the tide gauges are a fair sample of the global variability of the noise, then the mean error should average to zero. The standard deviations during each cycle are plotted as vertical bars and show that the mean errors are not significantly different than zero. Drifts of this curve away from zero can be used to monitor the stability of T/P.

introduced significant differences between the altimetric and *in situ* data sets. It was also shown to be possible to use the TOPEX heights as a check on the *in situ* data, and to identify sea level stations that have problems. Such checks have since been incorporated into the WSLC quality control procedures.

Evaluation such as this, however, is not a one-time thing. Monitoring the quality of altimetric heights should be a continuing process. As longer time series are obtained it is possible that more subtle problems with the altimeter will surface. One way of monitoring the health of the satellite over the long term (Mitchum, 1994) is shown in Fig. 2. This plot is from the differences between the WSLC sea level gauges (see Fig. 1) and the T/P heights at the point of nearest approach. The data are averaged over the 10-day T/P cycles and are therefore an indicator of the quality of the T/P data on time scales longer than about 10 days. Fig. 2 basically shows the time series of the mismatch between T/P and the gauges during each 10-day cycle averaged globally over the tide gauge locations to obtain an estimate of the globally

averaged error. The scatter estimate shown allows a determination as to whether the mean error is significantly different from zero. Such a plot could identify particular time periods when the altimeter performed badly, but fortunately no such periods are found. More importantly, estimation of the low frequency content of this time series could allow identification of a drift in the altimetric data. A paper expanding on this use of the WSLC sea levels is in preparation.

## Future plans

The WSLC now functions routinely, which means that the data set is updated every month on a strict schedule. The first priority is to maintain the data flow without interruption or compromise in its quality and significant effort is made to sustain the level of service that we have established. There are, however, two areas that require attention. The sea level network is still sparse in the Southern Ocean and in parts of the Atlantic and Pacific Oceans. Also, all of the time series have not been expanded backward to 1985. This is desirable in order to provide linkages between present altimeters (T/P and ERS-1), future ones (*e.g.*, ERS-2), and the past data from GEOSAT. In the Southern Ocean, a primary source of data is from the British ACCLAIM gauges. We will continue to work with

the data originators to obtain these data in a more timely fashion. Two Southern Ocean gauges are operated by C. Le Provost in the Indian Ocean. The data from these gauges are provided reliably and thanks are due to the French for this effort. Telemetry for these gauges is via Service ARGOS. Additional sites will soon be available from Australian groups. The WSLC will also continue to work with the appropriate national agencies to obtain additional data in the Pacific and Atlantic Oceans. The prospects for acquiring additional near-real data from those agencies already contributing to the TSLC and ISLP-Pac appear good.

## References

- Kilonsky, B., Satellite-transmitted sea level stations – 1983, 1984: University of Hawaii, Honolulu, Ref. HIG-84-2, 40pp.
- Kilonsky, B., and P. Caldwell, 1991: In the pursuit of high-quality sea level data. *IEEE Oceans Proceedings*, 2, 669–675.
- Mitchum, G., 1994: Comparison of TOPEX sea surface heights and tide gauge sea levels. *J. Geophys. Res.*, 99, 24541–24554.
- Mitchum, G., B. Kilonsky, and B. Miyamoto, 1994: Methods for maintaining a stable datum in a sea level monitoring system. *IEEE Oceans Proceedings*, 1, 25–30.

# The Global Lagrangian Drifter Data Assembly Center at NOAA/AOML

*Mark Bushnell, NOAA/AOML, 4301 Rickenbacker Causeway, Miami, FL 33149, USA*

## The drifters

The Global Drifter Program (GDP) provides worldwide observations of sea surface temperature (SST), surface currents, and sea level pressure (SLP) in support of a host of climate research programs. Using a standardized design developed at Scripps Institute of Oceanography (Sybrandt and Niiler, 1991), global lagrangian drifters (GLD) are deployed in all the world's oceans. The drifters are designed to be good water followers; they use a small surface float and a large drogue centred at fifteen metres depth, resulting in a slip of less than 1 cm/sec in winds of 10 m/sec. All drifters are fitted with a linear thermistor accurate to 0.1°C located on the lower half of the surface float, and a submergence sensor used to determine the presence of the drogue. Presently over 750 drifters are deployed worldwide, and their locations are shown in Fig. 1. About 10% of those are also fitted with a barometric SLP sensor, and they are primarily deployed in the Southern Ocean. In July 1995 a

new array of barometer drifters was established off the west coast of the United States in support of the US National Weather Service.

## The drifter data

Drifters transmit data every 90 seconds, and the data are received when a NOAA polar orbiting satellite passes overhead. The data are relayed to Service Argos, where positions are computed and the raw data are logged. Most drifters operate on a 1/3 duty cycle to reduce Argos fees, typically one day on and two days off or three hours on and six hours off. Due to the satellite passage schedule and the one third duty cycle, drifter positions and data are not uniformly distributed in time. The transmitted data are also highly redundant and contain occasional transmission errors, failed sensor errors, etc. Data are sent to the AOML DAC monthly on nine track tapes, from both Argos in Landover and in Toulouse.

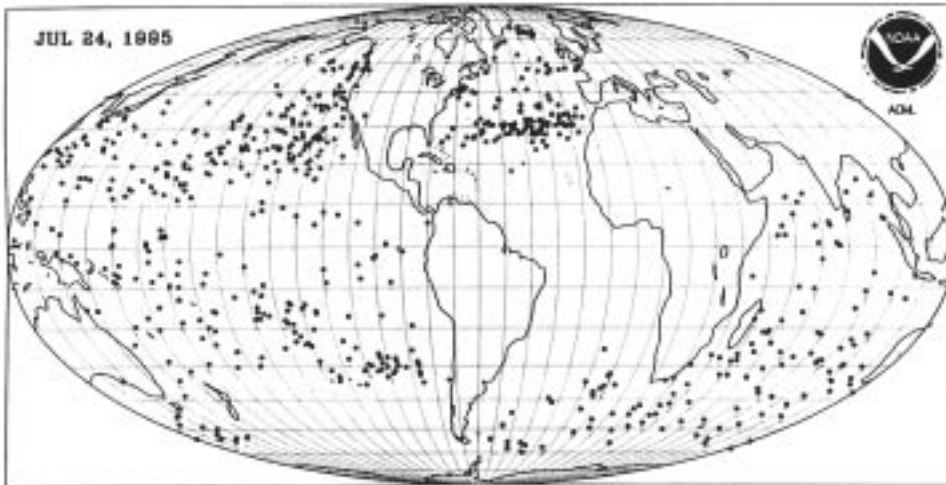


Figure 1. Status of the Global Drifter Array. Monthly updates of this map can be found on the WWW: <http://larry.aoml.erl.gov:8000/www/drifter.html>

## The Data Assembly Center

The Data Assembly Center (DAC) was established at AOML in 1988 to support the drifter data needs of the WOCE and TOGA programs. Funding for the DAC activities has taken place under various NOAA programs and it is presently supported by NOAA's Climate and Global Change Program. In 1995 the Global Drifter Center (GDC), which is responsible for shipping and deploying the drifters, moved from Scripps to AOML to facilitate the close coordination between these two centres.

The primary objective of the DAC is to create a research quality data set of surface velocity and SST by applying uniform quality control and processing to the drifter data. A secondary objective is to provide data products and services for monitoring and managing the global array of drifters. Data from 26 different Argos programs, 25 scientists, and 12 different countries are acquired at the drifter DAC. The raw data are quality controlled by removal of outliers, primarily by using rate of change constraints. A uniform time series of position and sensor data at six hour time steps is then created using optimum interpolation logic, including uncertainty estimates for each value. Data processing procedures are more fully described by Hansen and Poulain, 1995.

The DAC then provides the data set to the Canadian Marine Environmental Data Service (MEDS) for permanent archive and public dissemination. The DAC also returns database updates to contributing researchers, produces monthly maps of displacement vectors, and manages data distribution on the Global Telecommunications System (GTS) for US researchers. The DAC maintains a World-Wide Web (WWW) home page at <http://larry.aoml.erl.gov:8000/www/drifter.html>, from which several of the products may be obtained. Guest computer accounts are also available, such that cooperating researchers may access the data themselves using menu driven software to create specific products.

DAC products are used for research including ocean observation (Reynolds and Smith, 1994), ocean model evaluation (WCRP, 1995), and climate prediction research (CPC, 1995), to name a few. At last count, there were at least 150 manuscripts based at least in part on GLD observations.

Plans for the DAC include the acquisition of Argos data on a more frequent basis and improved access to more products using the WWW. The number of deployed drifters has increased five-fold since the DAC began in 1988, and it is expected that over 1000 GLDs will be in operation worldwide during FY 1996. Soon the SLP data from the US west coast array will be incorporated into NWS forecasts. Several new sensors such as wind speed and direction, and rainfall rate are under development, and it is expected that those data will be processed at the AOML DAC.

## References

- CPC, 1995: Experimental Long-lead Forecast Bulletin, June 1995, Vol. 4 No. 2. Climate Prediction Center, Washington, D.C. 20233, 45pp.
- Hansen, D.V., and P.M. Poulain, 1995: Quality control and interpolations of WOCE/TOGA drifter data. *J. Atmos. Oceanic Tech.*, submitted.
- Reynolds, R.W., and T.M. Smith, 1994: Improved global sea surface temperature analysis. *J. Climate*, 7, 929-948.
- Sybrandy, A.L., and P.P. Niiler, 1991: WOCE/TOGA Lagrangian drifter construction manual. SIO Ref. 91/6, WOCE Report 63, 58pp.
- WCRP, 1995: Comparison of TOGA tropical Pacific Ocean model simulations with the WOCE/TOGA Surface Velocity Program drifter data set. Global Drifter Center, Scripps Institution of Oceanography, La Jolla, CA, USA, 156pp.

## Exploring Oceanographic Data on the PC

*Reiner Schlitzer, Alfred-Wegener-Institute for Polar and Marine Research, Postfach 120161,  
27515 Bremerhaven, Germany*

Now, about five years after the start of the field work of WOCE, at a time when first WOCE datasets are distributed, the tasks of analyzing and managing these datasets become increasingly important. To assist and facilitate the scientific analysis of the oceanographic data I have developed a software package, OCEAN DATA VIEW (ODV), that can be of general use and can help exploring the evolving large datasets. This software is now publicly available.

ODV is a software package for the exploration and graphical analysis of oceanographic bottle, CTD, and XBT data running on PCs under MS-DOS, Windows or OS/2. Graphics output includes general property-property plots of one or more stations, colour property sections along cruise tracks and colour property distributions on general iso-surfaces. Any basic or derived variable can be used to define iso-surfaces (*e.g.*, depth horizons, isopycnals, isothermals, etc.) but property minimum or maximum layers, like, for instance, the salinity minimum layer (AAIW) in the South Atlantic, can be chosen as display-surface as well. Colour or black-and-white paper hard-copies of the screen graphics are obtained easily.

The data format of ODV is optimized to provide dense storage and direct data access and allows the creation and management of large sets of station data from, for instance, the World Ocean Circulation Experiment (WOCE), the NODC hydrographic data-archives or other data sources on relatively inexpensive and readily available desktop and notebook computers. ODV allows easy import of new data as well as re-export of some or all of the data stored in a collection. Hydrographic data in WOCE WHP format (distributed via Internet by the SAC, Hamburg) and data from the World Ocean Atlas 1994 (WOA94; distributed on CD-ROM by NODC, Washington) can directly be incorporated into the ODV system.

In addition to the basic, measured variables that are imported from data input files and that are stored in the data collection disk files, ODV can automatically calculate additional, derived variables which (once defined) are accessible for data exploration and graphical display in the same way as the basic variables. A suite of commonly used derived quantities including potential temperature, potential density, dynamic height (all referenced to arbitrary levels), Brunt-Väisälä Frequency, sound velocity, oxygen saturation and others are implemented in the software code and can be activated using a few mouse and keyboard operations. Other derived variables not included in the list of internally defined quantities can be added by means of macro files. Use of macro files for new derived quantities broadens the scope of ODV considerably and allows easy experimentation with new quantities not yet established in the scientific community.

The ODV software is equipped with a suite of options for the selection of data and for interactive modification of the data plots shown on the screen. These options are usually used to browse through the data and to adapt the graphics layout and the contents of the data windows according to specific needs. You can, for example, (1) focus on individual stations or even samples by clicking with the mouse on respective station or sample positions; (2) zoom into any of the data plots for investigation of small details; (3) perform automatic rescaling for full-range view of the data; (4) define sections following arbitrary cruise tracks or define arbitrary iso-surfaces; (5) select subsets of stations using a variety of different criteria for studies of, for instance, regional, seasonal or inter-annual trends; (6) define water-mass "patches" and identify their distribution along a section; (7) define and use derived quantities; (8) redefine the graphics layout (number of data-windows, their size and position on screen and hardcopy as well as variables displayed in data-window); (9) change the colour-scale for colour distributions. Once an interesting graphics screen has been obtained, a paper hardcopy can be produced easily.

ODV can operate in two display-modes: (1) original data points, and (2) gridded fields. In (1) the data are displayed at their original sampling locations in the property-property plots, colour sections and iso-surface plots and no gridding or mapping is performed on the data. This approach produces "honest" distributions of the data thereby instantly revealing regions of poor sampling and highlighting occasional bad data values. In regions with good data coverage the displayed fields appear quasi-continuous as if the data had been gridded (but note that the colour dots overlap in these areas and that some data points may be invisible). In (2) section and surface data are used to calculate gridded fields by averaging over nearby data. The averaged fields are then displayed on the screen or can be printed on a colour PostScript printer. These distributions are generally nicer to look at, but it is important to note that they are a data-product and that some small-scale features in the data might be lost due to the averaging. In both display-modes ODV allows the export of section or surface data to ASCII files suitable for dedicated gridding, shading and contouring software.

ODV is designed to be flexible and easy-to-use. A user does not require knowledge of any programming language nor does he (or she) need to know any details of the internal data storage format. The programs always display station maps on the screen and allow navigation through the data using the mouse. Typing-in of commands is kept to a minimum. The capability to create and maintain large data collections of up to 99,999 stations makes it feasible to keep large parts of the global historical

hydrographic data plus newly arriving, more recent data on readily available desktop or notebook PC for scientific analysis. In addition to actual research applications during oceanographic cruises or in the laboratory ashore, ODV could be useful for data quality evaluation work or for educational and classroom activities.

OCEAN DATA VIEW is available via Internet at no charge. If you are using a World-Wide-Web browser connect to

<http://www.awi-bremerhaven.de/GPH/ODV/>.

From the ODV page you can choose to download the ODV files by selecting OCEAN-DATA-VIEW, you can view ODV sample section- and surface plots and you can connect to the WOCE SAC (Hamburg) or the NODC (Washington), two sites that distribute data that can easily be incorporated into the ODV system.

To download the ODV package to your PC via

anonymous FTP perform the following steps:

```
ftp ftp.awi-bremerhaven.de (or: ftp 134.1.2.250)
anonymous
enter your e-mail address as password
cd /pub/GPH/ODV
get readme.txt
binary
get pkunzip.exe
get odv30d1.zip
get odv30d2.zip
bye
```

Then, print file *readme.txt* and follow its instructions.

ODV runs on PCs with 386 or higher processor, 4 MB of available extended memory, 5 MB of free hard-disk space and a mouse. For best results, SVGA graphics hardware capable of 256 colours and a graphics resolution of at least 800 x 600 pixels is recommended.

## WCRP PROGRAMMES: CLIVAR Has Begun

*R. Allyn Clarke, Bedford Institute of Oceanology, PO Box 1006, Dartmouth, N.S., Canada B2Y 4A2*

CLIVAR (Climate Variability and Predictability) became an active programme within the WCRP at the beginning of 1995 by taking over scientific responsibility for a number of ongoing projects begun by TOGA. In the early 1990's, the WCRP began thinking about what programmes it should have in place to succeed TOGA and WOCE. A study group, recommended that a programme be established to focus on climate variability and predictability over time scales of seasons to centuries.

The Scientific Steering Group for CLIVAR was established in April 1993 and immediately began working on its science plan. The CLIVAR science plan was approved by the SSG in June, 1995 and will be published as a WCRP report sometime in the fall. The science plan establishes four scientific objectives.

- To describe and understand the physical processes responsible for climate variability and predictability on seasonal, decadal and centennial time scales, through the collection and analysis of observations and the development and application of models of the coupled climate system, in co-operation with other relevant climate research and observing programmes.
- To extend the record of climate variability over the time scales of interest through the assembly of quality controlled paleoclimatic and instrumental data sets.
- To extend the range and accuracy of seasonal to interannual climate prediction through the development of global coupled predictive models.
- To understand and predict the response of the climate system to the growth of the radiatively active gases and aerosols and to compare these predictions to the observed climate system in order to detect the

anthropogenic modifications of the natural climate signal.

The Science Plan is to be followed by an implementation plan. Initially CLIVAR is to be organized into three components:

- CLIVAR-GOALS: A study of seasonal-to-inter-annual global climate variability and predictability,
- CLIVAR-DecCen: A study of decadal-to-centennial global variability and predictability, and
- CLIVAR-ACC: A study of the response of the climate system to the addition of radiatively active gases and aerosols to the atmosphere.

A CLIVAR project office has been established at the Institut für Meereskunde, Universität Hamburg and Dr Michael Coughlan has just taken up residence in Hamburg as its first director. The project office will be of immense help as CLIVAR develops its initial implementation plan.

A great deal of work has already been directed toward the development of an initial implementation plan for CLIVAR-GOALS since a programme needed to be in place to continue TOGA's observational and modelling activities directed toward ENSO prediction. A workshop was held in April, 1995 in Melbourne to discuss the Asian-Australian Monsoon, a subject of important interest to the CLIVAR-GOALS community and to the nations of this region.

Implementation is much less advanced with regard to CLIVAR DecCen and CLIVAR-ACC. The SSG called for the organization of three scientific workshops to be held over the next year and a half to examine several possible mechanisms causing decadal to century scale climate variability. These workshops will be:

- On the role of water mass transformation to be led by Fritz Schott,
- On the role of variations in large-scale ocean circulation to be led by Arnold Gordon, and
- On the role of large scale atmosphere/ocean interactions to be led by Ed Sarachik.

In addition to these workshops, the SSG has established two Numerical Experimentation Groups; one directed at the seasonal to interannual time scale and the other at the longer time scale and on anthropogenic changes. CLIVAR is also in the process of establishing an Upper Ocean Processes working group to provide scientific planning and oversight to the observation, analysis and modelling of air-sea fluxes and the upper ocean.

From the results of these workshops and the input of the NEG's and the Upper Ocean working group, the SSG will develop an initial implementation plan for CLIVAR. Since CLIVAR is to be a fifteen year programme, this implementation plan is likely to evolve in time, especially after the completion of WOCE's synthesis and analysis

phase.

CLIVAR like GEWEX is a broad programme that seeks to form new bridges between communities who have not worked particularly closely together in the past. CLIVAR seeks to study the coupled atmosphere-ocean system and needs to find atmospheric and ocean scientists willing to share their ideas and efforts. CLIVAR also seeks to look at time scales not resolved by our short instrumental records and hence needs to forge links with the paleoclimate community.

For more information contact:

International CLIVAR Project Office

Institut für Meereskunde

Universität Hamburg

Tropelwitzstrasse 7

D-22529 Hamburg

Germany.

Tel: 49-40-561017/18

Fax: 49-40-563990

e-mail: michael.coughlan@clivar.dkrz.d400.de.

## WOCE Hydrographic Programme Underway Data Submission - An Update

*Bertrand J. Thompson, WOCE DIU, University of Delaware, Lewes, USA*

Number 15 in this Newsletter series published February 1994 carried an article explaining the submission procedures for WHP underway data (surface salinity, meteorology, bathymetry, XBTs/XCTDs, currents (ADCP), and gases). Since that time, existing and new Data Assembly Centres (DACs) have been working with the WHP Office, PIs and National WOCE focal points to facilitate the submission of data. The procedures for underway data have been issued by the WHPO in "Requirements for WHP Data Reporting" WHP Manual 90-1 (Rev. 2) May 1994. Summaries of the underway data flow and availability are included in the WOCE Data Handbook, 2nd ed (Dec 1994), and with DAC status reports, are available on OCEANIC.

The general procedure for submission of underway data (except XBTs) is to submit the data as soon as possible after a cruise to the WHP Office, who forward the data to the appropriate DAC. DACs are seeking data from cruises which took place prior to the establishment of submission procedures, directly from PIs or National focal points. We urge all WOCE PIs holding or planning underway data to contact the appropriate DAC or the WHPO to coordinate the submission of data.

### Surface Salinity

To date, few WOCE underway Surface Salinity data sets have been submitted to the SS DAC in Brest, France. The existing data set is mainly composed of ship of opportunity data taken in association with XBT operations.

Contact Alain Dessier (dessier@orstom.fr or Fax 33-98-22-45-14) or see the World Wide Web server ([http://www.ifremer.fr/sismer/sommaire\\_e.htm](http://www.ifremer.fr/sismer/sommaire_e.htm)).

### XBT/XCTD

These data continue to follow the long standing IGOSS and IODE procedures and in a number of cases that means slowly. The real-time data move through the system efficiently but the delayed mode data, the category in which most WHP underway data would fall, are moving through to the DACs slowly. These data will not be available for synthesis at an early stage unless PIs and National focal points comply with the agreed submission guideline of one year after collection. Contact Bruce Hillard (b.hillard@unesco.org or Fax 33-1-45-68-30-96).

### Bathymetry

The Bathymetry Center now holds data from 18 WOCE cruises. The submission of bathymetry data does not seem to have become standard practice, though many PIs may still be unaware of the existence of the bathymetry DAC. The DAC has asked that it be given help in raising the awareness of it's mission and states it can accept data in any well documented format. Contact Tom Niichel (tniichel@ngdc.noaa.gov or Fax 1-303-497-6513) and view their World Wide Web server (<http://www.ngdc.gov/ngdc.html>).

## Meteorology

The Meteorology DAC has been aggressive in its efforts to collect data. About 20% of the WOCE cruises declare they have or will have meteorology data but it is the DAC's belief that all WOCE cruises (about 500) record surface meteorology and is, therefore, pursuing data from all cruises. They now have data from 125. The DAC has had some difficulty identifying contacts and convincing them to send data to the DAC. Contact David Legler (legler@coaps.fsu.edu or Fax 1-904-644-4841) and WWW (<http://www.coaps.fsu.edu/WOCE/>).

## ADCP

As of this writing the situation regarding ADCP data has changed little since early 1994 but it is proposed that the Japan Oceanographic Data Center (JODC) and the USA NODC unit at the University of Hawaii collaborate over archiving and distributing WOCE ADCP data. JODC and NODC have agreed to collaborate and await WOCE SSG approval. Besides collecting data and metadata, the

DAC will reformat the data into a common format without loss of data, maintain an on line inventory, and make the data and metadata available through the NODC web site in Hawaii. Special attention will be given to ensuring that the metadata are sufficient to allow assessment of the scientific quality of the data. JODC/NODC will be provided guidelines by the scientific community on the level of metadata required to achieve this.

This DAC will only obtain shipboard ADCP data. The existence of lowered and moored ADCP data will continue to be tracked by the WHP Office and DIU but these data should continue to reside with PIs. Until the DAC is truly established, please contact WOCE IPO (woceipo@soc.soton.ac.uk or Fax 44-1703-596204) and see OCEANIC (<http://www.cms.udel.edu/>).

## Gases

The responsibility for underway gas measurements remains with the JGOFS community, but you can contact the WHP Office (whpo@whpvax.whoi.edu or Fax 1-508-457-2165 and WWW <http://whpo.whoi.edu/>).

## Errata

In the article in WOCE Newsletter No. 19 entitled "A Hydrography in the Southern Philippine Sea: From WOCE Hydrographic Programme Section PR1S and PR24" there are a number of matters that need clarification or correction, as follows:

- (1) This article is a digest of a paper for a proceeding of the WESTPAC III at Bali, 1995. We authors would like to make the origin clear.
- (2) The precisions of our measurement during this cruise were 0.0005 PSS in Salinity, 0.5% in Oxygen, 0.6% in Nitrate, 0.4 in Silicate and 1.2% in Phosphate. These values are important to discuss the homogeneity of the deep water.
- (3) We made mistakes in Table 1:
  - The value 129.7 of the average of Silicate between 7600–4998 should be read 139.7  $\mu\text{mol/kg}$ .
  - The value 0.0002, 0.0003 and 0.0001 of the standard deviation of Salinity should be read 0.002, 0.003 and 0.01%.

Sincerely yours,

Takeshi Kawano  
Nani Hendiarti

## Meeting Timetable 1995/96

### WOCE Meetings

1995	October	26–27	SMWG-1	Boston
	October 31 – November 3		WOCE-22	WHOI
	October	10–12	WHPPC-14	Hamburg
	October	12–13	(C)WXXPPC-4	Ottawa
1996	February	5–9	DPC-9	Brest
	February		UOT/DAC-6	NODC
	February		GTSP-IV	NODC
	May		SVP-8	Argentina

### Science and other Meetings

1995	September	21–29	ICES 1995 Annual Science Conference, Copenhagen	
	September	26–29	42nd Annual Eastern Pacific Oceanic Conference (EPOC) Special topic: Eastern Boundary Currents, Fallen Leaf Lake, Calif.	
	September	25–29	IGBP - Global Analysis Interpretation and Modelling, Garmisch	
	October	10–14	5th International Conference on Paleoceanography, Halifax	
	October	16–20	Ewing Symposium on Applications of Trace Substance Measurements to Oceanographic Problems, Biosphere II, Arizona or Lamont	
	October	16–22	4th Annual Meeting of the North Pacific Marine Science Organisation (PICES) (with a session on circulation in the subarctic North Pacific and its marginal seas), Qingdao	
	October	24–27	WCRP Workshop on Air-Sea Flux Fields for Forcing Ocean Models and Validating GCMs, Reading, UK	
1996	February	12-16	Ocean Sciences Meeting (sponsored by the American Geophysical Union and the American Society of Limnology and Oceanography), San Diego	
	May	6–10	European Geophysical Society XX1 Assembly, Den Haag	
	July	8-11	The Oceanography Society (TOS) Meeting on Marine Environment and the Global Change Programs, Amsterdam	
	July	23–27	Western Pacific Geophysics Meeting (AGU), Brisbane	
1997	July	1–9	IAMOS/IAPSO XXII General Assembly, Melbourne	

For more information on the above meetings contact the IPO. If you are aware of any conferences or workshops which are suitable for the presentation of WOCE results and are not mentioned in the above list please let the IPO know.



## Note on Copyright

Permission to use any scientific material (text as well as figures) published in the International WOCE Newsletter should be obtained from the authors.

WOCE is a component of the World Climate Research Programme (WCRP), which was established by WMO and ICSU, and is carried out in association with IOC and SCOR. The scientific planning and development of WOCE is under the guidance of the JSC Scientific Steering Group for WOCE, assisted by the WOCE International Project Office. JSC is the main body of WMO-ICSU-IOC, formulating overall WCRP scientific concepts.

The WOCE Newsletter is edited at the WOCE IPO at the Southampton Oceanography Centre, Empress Dock, Southampton SO14 3ZH (Tel: 44-1703-596789, Fax: 44-1703-596204, e-mail: [woceipo@soc.soton.ac.uk](mailto:woceipo@soc.soton.ac.uk)).

We hope that colleagues will see this Newsletter as a means of reporting work in progress related to the Goals of WOCE as described in the Scientific Plan. The SSG will use it also to report progress of working groups, experiment design and models.

The editor will be pleased to send copies of the Newsletter to institutes and research scientists with an interest in WOCE or related research.